THESE TERMS GOVERN YOUR USE OF THIS DOCUMENT

Your use of this electronic information product ("EIP"), and the digital data files contained on it (the "Content"), is governed by the terms set out on this page ("Terms of Use"). By opening the EIP and viewing the Content, you (the "User") have accepted, and have agreed to be bound by, the Terms of Use.

EIP and Content: This EIP and Content is offered by the Province of Ontario's *Ministry of Energy, Northern Development and Mines* (ENDM) as a public service, on an "as-is" basis. Recommendations and statements of opinions expressed are those of the author or authors and are not to be construed as statement of government policy. You are solely responsible for your use of the EIP and its Content. You should not rely on the Content for legal advice nor as authoritative in your particular circumstances. Users should verify the accuracy and applicability of any Content before acting on it. ENDM does not guarantee, or make any warranty express or implied, that the Content is current, accurate, complete or reliable or that the EIP is free from viruses or other harmful components. ENDM is not responsible for any damage however caused, which results, directly or indirectly, from your use of the EIP or the Content. ENDM assumes no legal liability or responsibility for the EIP or the Content whatsoever.

Links to Other Web Sites: This EIP or the Content may contain links, to Web sites that are not operated by ENDM. Linked Web sites may not be available in French. ENDM neither endorses nor assumes any responsibility for the safety, accuracy or availability of linked Web sites or the information contained on them. The linked Web sites, their operation and content are the responsibility of the person or entity for which they were created or maintained (the "Owner"). Both your use of a linked Web site, and your right to use or reproduce information or materials from a linked Web site, are subject to the terms of use governing that particular Web site. Any comments or inquiries regarding a linked Web site must be directed to its Owner.

Copyright: Canadian and international intellectual property laws protect the Content. Unless otherwise indicated, copyright is held by the Queen's Printer for Ontario.

It is recommended that reference to the Content be made in the following form:

Ontario Geological Survey 2018. Survey report on Sandy Lake–Favourable Lake area, 77p. [PDF document]; *in* Ontario airborne geophysical surveys, magnetic and electromagnetic data, grid and profile data (ASCII format) and vector data, Ontario Geological Survey, Geophysical Data Set 1085a.

Ontario Geological Survey 2018. Survey report on Sandy Lake–Favourable Lake area, 77p. [PDF document]; *in* Ontario airborne geophysical surveys, magnetic and electromagnetic data, grid and profile data (Geosoft® formats) and vector data, Ontario Geological Survey, Geophysical Data Set 1085b.

Use and Reproduction of Content: The EIP and the Content may be used and reproduced only in accordance with applicable intellectual property laws. *Non-commercial* use of unsubstantial excerpts of the Content is permitted provided that appropriate credit is given and Crown copyright is acknowledged. Any substantial reproduction of the Content or any *commercial* use of all or part of the Content is prohibited without the prior written permission of ENDM. Substantial reproduction includes the reproduction of any illustration or figure, such as, but not limited to graphs, charts and maps. Commercial use includes commercial distribution of the Content, the reproduction of multiple copies of the Content for any purpose whether or not commercial, use of the Content in commercial publications, and the creation of value-added products using the Content.

Contact:

FOR FURTHER INFORMATION ON	PLEASE CONTACT:	BY TELEPHONE:	BY E-MAIL:
The Reproduction of the EIP or Content	ENDM Publication Services	Local: (705) 670-5691 Toll-Free: 1-888-415-9845, ext. 5691 (inside Canada, United States)	Pubsales.ndm@ontario.ca
The Purchase of ENDM Publications	ENDM Publication Sales	Local: (705) 670-5691 Toll-Free: 1-888-415-9845, ext. 5691 (inside Canada, United States)	Pubsales.ndm@ontario.ca
Crown Copyright	Queen's Printer	Local: (416) 326-2678 Toll-Free: 1-800-668-9938 (inside Canada, United States)	Copyright@ontario.ca

Ontario

Ontario Airborne Geophysical Surveys
Magnetic and Electromagnetic Data
Sandy Lake–Favourable Lake Area

ONTARIO GEOLOGICAL SURVEY

Geophysical Data Set 1085

2018

Ontario

ONTARIO GEOLOGICAL SURVEY

Geophysical Data Set 1085

Ontario Airborne Geophysical Surveys
Magnetic and Electromagnetic Data
Sandy Lake–Favourable Lake Area

by

Ontario Geological Survey

2018

Ontario Geological Survey
Ministry of Energy, Northern Development and Mines
Willet Green Miller Centre, 933 Ramsey Lake Road,
Sudbury, Ontario P3E 6B5 Canada

Contents

FIGURES

TABLES

CREDITS

List of accountabilities and responsibilities.

- Renée-Luc Simard, Senior Manager, Earth Resources and Geoscience Mapping Section, Ontario Geological Survey (OGS), Ministry of Energy, Northern Development and Mines (MENDM)—accountable for the geophysical survey projects, including contract management
- Edna Mueller–Markham, Senior Consulting Geophysicist, Paterson, Grant and Watson Limited (PGW), Toronto, Ontario, Geophysicist under contract to MENDM—responsible for the airborne geophysical survey project management, quality assurance (QA) and quality control (QC)
- Tom Watkins, Manager, Publication Services Unit, GeoServices Section, Ontario Geological Survey, MEND—managed the project-related hard-copy products
- Desmond Rainsford, Senior Geoscience Leader, Geophysics, Earth Resources and Geoscience Mapping Section, Ontario Geological Survey—responsible for final quality assurance (QA), quality control (QC) of published digital products
- Geotech Ltd., Aurora Ontario – data acquisition and data compilation

DISCLAIMER

Every possible effort has been made to ensure the accuracy of the information presented in this report and the accompanying data; however, the Ministry of Energy, Northern Development and Mines does not assume liability for errors that may occur. Users should verify critical information.

CITATION

Parts of this publication may be quoted if credit is given. It is recommended that reference to this publication be made in the following form:

Ontario Geological Survey 2018. Survey report on Sandy Lake–Favourable Lake area, 77p. [PDF document]; *in* Ontario airborne geophysical surveys, magnetic and electromagnetic data, grid and profile data (ASCII format) and vector data, Ontario Geological Survey, Geophysical Data Set 1085a.

Ontario Geological Survey 2018. Survey report on Sandy Lake–Favourable Lake area, 77p. [PDF document]; *in* Ontario airborne geophysical surveys, magnetic and electromagnetic data, grid and profile data (Geosoft® formats) and vector data, Ontario Geological Survey, Geophysical Data Set 1085b.

NOTE

Users of OGS products are encouraged to contact those Aboriginal communities whose traditional territories may be located in the mineral exploration area to discuss their project.

1. Introduction

This report describes a helicopter-borne combined aeromagnetic and electromagnetic survey carried out by Geotech Limited for the Ministry of Energy, Northern Development and Mines (MENDM) performed as part of the Ontario Geological Survey (OGS) geoscience program in the Sandy Lake and Favourable Lake area in northwestern Ontario.

The airborne survey contracts were awarded through a Request for Proposal and Contractor Selection process. The system and contractor selected for each survey area were judged on many criteria, including the following:

- applicability of the proposed system to the local geology and potential deposit types
- aircraft capabilities and safety plan
- experience with similar surveys
- QA/QC plan
- capacity to acquire the data and prepare final products in the allotted time price-performance.

2. Survey Location and Specifications

2.1. SURVEY LOCATION

Geotech Ltd. conducted a helicopter-borne geophysical survey over the Sandy, Finger and Favourable lakes area in northwestern Ontario (Figure 1).

The geophysical survey consisted of a combined helicopter-borne electromagnetic (EM) survey using the versatile time-domain electromagnetic (VTEM®Plus) system with X-, Y- and Z-component measurements and an aeromagnetic survey using a cesium magnetometer. A total of 17 511 line-kilometres of geophysical data were acquired during the survey.

The crew was based out of the community of Sandy Lake, Ontario (*see* Figure 2) for the acquisition phase of the survey. The survey was flown between July 1, 2017 and March 18, 2018.

The geophysical survey was flown in 2 distinct blocks, the Sandy Lake Block to the northeast and the Favourable Lake Block to the southwest. The outline of the survey area and the flight path layout is shown in Figure 2 below.

Figure 1. Location map of the Sandy Lake–Favourable Lake area geophysical survey.

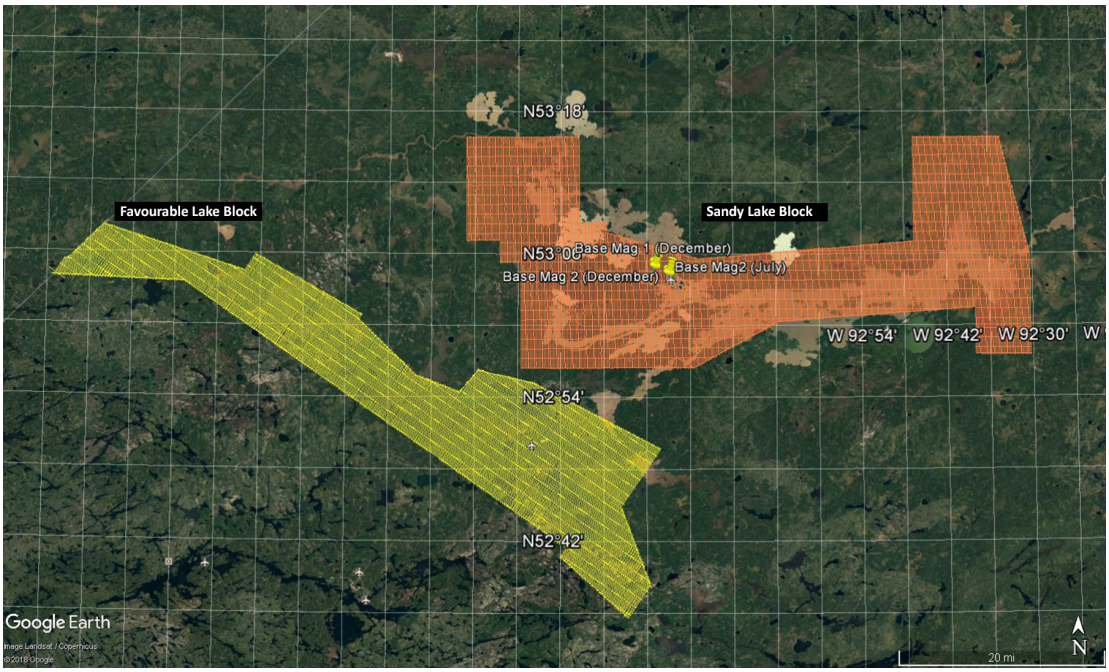

Figure 2. Flight path and magnetic base station locations displayed on Google Earth™ image.

2.2. TOPOGRAPHIC RELIEF AND CULTURAL FEATURES

Topographically, the blocks exhibits a shallow relief with an elevation ranging from 270 to 386 m above mean sea level over an area of 3 075 km^2 (Figure 3).

The survey blocks cover rivers and streams throughout the survey area which connect various lakes and wetlands. The most notable lake is Sandy Lake located in the middle of Sandy Lake Block. There are visible signs of culture, such as winter roads, and the Sandy Lake First Nation community, located in the survey area.

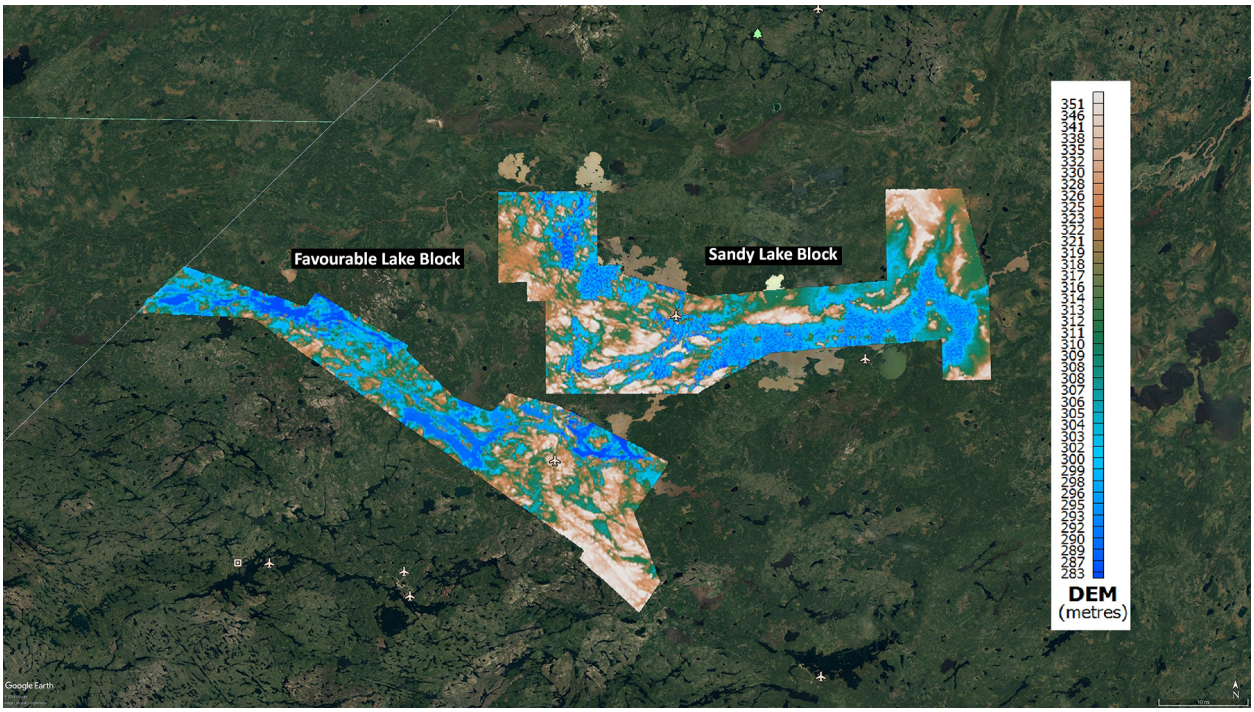

Figure 3. Digital Elevation Model (DEM) over Google Earth™ Image.

2.3. SURVEY AND SYSTEM SPECIFICATIONS

Data quality control and quality assurance, and preliminary data processing were carried out on a daily basis during the acquisition phase of the project. Final data processing followed immediately after completion of the survey. Final reporting, data presentation and archiving were completed at the Geotech Aurora office in June 2018.

The Sandy Lake Block was flown in a northward direction (0°), with traverse line spacing of 200 metres as depicted in Figure 2. Tie lines were flown perpendicular to the traverse lines (90°) at a spacing of 1500 metres. The Favourable Lake Block was flown in a southwest to northeast direction (35°), with traverse line spacing of 200 metres as depicted in Figure 2. Tie lines were flown perpendicular to the traverse lines (125°) at a spacing of 1500 metres. For more detailed information on the flight spacing and direction see Table 1.

2.4. DATA ACQUISITION

2.4.1. FLIGHT LINE SPECIFICATIONS

The survey block (*see* Figure 2) and general flight specifications are as follows.

Table 1. Flight line specifications

Survey block	Traverse Line spacing (m)	Area (Km^2)	Planned[1] Line-km	Actual Line-km	Flight direction	Line numbers
Sandy Lake Block	Traverse: 200	1800	7052	7287	0° / 180°	L1000 – L5400
	Tie: 1500				90° / 270°	T6000 – T7050
Favourable Block	Traverse: 200	1275	10081	10224	35° / 215°	L8000-L13210
	Tie: 1500				125° / 315°	T14000-T15100
TOTAL		3075	17133	17511		

Survey block boundary co-ordinates are provided in Appendix H.

As per agreement with the Sandy Lake First Nation, the data over the reserve has been delivered exclusively to the First Nation and is not included in this geophysical data set. The total line kilometres flown over the Sandy Lake reserve is approximately 257.

2.4.2. SURVEY OPERATIONS

Survey operations were based out of Sandy Lake, Ontario from July 1, 2017 to March 18, 2018. The flight schedule for the survey is outlined in Table 2 below.

Table 2. Survey flight schedule.

Date	Flight #	Flown km	Block	Crew location	Comments
1-Jul-17				Sandy Lake, ON	Mobilization
2-Jul-17				Sandy Lake, ON	System assembly
3-Jul-17				Sandy Lake, ON	System assembly
4-Jul-17				Sandy Lake, ON	System Testing
5-Jul-17				Sandy Lake, ON	System Testing
6-Jul-17				Sandy Lake, ON	System Testing
7-Jul-17				Sandy Lake, ON	System Testing
8-Jul-17				Sandy Lake, ON	System Testing
9-Jul-17				Sandy Lake, ON	System Testing
10-Jul-17				Sandy Lake, ON	System Testing
11-Jul-17				Sandy Lake, ON	System Testing
12-Jul-17				Sandy Lake, ON	System Testing
13-Jul-17				Sandy Lake, ON	Mobilization to survey area
14-Jul-17				Sandy Lake, ON	Mobilization to survey area
15-Jul-17				Sandy Lake, ON	Mobilization to survey area
16-Jul-17				Sandy Lake, ON	Mobilization to survey area
17-Jul-17				Sandy Lake, ON	Local Logistics
18-Jul-17				Sandy Lake, ON	System assembly
19-Jul-17				Sandy Lake, ON	Testing/ System assembly
20-Jul-17				Sandy Lake, ON	Testing Testing/ System assembly
21-Jul-17				Sandy Lake, ON	Testing/ System assembly

Date	Flight #	Flown km	Block	Crew location	Comments
22-Jul-17				Sandy Lake, ON	Testing/ System assembly
23-Jul-17				Sandy Lake, ON	Testing/ System assembly
24-Jul-17				Sandy Lake, ON	Test flights
25-Jul-17	1	80	A1	Sandy Lake, ON	80km flown limited due to weather
26-Jul-17				Sandy Lake, ON	No production due to weather
27-Jul-17	2,3,4	443	A1	Sandy Lake, ON	443km flown
28-Jul-17	5,6	324	A1	Sandy Lake, ON	324km flown
29-Jul-17	7,8	165	A1	Sandy Lake, ON	165km flown
30-Jul-17	9,10,11	329	A1	Sandy Lake, ON	329km flown
31-Jul-17				Sandy Lake, ON	Flight aborted due to weather
1-Aug-17	12	72	A1	Sandy Lake, ON	72km flown
2-Aug-17	13,14	269	A1	Sandy Lake, ON	269km flown
3-Aug-17				Sandy Lake, ON	No production due to technical issues
4-Aug-17				Sandy Lake, ON	Troubleshooting
5-Aug-17	15	20	A1	Sandy Lake, ON	20km flown
6-Aug-17				Sandy Lake, ON	No production due to technical issues
7-Aug-17				Sandy Lake, ON	No production due to technical issues
8-Aug-17				Sandy Lake, ON	No production due to technical issues
9-Aug-17				Sandy Lake, ON	System assembly
10-Aug-17				Sandy Lake, ON	
11-Aug-17				Sandy Lake, ON	
12-Aug-17				Sandy Lake, ON	
13-Aug-17				Sandy Lake, ON	
14-Aug-17				Sandy Lake, ON	
15-Aug-17				Sandy Lake, ON	
28-Jul-17				Sandy Lake, ON	Testing /troubleshooting
29-Jul-17				Sandy Lake, ON	Testing /troubleshooting
30-Jul-17				Sandy Lake, ON	Testing /troubleshooting
31-Jul-17				Sandy Lake, ON	Waiting for client to review data
1-Aug-17				Sandy Lake, ON	Waiting for client to review data
2-Aug-17				Sandy Lake, ON	No production due to weather
3-Aug-17	1, 2, 217, A2			Sandy Lake, ON	217km flown
4-Aug-17	3, 37, A2			Sandy Lake, ON	37km flown
5-Aug-17				Sandy Lake, ON	No production due to technical issues
6-Aug-17				Sandy Lake, ON	No production due to technical issues
7-Aug-17				Sandy Lake, ON	No production due to technical issues
8-Aug-17	4, 22, A2			Sandy Lake, ON	22km flown
9-Aug-17				Sandy Lake, ON	
10-Aug-17				Sandy Lake, ON	
11-Aug-17				Sandy Lake, ON	
12-Aug-17				Sandy Lake, ON	
13-Aug-17				Sandy Lake, ON	
14-Aug-17				Sandy Lake, ON	
15-Aug-17				Sandy Lake, ON	
16-Aug-17	214	159	A1	Sandy Lake, ON	1st system testing was completed and is approved for production, no production flights due to weather. 159km flown with 2nd system. Limited production due to weather.
17-Aug-17				Sandy Lake, ON	No production for either system due to weather, rain and thunderstorms.
18-Aug-17	16, 17, 215, 216	403	A1	Sandy Lake, ON	403km flown.
19-Aug-17	18, 19	271	A1	Sandy Lake, ON	271km flown. Second system had a technical issue which was resolved mid-afternoon. No production was possible due to strong gusty winds.
20-Aug-17				Sandy Lake, ON	No production due to weather, rain turning to sting gusty winds in the afternoon.
21-Aug-17				Sandy Lake, ON	No production due to weather, strong gusty winds throughout the day.

Date	Flight #	Flown km	Block	Crew location	Comments
22-Aug-17				Sandy Lake, ON	No production due to weather, low ceiling and rain throughout the day.
23-Aug-17	20, 21, 22, 217, 218, 219	730	A1	Sandy Lake, ON	730km flown
24-Aug-17	23, 24, 220, 221, 222	574	A1	Sandy Lake, ON	574km flown
25-Aug-17	25, 26, 27	321	A1	Sandy Lake, ON	321km flown. No production with second system due to helicopter technical issues, parts were ordered and arrived.
26-Aug-17	28, 223, 224, 225	452	A1	Sandy Lake, ON	Limited production due to scheduled helicopter maintenance with first system. 452km flown.
27-Aug-17				Sandy Lake, ON	No production due to rain and low ceiling throughout the day.
28-Aug-17	226, 227	191	A1	Sandy Lake, ON	191km flown. No further flights could be performed due to weather, strong gusty winds
29-Aug-17	29, 228	133	A1	Sandy Lake, ON	Late start due to rain in the morning, 133km flown. Flights were cut short due to heavy smoke/haze from nearby Manitoba forest fires.
30-Aug-17	30, 31, 229, 230	489	A1	Sandy Lake, ON	489km flown. No further production due to high winds and low ceilings.
31-Aug-17	32, 231	168	A1	Sandy Lake, ON	168km flown, limited production due to active magnetic diurnal in the morning and high winds in the afternoon.
1-Sept-17				Sandy Lake, ON	With permission from the community the crew performed calibration testing in preparation for the break in the survey.
2-Sept-17				Sandy Lake, ON	Demob commenced, crew started disassembly of the two VTEM systems and arrangements were made for local storage.
3-Sept-17				Sandy Lake, ON	Disassembly was completed
4-Sept-17				Sandy Lake, ON	Systems were moved into storage and final packing/ preparations for storage were started.
5-Sept-17				Sandy Lake, ON	Crew will finalize packing and storage of the system and demobilize from Sandy Lake.
6-Sept-17				Sandy Lake, ON	Crew will fly out of Sandy Lake
7-Sept-17					Survey break due to hunting season.
8-Dec-17				Sandy Lake, ON	Crew mobilized to Sandy Lake.
9-Dec-17				Sandy Lake, ON	Unpack storage; commence VTEM15 assembly, aircraft arrival.
10-Dec-17				Sandy Lake, ON	Continue VTEM15 assembly, continue to unpack storage.
11-Dec-17				Sandy Lake, ON	Set up mag and gps bases, 1 mag base will require troubleshooting. Completed loop assembly.
12-Dec-17				Sandy Lake, ON	Mag sensor replaced, heli install completed. Spares and radar parts shipped from the office. Rented generator to heat the heli while at airport.
13-Dec-17				Sandy Lake, ON	Crew arrived and waited for Morning prayer/Elder Blessing no elders arrived, alternate date and time has yet to be scheduled, begin system testing.
14-Dec-17				Sandy Lake, ON	Continued with system testing, few completed due to low ceilings will continue tomorrow.
15-Dec-17				Sandy Lake, ON	Elders Blessing in the morning. Late start due to temperatures below aircraft limitations, continued with system testing. Submitted previous days test for MNDM review.
16-Dec-17				Sandy Lake, ON	Standby for data review.
17-Dec-17				Sandy Lake, ON	Began troubleshooting, test flights completed.
18-Dec-17				Sandy Lake, ON	Continue troubleshooting, performed test flights.
19-Dec-17				Sandy Lake, ON	No testing due to weather, strong winds and low ceilings throughout the day.
20-Dec-17				Sandy Lake, ON	Completed system testing.
21-Dec-17				Sandy Lake, ON	Test data submitted for approval. Low ceiling and temp below aircraft limitations in the morning, completed recon of Favourable Lake block in the afternoon, located possible fuel cache. Test data approved. Equipment prepared for storage for the break.
22-Dec-17				Sandy Lake, ON	Crew to demob from Sandy Lake.
23-Jan-18				Sandy Lake, ON	Continued testing and troubleshooting. Arrival of 2nd aircraft delayed due to weather.
3-Jan-18				Sandy Lake, ON	First crew arrived in Sandy Lake.

Date	Flight #	Flown km	Block	Crew location	Comments
4-Jan-18				Sandy Lake, ON	Coordinate local logistics. Unpack storage, set up bases.
5-Jan-18				Sandy Lake, ON	No production due to temperature below aircraft limitations. Unpacked storage, commenced assembly on VTEM07.
6-Jan-18	33	38	A1	Sandy Lake, ON	Short production flight completed in the morning, 38km flown, no further production due to strong winds. Continued assembly on VTEM07.
7-Jan-18				Sandy Lake, ON	No production due to snow and low ceilings. Continued assembly on VTEM07.
8-Jan-18	34	38	A1	Sandy Lake, ON	Standby in the morning due to high winds and low ceilings, 38km flown. Continued assembly on VTEM07.
9-Jan-18	35, 36	383	A1	Sandy Lake, ON	383km flown. Continued assembly on VTEM07.
10-Jan-18				Sandy Lake, ON	No flights due to weather, snow and low ceilings throughout the day. Continued assembly on VTEM07.
11-Jan-18				Sandy Lake, ON	No flights due to aircraft limitations.
12-Jan-18				Sandy Lake, ON	No flights due to aircraft limitations.
13-Jan-18	37	172	A1	Sandy Lake, ON	172km flown
14-Jan-18	38, 39	147	A1	Sandy Lake, ON	147km flown
15-Jan-18	40	63	A1	Sandy Lake, ON	Late start due to aircrafts weather limitations, 63km flown.
16-Jan-18	41	151	A1	Sandy Lake, ON	Late start due Heli maintenance, 151km flown. Heli maintenance on the Koala to be completed.
17-Jan-18				Sandy Lake, ON	Koala maintenance.
18-Jan-18				Sandy Lake, ON	Koala maintenance, Expedition helicopters arrived in Sandy Lake.
19-Jan-18				Sandy Lake, ON	Completed Heli Install, no testing due to weather, fog and low ceiling throughout the day.
20-Jan-18				Sandy Lake, ON	Commence system testing.
21-Jan-18				Sandy Lake, ON	Some troubleshooting required on system in the morning. Continued testing.
22-Jan-18				Sandy Lake, ON	Continued testing and troubleshooting.
23-Jan-18				Sandy Lake, ON	Continued testing and troubleshooting. Arrival of 2nd aircraft delayed due to weather.
24-Jan-18				Sandy Lake, ON	Completed testing, replacement aircraft to arrive tomorrow. 2nd aircraft arrived in Sandy Lake.
25-Jan-18				Sandy Lake, ON	Replacement aircraft arrived in Sandy lake. Completed install on 2nd aircraft, began testing.
26-Jan-18				Sandy Lake, ON	Completed install on replacement aircraft, limited testing on both systems due to weather.
27-Jan-18				Sandy Lake, ON	Continued some system tests, unable to complete test flights due to weather, low ceilings.
28-Jan-18				Sandy Lake, ON	Low ceilings throughout the day. Completed ground testing on VTEM07, tree strike occurred while moving system to complete calibration causing minor damage, repairs on system completed.
29-Jan-18				Sandy Lake, ON	Late start due to weather. Completed testing on VTEM15. Continued testing on VTEM07.
30-Jan-18				Sandy Lake, ON	Complete testing VTEM07, await data approval.
31-Jan-18				Sandy Lake, ON	No production due to weather.
1-Feb-18	42, 43, 232	435	A1	Sandy Lake, ON	Late start due to cold temperatures, 435km flown.
2-Feb-18	44, 45, 233, 234	588	A1	Sandy Lake, ON	Late start due to weather, 588km flown.
3-Feb-18	46, 47, 235, 236	558	A1	Sandy Lake, ON	558km flown
4-Feb-18	237	21	A1	Sandy Lake, ON	21km flown. No further production due to weather, high winds and low ceilings throughout the day.
5-Feb-18	238, 239	358	A1	Sandy Lake, ON	358km flown. VTEM15 attempted lines on Favorable Lake before tree strike occurred; system returned to airport and began loop reconstruction.
6-Feb-18	48, 240	166	A1, A2	Sandy Lake, ON	166km flown. Set up fuel cache at Favorable lake, began lines on Favorable Lake block.
7-Feb-18	49, 50, 241, 242, 243	407	A1, A2	Sandy Lake, ON	407km flown. Completed Sandy Lake block.
8-Feb-18	51, 52, 53, 244, 245	523	A2	Sandy Lake, ON	523km flown.
9-Feb-18				Sandy Lake, ON	No production due to weather, high winds throughout the day.
10-Feb-18	54, 55, 246	319	A2	Sandy Lake, ON	319km flown.

Date	Flight #	Flown km	Block	Crew location	Comments
11-Feb-18	247	124	A2	Sandy Lake, ON	Minor system repairs required and completed to VTEM15 then performed test flight in the morning. 124km flown with VTEM07. No further flights due to weather, high winds.
12-Feb-18	248	73	A2	Sandy Lake, ON	73km flown. No further production due to weather, high winds throughout the day.
13-Feb-18				Sandy Lake, ON	No production due to weather, high winds throughout the day.
14-Feb-18				Sandy Lake, ON	No production due to weather, high winds and low ceilings throughout the day.
15-Feb-18	249, 250	364	A2	Sandy Lake, ON	364km flown.
16-Feb-18	251, 252	291	A2	Sandy Lake, ON	291km flown. Tree strike on VTEM15 during flight, causing minor damage, repairs on system began.
17-Feb-18	253, 254	233	A2	Sandy Lake, ON	233km flown. Completed repairs on system, completed test flight.
18-Feb-18	56, 57, 255, 256, 257	457	A2	Sandy Lake, ON	Some troubleshooting was required and completed on VTEM15 in the morning, production in the afternoon. 457km flown.
19-Feb-18	58, 59, 258, 259	271	A2	Sandy Lake, ON	Late start due to temperature below aircraft operating limit. 271km flown.
20-Feb-18	60, 61, 260	300	A2	Sandy Lake, ON	300km flown. No further flights due to weather.
21-Feb-18	62, 63, 261	182	A2	Sandy Lake, ON	182km flown. Flights were cut short in the afternoon due high gusting winds, some maintenance on VTEM15 required. No further flights due to weather, high winds.
22-Feb-18				Sandy Lake, ON	Production was attempted in the morning but aborted due to very high winds, no flights for the day due to weather. Continued with loop maintenance.
23-Feb-18	262, 263	245	A2	Sandy Lake, ON	245km flown. Continued with loop maintenance.
24-Feb-18				Sandy Lake, ON	Attempted production but aborted due to strong winds, no further flights due to weather. Continued with loop maintenance.
25-Feb-18				Sandy Lake, ON	Attempted production but aborted due to low visibility, no further flights due to weather. Continued with loop maintenance.
26-Feb-18	264, 265, 266	352	A2	Sandy Lake, ON	352km flown. Began testing VTEM15.
27-Feb-18	267	144	A2	Sandy Lake, ON	144km flown, no further flights due to low ceilings. Continued testing and troubleshooting on VTEM15
28-Feb-18	268, 269, 270	199	A2	Sandy Lake, ON	199km flown. Continued troubleshooting on VTEM15.
1-Mar-18	271, 272, 273	505	A2	Sandy Lake, ON	505km flown. Continued troubleshooting on VTEM15.
2-Mar-18				Sandy Lake, ON	Crew on Standby due to logistical issues with motel.
3-Mar-18				Red Lake, ON	Crew mobilized to Red lake.
4-Mar-18				Red Lake, ON	Complete local logistics and operational issues from new base.
5-Mar-18				Red Lake, ON	No production due to weather, high winds throughout the day. Completed maintenance on VTEM15.
6-Mar-18	274	152	A2	Red Lake, ON	152km flown. Completed testing on VTEM15.
7-Mar-18				Red Lake / Sandy Lake, ON	No production due to weather, low ceilings and poor visibility throughout the day. 2 crew members return to Sandy Lake with current availability, other members continue to operate from Red Lake.
8-Mar-18	275, 276	288	A2	Red Lake / Sandy Lake, ON	288km flown. Completed test flight with VTEM15. Edna arrived in Red Lake, travelled to Sandy Lake with crew to complete site/operations visit.
9-Mar-18	277, 278	349	A2	Red Lake / Sandy Lake, ON	349km flown. Edna departed Red Lake. VTEM15 will be reassembled.
10-Mar-18	279, 280	398	A2	Red Lake / Sandy Lake, ON	398km flown.
11-Mar-18				Red Lake / Sandy Lake, ON	Troubleshooting VTEM07 in the morning, later repositioned aircraft to Red Lake to begin 100hr inspection. Begin disassembly on VTEM15.
12-Mar-18				Red Lake / Sandy Lake, ON	Completed 100hr inspection on aircraft. Completed disassembly on VTEM15.

Date	Flight #	Flown km	Block	Crew location	Comments
13-Mar-18				Red Lake / Sandy Lake, ON	Mob to Sandy Lake, production attempted but aborted due to high winds. Started re-building on VTEM15.
14-Mar-18				Red Lake / Sandy Lake, ON	Troubleshoot and testing of VTEM07. Continue re-building on VTEM15.
15-Mar-18	281, 282	180	A2	Red Lake / Sandy Lake, ON	180km flown. Completed re-building VTEM15.
16-Mar-18	283, 284, 285	5	A2	Red Lake / Sandy Lake, ON	5km flown due to data collection issue.
17-Mar-18	286	215	A2	Sandy Lake, ON	215km flown. No further production due to weather, low ceilings.
18-Mar-18	287, 288	376	A2	Sandy Lake, ON	376km flown
19-Mar-18	289, 290	13	A2	Sandy Lake, ON	Completed final tie line and post survey test flights (VTEM07), 13km flown. Flight path completed.
20-Mar-18				Red Lake, ON	Collected fuel drums from fuel cache locations, packed gps and mag base stations, organized storage. Crew, A/C and VTEM07 mobilized to Red Lake. Ran GPS static test on VTEM07 overnight, base stations re-positioned in Red Lake.
21-Mar-18				Red Lake, ON	Completed static test on VTEM07 early morning and uploaded for review, VTEM07 testing completed. Switchover system/equipment to VTEM15 and began post survey testing.
22-Mar-18				Red Lake, ON	Continued VTEM15 post survey testing, VTEM07 approved for demob.
23-Mar-18				Red Lake, ON	Continued VTEM15 post survey testing, troubleshooting Y-coil data.
24-Mar-18				Red Lake, ON	Completed post survey testing on VTEM15, demob approval received
25-Mar-18				Sandy Lake, ON	Aircraft demob from Red Lake, operators travel to Sandy Lake to prepare storage items for shipping.
26-Mar-18				Red Lake / Sandy Lake, ON	Shipped storage items out of Sandy Lake, crew demob from Sandy lake.
27-Mar-18				Red Lake, ON	Continue demob from Red Lake.

3. Survey Area Geology

The following description of the regional geology of the area is drawn partly from Satterly (1938) and Stone (1998). The area is largely underlain by the Archean Sandy Lake and Favourable Lake greenstone belts which are located in the Sachigo Subprovince.

The Sandy Lake greenstone belt (Figure 4) has an east to west extent of approximately 70 km and bifurcates at the western end. The greenstone belt comprises sequences of metavolcanic and metasedimentary rocks. Gabbro sills are intruded along the southern parts of the belt and oxide iron formations are present in the eastern end of the belt. Shear zones with dextral offset, extending nearly the entire length of the belt, have been mapped. Gold and a few copper showings, located in the northwestern and eastern parts of the belt, have been known since the area was first mapped in the 1930s.

The Favourable Lake greenstone belt (*see* Figure 4) is oriented approximately northwest to southeast and extends 110 km in a southeasterly direction from the Manitoba border to join the North Spirit Lake greenstone belt. The greenstone belt is generally narrow and ranges in width from about 2 to 13 km. The geology consists of metavolcanic and metasedimentary rocks. The metavolcanic rocks are mafic to felsic in composition and the metasedimentary rocks range in composition from argillite, through sandstones and conglomerates. Numerous gold, silver and copper occurrences within the metavolcanic rocks have been documented in the southeastern part of the Favourable Lake greenstone belt. Most notable are the No. 1 and 3 veins which were mined between 1939 and 1948, producing 158,000 ounces of gold and 5.8 million ounces of silver.

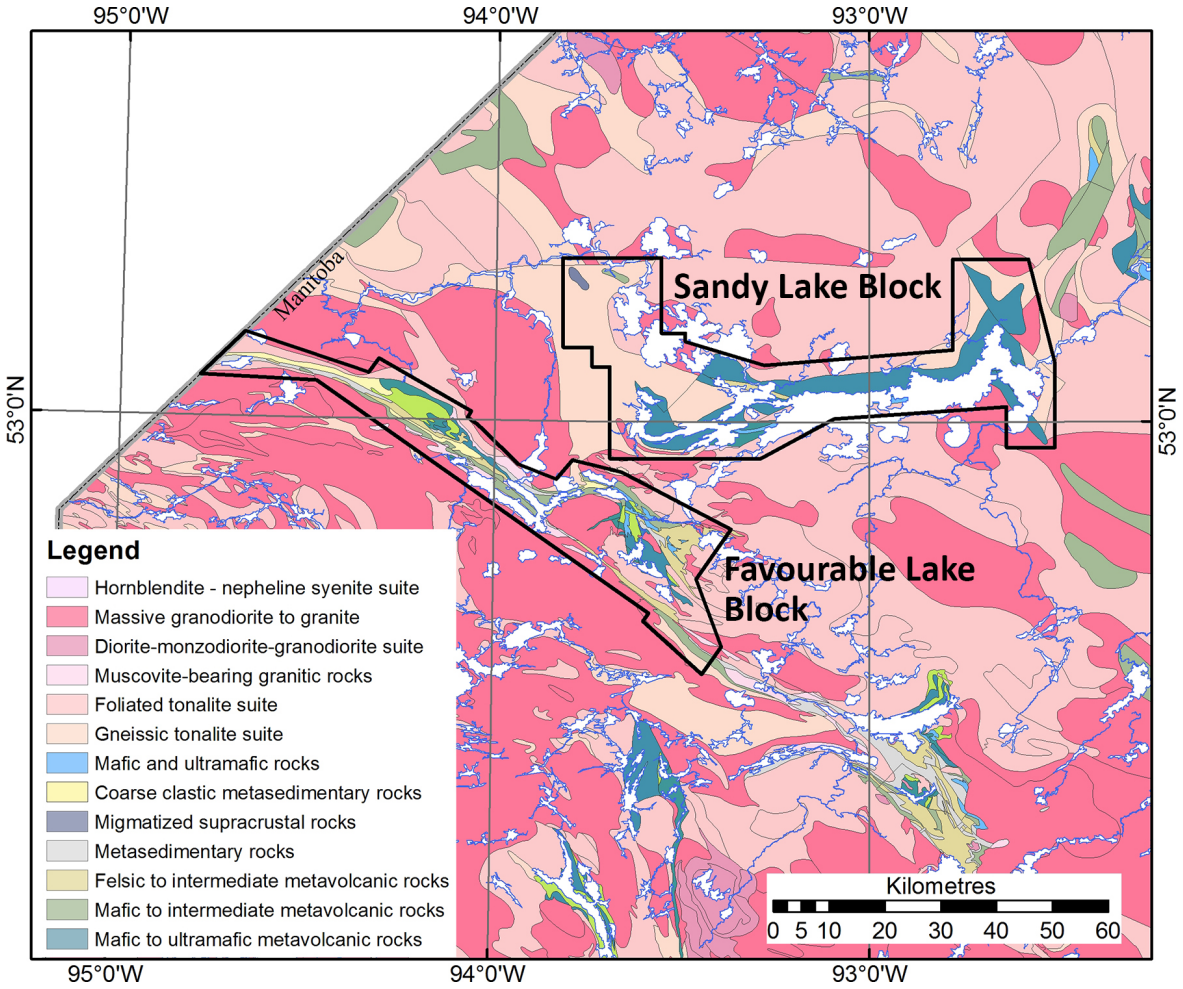

Figure 4. Sandy Lake–Favourable Lake geophysical survey area outlined on map of simplified bedrock geology of the area, northwest Ontario (*from* Ontario Geological Survey 2011).

4. Aircraft, Equipment and Personnel

4.1. FLIGHT LOGISTICS

During the survey, the helicopter was maintained at a mean altitude of 94.6 m above the ground with an average survey speed of 80 km/hour. This allowed for an average EM bird terrain clearance of 43 m and a magnetic sensor clearance of 52 m.

The on-board operator was responsible for monitoring the system integrity. He also maintained a detailed flight log during the survey, tracking the times of the flight as well as any unusual geophysical or topographic features.

Upon return to base camp, the survey data were transferred from a compact flash card (PCMCIA) to the data processing computer. The data were then uploaded via ftp to the Geotech office in Aurora for daily quality assurance and quality control by qualified personnel.

4.2. AIRCRAFT AND EQUIPMENT

4.2.1. SURVEY AIRCRAFT

The survey was flown using a Eurocopter Aerospatiale (Astar) 350 B3 helicopter, registration C-FKOI and C-FBZN. The helicopter is owned and operated by Geotech Aviation. Installation of the geophysical and ancillary equipment was carried out by Geotech Ltd crew.

4.2.2. ELECTROMAGNETIC SYSTEM

The electromagnetic system was a Geotech Time Domain EM (VTEM®Plus) with full receiver-waveform streamed data recording at 192 kHz. The full waveform VTEM system uses the streamed half-cycle recording of transmitter and receiver waveforms to obtain a complete system response calibration throughout the entire survey flight. VTEM with the Serial number 07 and 15 had been used for the survey. The configuration is as indicated in Figure 6.

The VTEM Receiver and transmitter coils were in concentric-coplanar and Z-direction oriented configuration. The receiver system for the project also included coincident-coaxial X-direction and Y-direction coils to measure the in-line and off-line dB/dt, respectively, and calculate B-Field responses. The EM bird was towed at a mean distance of 42.6 m below the aircraft as shown in Figure 6 and Figure **7**. The VTEM transmitter current waveform is shown diagrammatically in Figure 5. The receiver decay recording scheme is shown in Table 3.

The VTEM decay sampling scheme is shown in Table 3 below. Forty-three time measurement gates were used for the final data processing in the range from 0.021 to 8.083 msec. Zero time for the off-time sampling scheme is equal to the current pulse width and is defined as the time near the end of the turn-off ramp where the dI/dt waveform falls to 1/2 of its peak value.

Table 3. VTEM decay sampling scheme (Milliseconds) – X, Y.

index	Start	End	Middle	Width
20	0.206	0.236	0.220	0.030
21	0.236	0.271	0.253	0.035
22	0.271	0.312	0.290	0.040
23	0.312	0.358	0.333	0.046
24	0.358	0.411	0.383	0.053
25	0.411	0.472	0.440	0.061
26	0.472	0.543	0.505	0.070
27	0.543	0.623	0.580	0.081
28	0.623	0.716	0.667	0.093
29	0.716	0.823	0.766	0.107
30	0.823	0.945	0.880	0.122
31	0.945	1.086	1.010	0.141
32	1.086	1.247	1.161	0.161
33	1.247	1.432	1.333	0.185
34	1.432	1.646	1.531	0.214
35	1.646	1.891	1.760	0.245
36	1.891	2.172	2.021	0.281
37	2.172	2.495	2.323	0.323
38	2.495	2.865	2.667	0.370
39	2.865	3.292	3.063	0.427
40	3.292	3.781	3.521	0.490

index	Start	End	Middle	Width
41	3.781	4.341	4.042	0.560
42	4.341	4.987	4.641	0.646
43	4.987	5.729	5.333	0.742
44	5.729	6.581	6.125	0.852
45	6.581	7.560	7.036	0.979
46	7.560	8.685	8.083	1.125

Table 4. VTEM decay sampling scheme (Milliseconds) – Z.

index	Start	End	Middle	Width
4	0.018	0.023	0.021	0.005
5	0.023	0.029	0.026	0.005
6	0.029	0.034	0.031	0.005
7	0.034	0.039	0.036	0.005
8	0.039	0.045	0.042	0.006
9	0.045	0.051	0.048	0.007
10	0.051	0.059	0.055	0.008
11	0.059	0.068	0.063	0.009
12	0.068	0.078	0.073	0.010
13	0.078	0.090	0.083	0.012
14	0.090	0.103	0.096	0.013
15	0.103	0.118	0.110	0.015
16	0.118	0.136	0.126	0.018
17	0.136	0.156	0.145	0.020
18	0.156	0.179	0.167	0.023
19	0.179	0.206	0.192	0.027
20	0.206	0.236	0.220	0.030
21	0.236	0.271	0.253	0.035
22	0.271	0.312	0.290	0.040
23	0.312	0.358	0.333	0.046
24	0.358	0.411	0.383	0.053
25	0.411	0.472	0.440	0.061
26	0.472	0.543	0.505	0.070
27	0.543	0.623	0.580	0.081
28	0.623	0.716	0.667	0.093
29	0.716	0.823	0.766	0.107
30	0.823	0.945	0.880	0.122
31	0.945	1.086	1.010	0.141
32	1.086	1.247	1.161	0.161
33	1.247	1.432	1.333	0.185
34	1.432	1.646	1.531	0.214
35	1.646	1.891	1.760	0.245
36	1.891	2.172	2.021	0.281
37	2.172	2.495	2.323	0.323
38	2.495	2.865	2.667	0.370
39	2.865	3.292	3.063	0.427
40	3.292	3.781	3.521	0.490
41	3.781	4.341	4.042	0.560
42	4.341	4.987	4.641	0.646
43	4.987	5.729	5.333	0.742
44	5.729	6.581	6.125	0.852
45	6.581	7.560	7.036	0.979
46	7.560	8.685	8.083	1.125

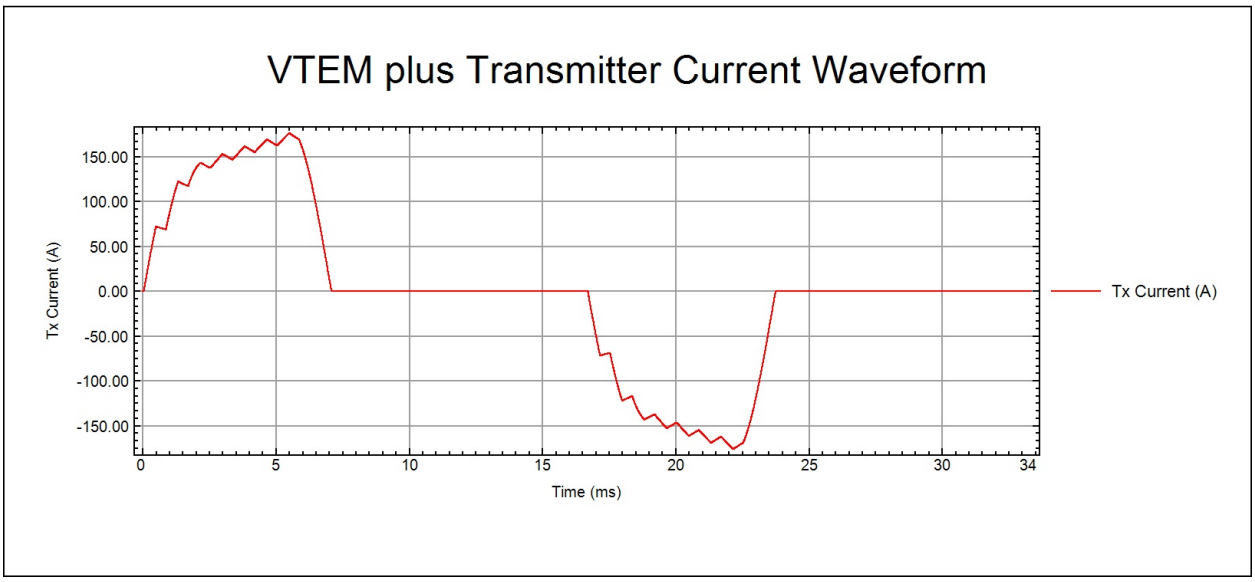

Figure 5. VTEM current waveform.

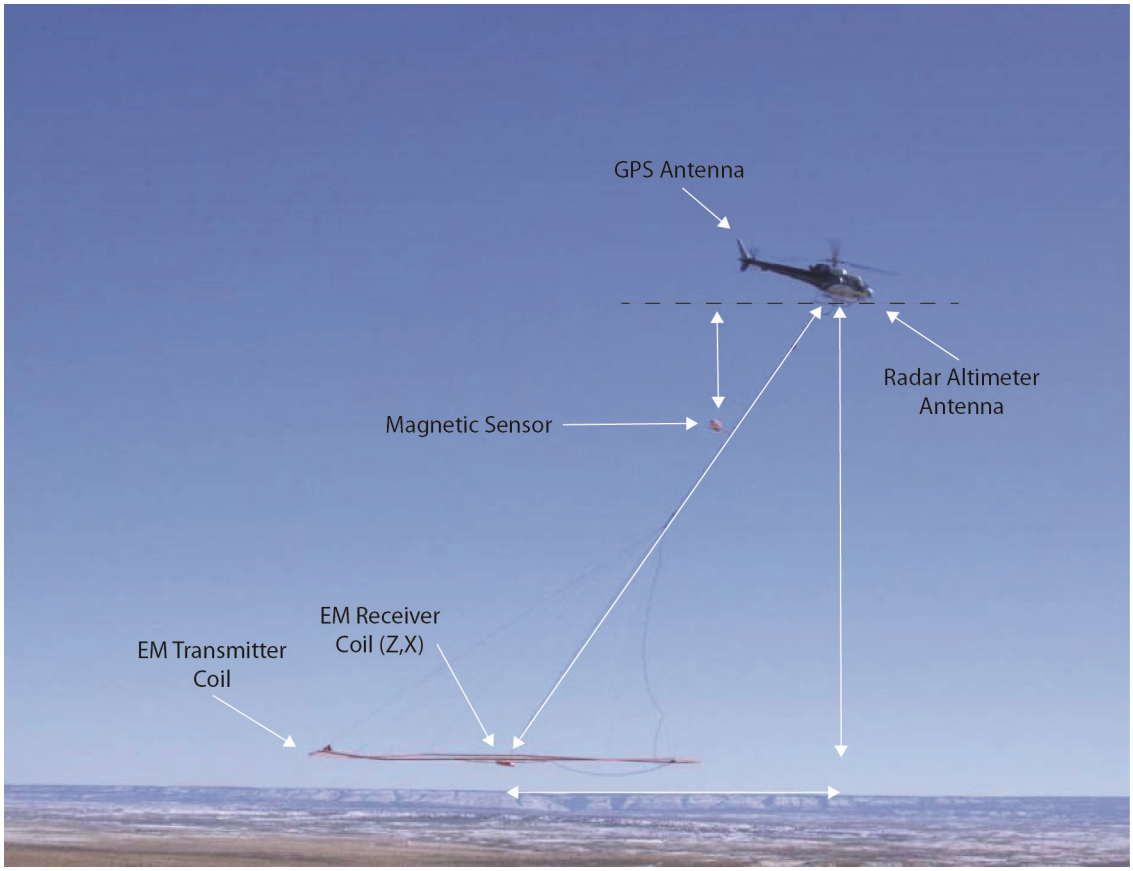

Figure 6. VTEM®Plus configuration, with magnetometer.

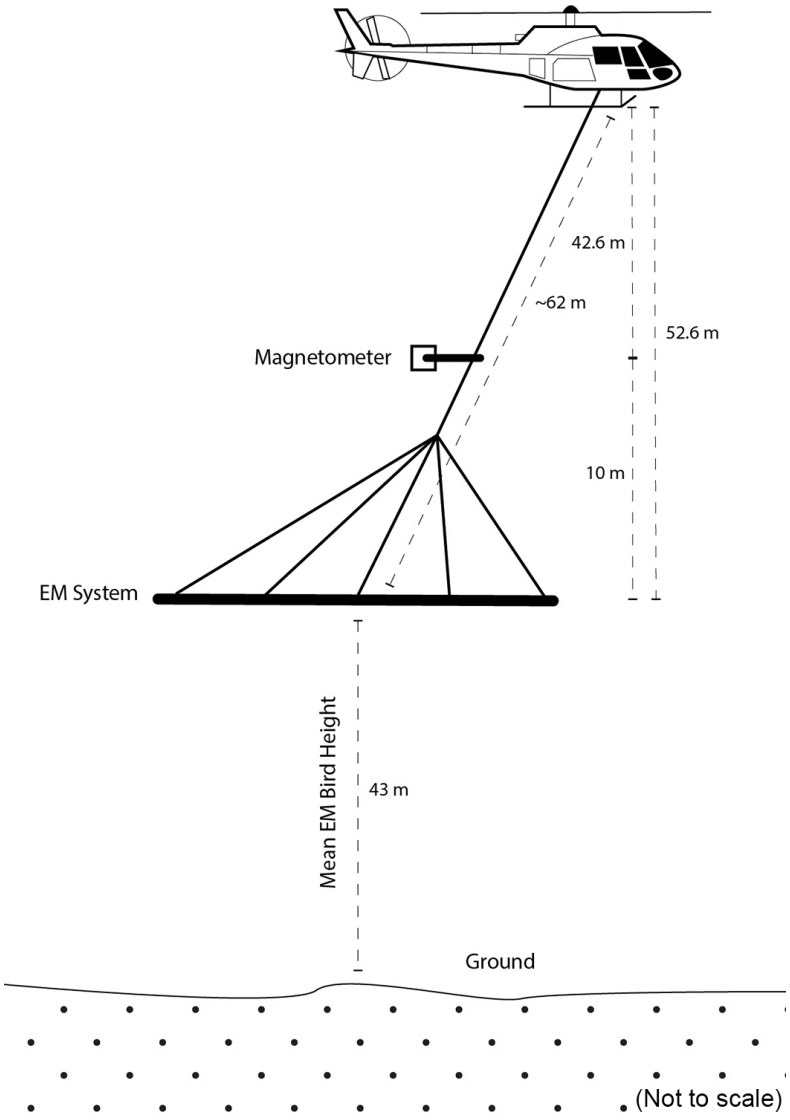

Figure 7. VTEM® Plus system configuration.

4.2.3. VTEM® PLUS SYSTEM SPECIFICATION

- Transmitter
- Transmitter loop diameter: 26 m
- Effective transmitter loop area: 2123.7 m^2
- Number of turns: 4
- Transmitter base frequency: 30 Hz
- Peak current: 172.6 A
- Pulse width: 7.047 ms
- Wave form shape: trapezoid
- Peak dipole moment: 395 967 nIA
- Average EM Bird terrain clearance: 43 m above the ground

Receiver

- X and Y Coil diameter: 0.32 m
- Number of turns: 245
- Effective coil area: 19.69 m^2
- Z-Coil diameter: 1.2 m
- Number of turns: 100
- Effective coil area: 113.04 m^2

4.2.4. AIRBORNE MAGNETOMETER

The magnetic sensor utilized for the survey was a Geometrics® Model G822A optically pumped cesium-vapour magnetic field sensor mounted 42.6 m below the helicopter, as shown in Figure 7. The sensitivity of the magnetic sensor is 0.001 nanotesla (nT) at a sampling interval of 0.1 seconds.

4.2.5. RADAR ALTIMETER

A Terra TRA 3000/TRI 40 radar altimeter was used to record terrain clearance. The antenna was mounted beneath the bubble of the helicopter cockpit (*see* Figure 7).

4.2.6. DIGITAL ACQUISITION SYSTEM

A Geotech data acquisition system recorded the digital survey data on an internal compact flash card. Data are displayed on an LCD screen as traces to allow the operator to monitor the integrity of the system. The data type and sampling interval as provided in Table 5.

Table 5. Acquisition sampling rates.

Data Type	Sampling
TDEM	0.1 sec
Magnetometer	0.1 sec
GPS Position	0.1 sec
Radar Altimeter	0.2 sec

4.2.7. BASE STATION MAGNETOMETER

A dedicated computer connected to a high sensitivity Geometrics® G822B cesium magnetometer and integrated GPS unit, for the accurate time synchronization, was employed to record magnetic activity. The magnetometer had a sensitivity of better than 0.01 nT at a sampling interval of 0.1 s. Digital data from the base station magnetometer were recorded at all times during the survey. The digital data included the date, an absolute magnetic value, and GPS time with accurate synchronization to the aircraft data acquisition system.

The Base Mag1 (July) station magnetometer sensor was installed at 53° 4'43.76"N, 93°23'11.55"W, Base Mag2 (July) at 53° 4'3.49"N, 93°21'16.40"W, Base Mag1 (December) at 53° 4'21.65"N, 93°23'12.62"W and Base Mag2 (December) at 53° 3'47.29"N, 93°21'16.74"W away from electric transmission lines and moving metal (iron) objects such as motor vehicles. The base station data were backed-up to the data processing computer at the end of each survey day.

4.2.8. GPS GROUND BASE STATION

A dedicated Novatel® ProPak™ V3-RT2-G WAAS GPS receiver and ground-based GPS antenna was used with a 0.1 s raw GPS data recording interval. Post-flight differential GPS data processing, utilizing Novatel® GrafNav 8.3 software, was used to produce sub-meter accuracy of the airborne system location at 10 Hz sampling interval. The GPS ground base station was positioned at each survey base of operations and setup in the same vicinity as the base station magnetometer.

4.2.9. GPS NAVIGATION SYSTEM

The navigation system used a Geotech PC104 based navigation system utilizing the NovAtel WAAS (Wide Area Augmentation System) enabled GPS receiver, Geotech navigation software, a full screen display with controls in front of the pilot to direct the flight and a NovAtel GPS antenna mounted on the helicopter tail (*see* Figure 6). As many as 11 GPS and 2 WAAS satellites may be monitored at any one time. The positional accuracy or circular error probability (CEP) is 1.8 m, with WAAS active, it is 1.0 m. The co-ordinates of the regional AEM survey were set-up prior to the survey and the information was fed into the airborne navigation system.

4.3. PERSONNEL

The following personnel were involved with the survey.

Field

Project Manager:	Darren Tuck (Office) Shauna-lee Hewitt (Office)
Data QC:	Neil Fiset (Office) Nick Venter (Office) Shei (Office) Shauna-lee Hewitt (Office) Kanita Khaled (Office)
Crew chief:	Paul Taylor Juan Carlos Osorio
Operator:	Matthew Dyer Emil Simanian Kirill Golubev Roberto Di Bari
Pilot:	Andre Vandrie Walter Zec Gord Bean Rob Girard
Mechanical Engineer:	Charles Picard

The survey pilot and the mechanical engineer were employed directly by the helicopter operator, Geotech Aviation.

Office

Preliminary Data Processing:	Neil Fiset Nick Venter
Interim Data Processor:	Keeme Mokubung Dmitriy Danchenko Zihao Han Nikolas Gazo
Supervisor of Data QC:	Alexander Prikhodko, P.Geo Kanita Khaled
Reporting/Mapping:	Joseli Soares

The data acquisition phase was carried out under the supervision of Alexander Prikhodko, P.Geo, PhD, and Director of Geophysics. The processing and interpretation phase was under the supervision of Alexander Prikhodko, P.Geo, PhD, and Director of Geophysics. Customer relations were looked after by David Hitz.

5. Data Processing

Data compilation and processing were carried out using Geosoft OASIS montaj® and programs proprietary to Geotech Ltd.

5.1. FLIGHT PATH

The flight path, recorded by the data acquisition program as WGS 84 latitude/longitude datum and co-ordinate system, was converted to NAD83, UTM Zone 15 North co-ordinate system in Oasis montaj®.

The flight path was drawn using linear interpolation between x, y positions from the navigation system. Positions are updated every second and expressed as UTM easting (x) and UTM northing (y).

5.2. ELECTROMAGNETIC DATA

As the data were acquired by the data acquisition system on the helicopter, they go through a digital filter to reject major sferic events and are stacked to further reduce system noise. Afterward, the streamed data are processed by applying a system response correction, B-field integration, time window binning, compensation, filtering, and leveling.

The Full Waveform EM specific data processing operations included:

- Half cycle stacking (performed at time of acquisition);
- System response correction;
- Parasitic and drift removal

The digital filtering process is a three-stage filter used to reject major sferic events and reduce system noise. Local sferic activity can produce sharp, large-amplitude events that cannot be removed by conventional filtering procedures. Smoothing or stacking will reduce their amplitude but leave a broader residual response that can be confused with geological phenomena. To avoid this possibility, a computer algorithm searches out and rejects the major sferic events. The data was then stacked using 18 half cycles, 0.3 seconds, to create a calibration file consisting of a single stacked half-cycle waveform at 0.1 second intervals. The stacking coefficients are tapered with a shape that approximates a Gaussian function. The purpose of the stacking is to attenuate natural and man-made signals.

During post-flight processing, the streamed data have a sensor response correction applied which corrects the receiver channels and current monitor to a common impulse response based on the Full Waveform Calibration. The B-field data are calculated by integrating the dB/dt cycles from the 192 kHz streamed data. The streamed data are then converted into a set of time window channels to reduce noise levels further.

The data have noise levels reduced further by the use of an EM compensation procedure which removes characteristic noise from each fiducial determined by the difference between the transmitter and bucking loop fields at the receiver during the flight. This is achieved by a statistical correlation between each time window channel and the primary field measurement taken during the on-time.

Next, filtering of the electromagnetic data was performed in 2 steps. The first is a 4 fiducial wide, non-linear filter to eliminate any large spikes remaining in the dataset. The second filter is a low-pass, symmetric, linear, digital filter that has zero phase-shift which prevents any lag or peak displacement from occurring, and it suppresses only variations with a wavelength less than about 1 second or 25 metres.

The VTEM system has 3 receiver coil orientations: X, Y and Z. Generalized modelling results of the VTEM system are shown in Appendix I.

A parallax correction was applied to the EM data to account for the distance by which the EM transmitter-receiver loop lags behind GPS. In this parallax correction the EM data are adjusted by the nearest integer number of fiducials that it would take to travel the horizontal distance from the center of the loop to the GPS.

The Z-axis receiver coil was oriented parallel with the transmitter coil axis and both were horizontal to the ground. The Z-component data produce double peak type anomalies for “thin” sub vertical targets and single peak anomalies for “thick” targets. The limits and changeover of “thin-thick” depends on dimensions of the TEM system (Appendix I).

The X-axis coil is oriented parallel with the ground and along the line-of-flight. The Y-axis coil is oriented parallel with the ground and perpendicular to the line-of-flight. The combination of the X and Z coils configuration provides information on the position, depth, dip and thickness of a conductor.

The X-component data produce cross-over type anomalies: from “+ to – ” in flight direction of flight for “thin” sub vertical targets and from “- to +” in direction of flight for “thick” targets.

Because the X component polarity is dependent on flight line direction, a convolution Fraser Filter (FF) (middle panel in Figure 8) is applied to X component. In this case, positive FF anomalies always correspond to “plus-to-minus” X data crossovers independent of the flight direction.

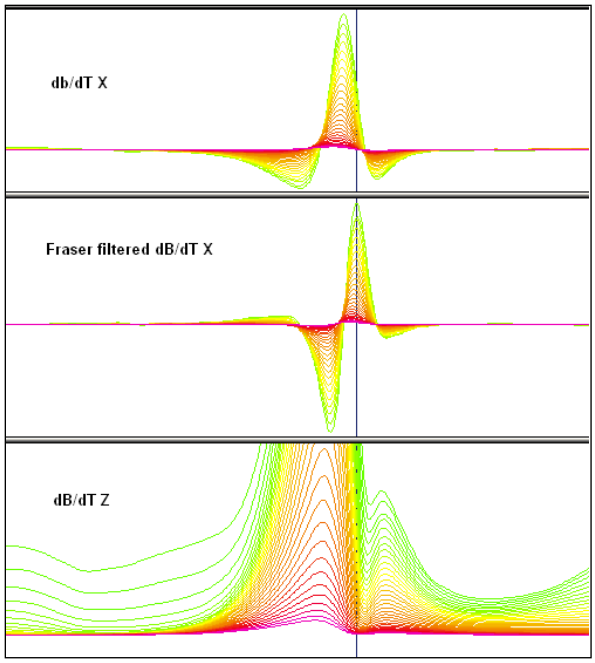

Figure 8. The Z, X and Fraser filtered X (FFx) components for "thin" target.

5.3. CONDUCTIVITY DEPTH IMAGING (CDI)

A set of conductivity depth images (CDI) were generated using Geotech in-house CDI algorithm, developed by Geotech Ltd. A total of 43 dB/dt Z-component channels, starting from channel 4 (21 µsec) to channel 46 (8685 µsec), were used for the CDI calculation for the data.

The used CDI algorithm is based on scheme of the apparent resistivity transform of Maxwell (Meju 1998) and TEM response from conductive half-space. The software was developed by Geotech and depth calibrated based on forward plate modelling for VTEM system configuration. For more information on the CDI algorithm refer to Appendix K.

The apparent conductivity and depth information for the survey area was visualized in 3D space in the form of a Geosoft Voxel. The apparent conductivity Voxel has its depth relative to surface of the earth and increases down (negative). Apparent conductivity depth-slices were extracted from the voxel with intervals every 25 m for 28 levels of depth below ground level (-25 m, -50 m, and -700 m).

5.4. ANOMALY SELECTION

The EM data were subjected to an anomaly recognition process using all the channels of the dBz/dt profiles. The resulting EM anomaly picks are presented as overlays on the maps and correspond to the approximate position of the conductors' centres projected to surface.

Each individual conductor pick is represented by an anomaly symbol classified according to the calculated conductance. Conductance values were obtained from the dBz/dt and B-Field EM time constants (Tau) whose relationships to Tau were calculated using the oblate spheroid model of McNeill (1980). Identified anomalies were classified into one of eight categories, as presented in Figure 9. The anomaly symbol is accompanied by postings denoting the number of Channels Deflected (upper-right),

the dBz/dt Apparent Conductance (lower-right), the Apparent Depth (lower-left) and the Identification of the Anomaly (upper left), a unique number to each flight line.

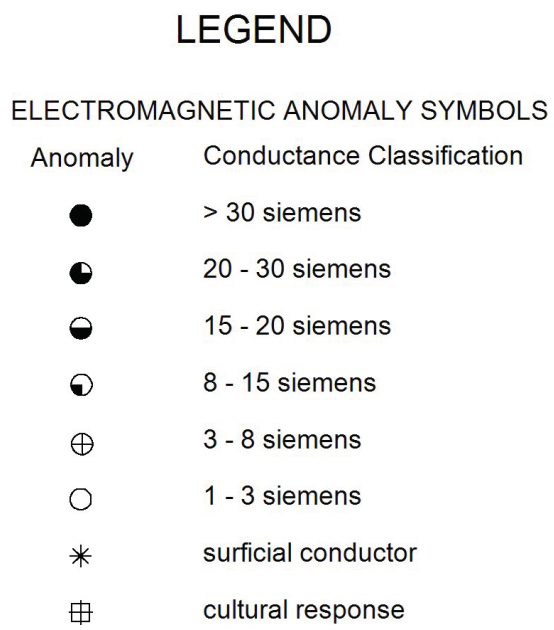

Figure 9. EM anomaly symbols.

The anomalous responses have been picked, reviewed and edited by an interpreter on a line-by-line basis to discriminate between bedrock, overburden and culture conductors. The accepted channels are provided in a Geosoft® database.

5.5. MAGNETIC MICROLEVELLING

Microlevelling is the process of removing residual flight line noise that remains after conventional levelling using control lines. It has become increasingly important as the resolution of aeromagnetic surveys has improved and the requirement of interpreting subtle geophysical anomalies has increased.

To isolate and remove this noise, the following procedure was employed. An elliptical reject filter, aligned with the flight lines, was first applied to the levelled total magnetic field grid. This filter removes features with a long wavelength in the flight line direction, but a short wavelength in the transverse direction. While removing the unwanted residual levelling errors, it also significantly distorts higher amplitude anomalies.

In order to minimize the effect on real anomalies, the flight path was ‘threaded’ through the filtered grid and a database profile channel was created from the grid. The difference between the control line levelled magnetic profile and this filtered profile was calculated. The difference profile was clipped to the amplitude of the observed noise in the grid. A half cosine roll-off filter was then applied to this channel and a final correction profile was derived with wavelengths longer than 1 km. This microlevel correction profile was applied to the levelled magnetic profile and a final magnetic profile channel was created.

5.6. KEATING CORRELATION COEFFICIENTS

Possible kimberlite targets are recognized from the residual magnetic intensity data, based on the identification of roughly circular anomalies. This procedure is automated by using a pattern recognition technique (Keating 1995), which consists of computing, over a moving window, a first-order regression between a vertical cylinder model anomaly and the gridded magnetic data. Only the results, where the absolute value of the correlation coefficient is above a threshold of 75%, were retained. On the magnetic maps, the results are depicted as circular symbols, scaled to reflect the correlation value. The most favourable targets are those that exhibit a cluster of high-amplitude solutions. Correlation coefficients with a negative value correspond to reversely magnetized sources.

The cylinder model parameters are as follows:

Sandy Lake Block:

- Cylinder diameter: 200 m
- Cylinder length: infinite
- Overburden thickness: 4.2 m
- Magnetic inclination: 77.1°
- Magnetic declination: 1.3°W
- Magnetization scale factor: 100
- Model window size: 13 x 13 cells (520 m x 520 m)
- Model window grid cell size: 40 m

Favourable Lake Block:

- Cylinder diameter: 200 m
- Cylinder length: infinite
- Overburden thickness: 5.5 m
- Magnetic inclination: 76.9°
- Magnetic declination: 0.5°W
- Magnetization scale factor: 100
- Model window size: 13 x 13 cells (520 m x 520 m)
- Model window grid cell size: 40 m

It is important to be aware that other magnetic sources may correlate well with the vertical cylinder model, whereas some kimberlite pipes of irregular geometry may not. The user should study the magnetic anomaly that corresponds with the Keating symbols, to determine whether it does resemble a kimberlite pipe signature, reflects some other type of source or even noise in the data e.g. a boudinage (beading) effect of the gridding algorithm. All available geological information should be incorporated into kimberlite pipe target selection.

5.7. GEOLOGICAL SURVEY OF CANADA DATA LEVELLING

In 1989, as part of the requirements for the contract with the Ontario Geological Survey (OGS) to compile and level all existing Geological Survey of Canada (GSC) aeromagnetic data (flown prior to 1989) in Ontario, Paterson, Grant and Watson Ltd. developed a robust method to level the magnetic data of various base levels to a common datum provided by the GSC as 812.8 m grids. The essential theoretical aspects of the levelling methodology were fully discussed in Gupta et al. (1989) and Reford et al. (1990). The method was later applied to the remainder of the GSC data across Canada and the high-resolution, combined aeromagnetic and EM (AMEM) surveys flown by the OGS. It has since been applied to all newly acquired OGS aeromagnetic surveys.

5.7.1. TERMINOLOGY

The Master grid refers to the 200 m Ontario magnetic grid compiled and levelled to the 812.8 m magnetic datum from the Geological Survey of Canada.

GSC levelling is the process of levelling profile data to a master grid, first applied to GSC data.

Intrasurvey levelling or microlevelling refers to the removal of residual line noise described earlier in this chapter; the wavelengths of the noise removed are usually shorter than tie line spacing.

Intersurvey levelling or GSC levelling refers to the level adjustments applied to a block of data; the adjustments are the long wavelength (in the order of tens of kilometres) differences with respect to a common datum, in this case, the 200 m Ontario master grid, which was derived from all pre-1989 GSC magnetic data and adjusted, in turn, by the 812.8 m GSC Canada wide grid.

5.7.2. THE GSC LEVELLING METHODOLOGY

The GSC levelling methodology is described below, using the Vickers survey flown for OGS as an example.

Several data processing procedures are assumed to be applied to the survey data prior to levelling, such as microlevelling, IGRF calculation and removal. The final levelled data are gridded at 1/5 of the line spacing. If a survey was flown as several distinct blocks with different flight directions, then each block is treated as an independent survey.

The steps in the GSC levelling process are as follows:

1. Create an upward continuation of the survey grid to 305 m

   Almost all recent surveys (1990 and later) to be compiled were flown at a nominal terrain clearance of 100 m or less. The first step in the levelling method is to upward continue the survey grid to 305 m, the nominal terrain clearance of the Ontario Master Grid (Figure 10). The grid cell size for the survey grids is set at 100 m. Since the wavelengths of level corrections will be greater than 10 to 15 km, working with 100 m or even 200 m grids at this stage will not affect the integrity of the levelling method. Only at the very end, when the level corrections are imported into the databases, will the level correction grids be re-gridded to 1/5 of line spacing.

   The unlevelled 100 m grid is extended by at least 2 grid cells beyond the actual survey boundary, so that, in the subsequent processing, all data points are covered.

2. Create a difference grid between the survey grid and the Ontario master grid.

   The difference between the upward continued survey grid and the Ontario master grid, re-gridded at 100 m, is computed (Figure 11). The short wavelengths represent the higher resolution of the survey grid. The long wavelengths represent the level difference between the two grids.

3. Rotate difference grid so that flight line direction is parallel with grid column or row, if necessary.

4. Apply the first pass of a non-linear filter (Naudy and Dreyer, 1968) of wavelength on the order of 15 to 20 km along the flight line direction. Reapply the same non-linear filter across the flight line direction.

5. Apply the second pass of a non-linear filter of wavelength on the order of 2000 to 5000 m along the flight line direction. Reapply the same non-linear filter across the flight line direction.

6. Rotate the filtered grid back to its original (true) orientation (Figure 12).

7. Apply a low pass filter to the non-linear filtered grid.

   Streaks may remain in the non-linear filtered grid, mostly caused by edge effects. They must be removed by a frequency-domain, low pass filter with the wavelengths in the order of 25 km (Figure 13).

8. Re-grid to 1/5 line spacing and import level corrections into database.

9. Subtract the level correction channel from the un-levelled channel to obtain the level corrected channel.

10. Make final grid using the gridding algorithm of choice with grid cell size at 1/5 of line spacing.

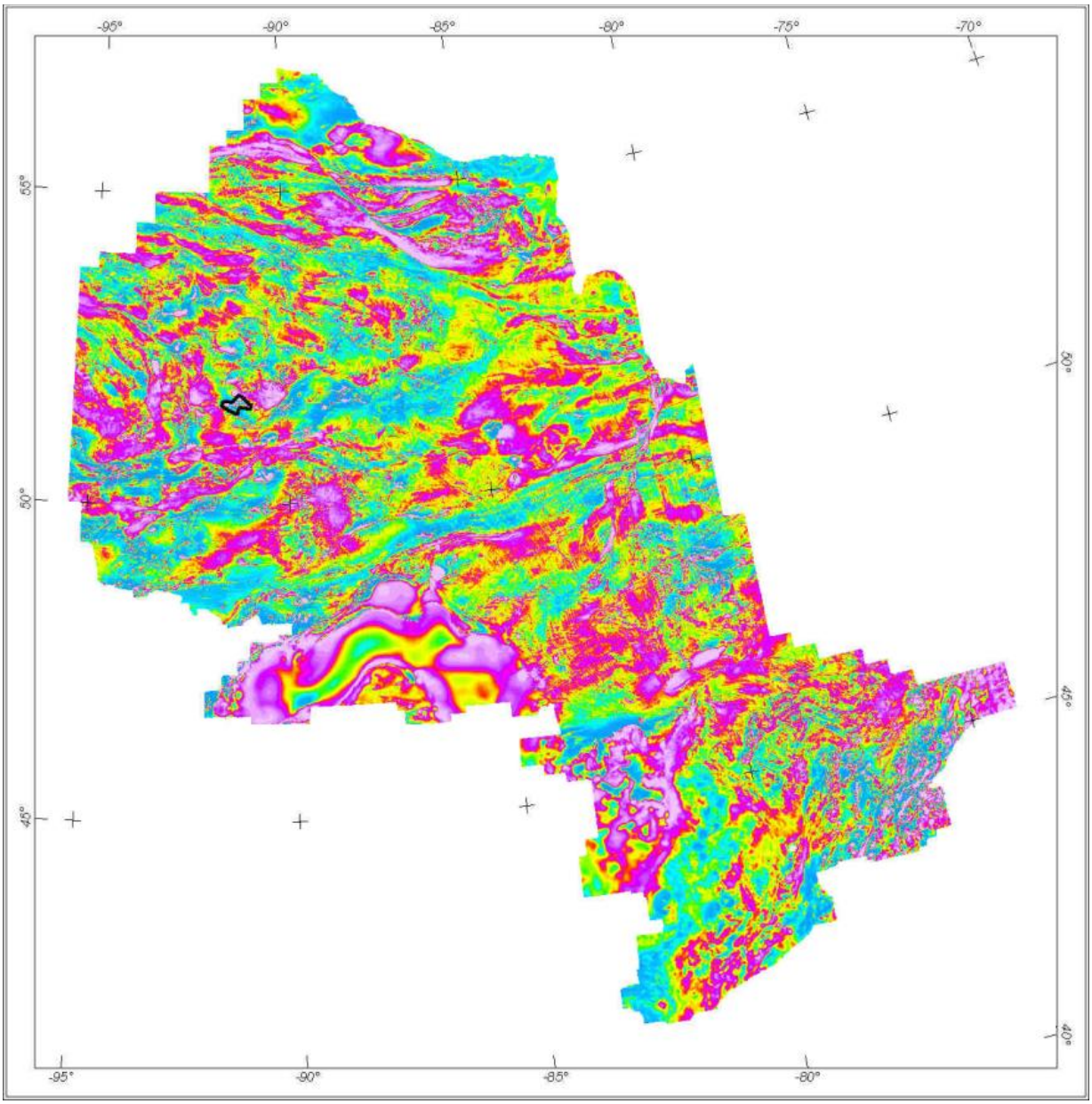

Figure 10. The Ontario Master Aeromagnetic Grid (Ontario Geological Survey 1999). The outline for the sample data set to be levelled (Vickers) is shown.

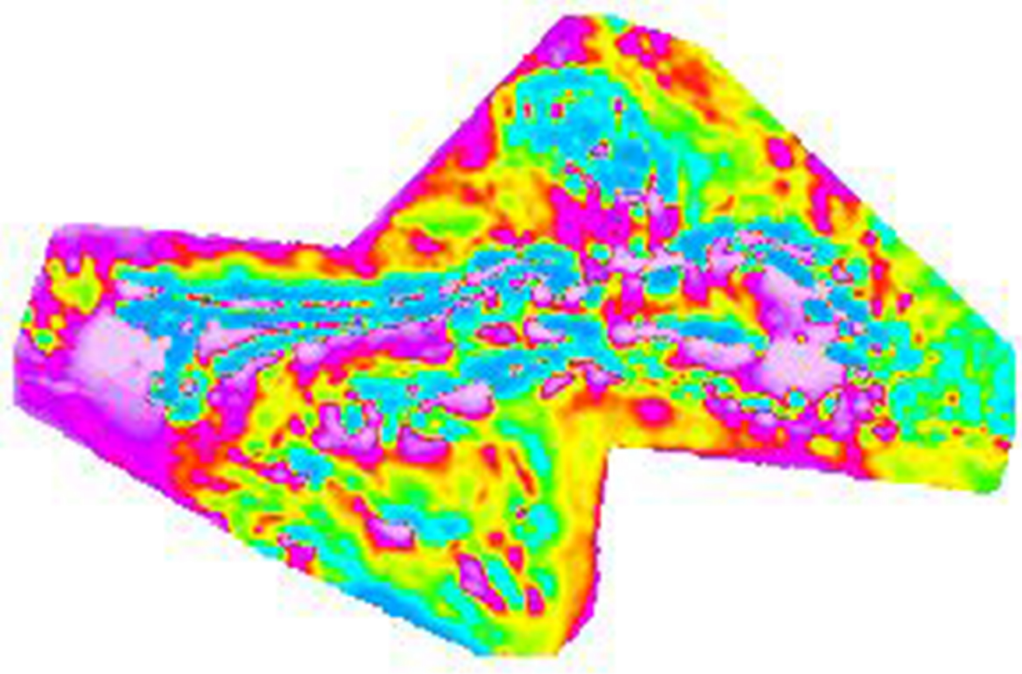

Figure 11. Difference grid (difference between survey grid and master grid), Vickers survey (Ontario Geological Survey 2003).

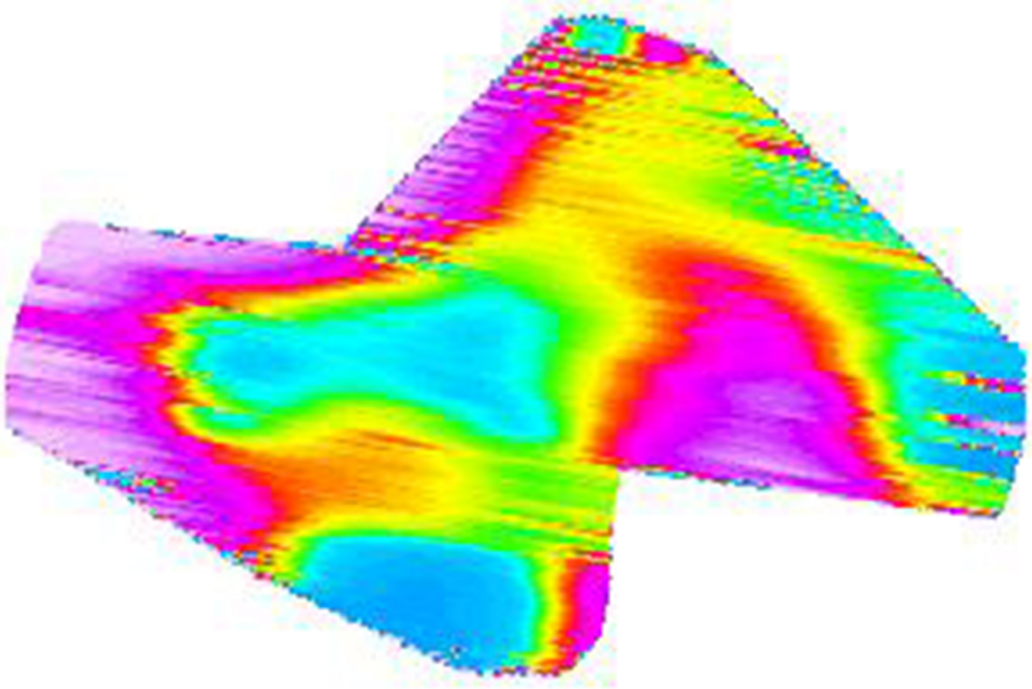

Figure 12. Difference grid after application of non-linear filtering and rotation, Vickers Survey.

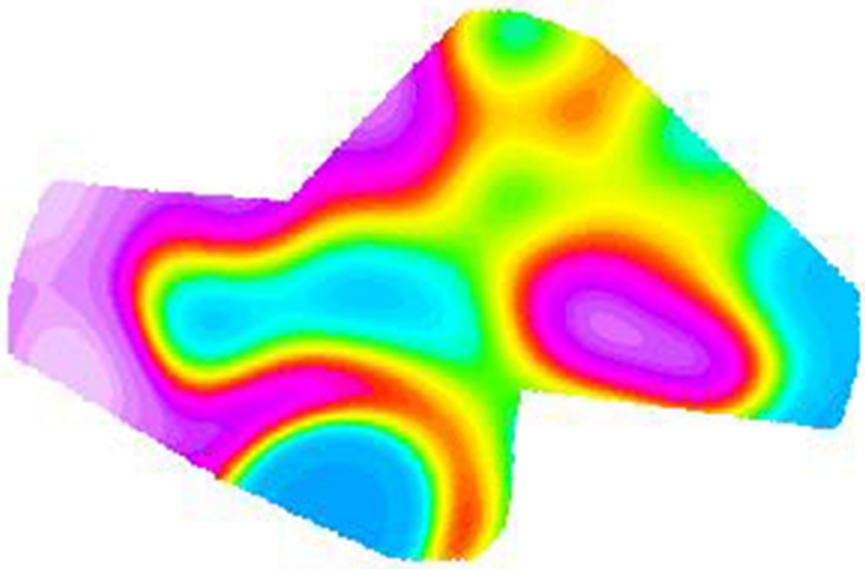

Figure 13. Level correction grid, Vickers survey.

Survey Specific Parameters

The following GSC levelling parameters were used in the Sandy Lake–Favourable Lake survey:

- Upward continuation of 224.9 for Sandy Lake Block and 214.6 for Favourable Lake Block
- OGS 200 m grid re-gridded to 100 m (Ontario-wide TMI grid)
- Residual grid re-gridded to 100 m
- Calculate difference grid between OGS_100 and Residual_100
- Difference grid of Favourable Lake Block was rotated to north-south; no need to rotate the difference grid of Sandy Lake Block
- Difference grid filtered with regrid.gx using LP=10 000m (1st pass) and 2500 m (2nd pass)
- Difference grid of Favourable Block rotated back to survey azimuth; no need to rotate grid of block 1
- Magmap filtered with LP=15 000 m
- Difference grid re-gridded to 40 m cell size
- Sampled back to database
- Correction subtracted from residual magnetic intensity channel

6. Final Products

The following products were delivered to MENDM.

6.1. PROFILE AND ANOMALY DATABASES

The following databases are provided in both Geosoft® *.gdb* and ASCII format.

- Magnetic and electromagnetic profile database
- EM anomaly database
- Keating correlation coefficient database
- Waveform database
- CDI database

6.2. GRIDDED DATA

The following data, gridded from co-ordinates in UTM Zone 15, NAD83 datum, are provided in both Geosoft® *.grd* and *.gxf* formats.

- digital elevation model
- GSC levelled residual magnetic field
- calculated second vertical derivative of the GSC levelled residual magnetic field
- TDEM decay constant Z-component
- apparent conductivity depth slices

6.3. MAPS

Final maps were produced at a scale of 1:20 000 and 1:50 000 for best representation of the survey size and line spacing. The co-ordinate and/or projection system used was NAD83 Datum, UTM Zone 15 North. The following maps were created:

Residual magnetic field contours, electromagnetic anomalies, Keating coefficients, flight path and base, 1:20 000 scale. Map numbers are shown in Figure 14.

Colour residual magnetic field grid, contours, electromagnetic anomalies and base, 1:50 000 scale. Map numbers are shown in Figure 15.

Colour Shaded second vertical derivative grid + Keating coefficients + base, 1:50 000 scale. Map numbers are shown in Figure 16.

Colour TDEM decay constant grid, contours, electromagnetic anomalies and base, 1:50 000 scale. Map numbers are shown in Figure 17.

Colour TDEM apparent conductivity, contours, electromagnetic anomalies and base, 1:50 000 scale. Map numbers are shown in Figure 18.

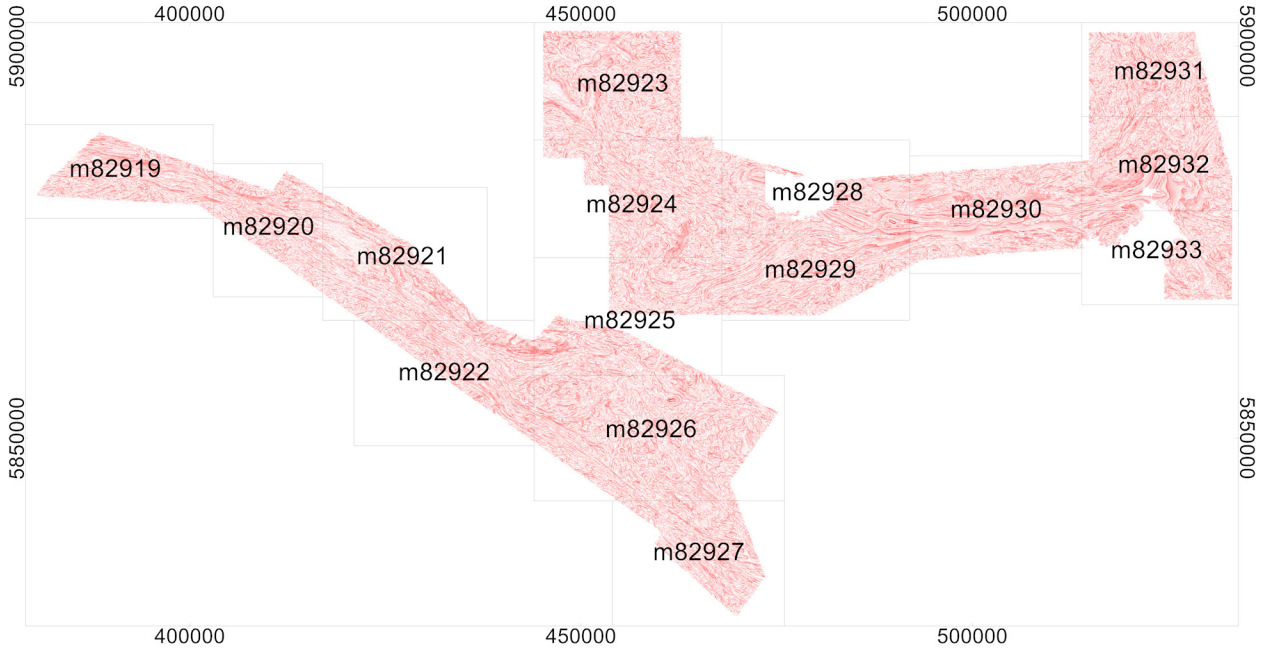

Figure 14. The tile layout for the digital 1:20 000 scale maps with a topographic layer is shown with associated map numbers where "M82XXX" indicates OGS Map 82XXX. The map exhibits residual magnetic contours with electromagnetic anomalies with Keating coefficients and flight lines.

Digital 1:50 000 scale maps in Geosoft® MAP format, with a topographic layer, of the following:

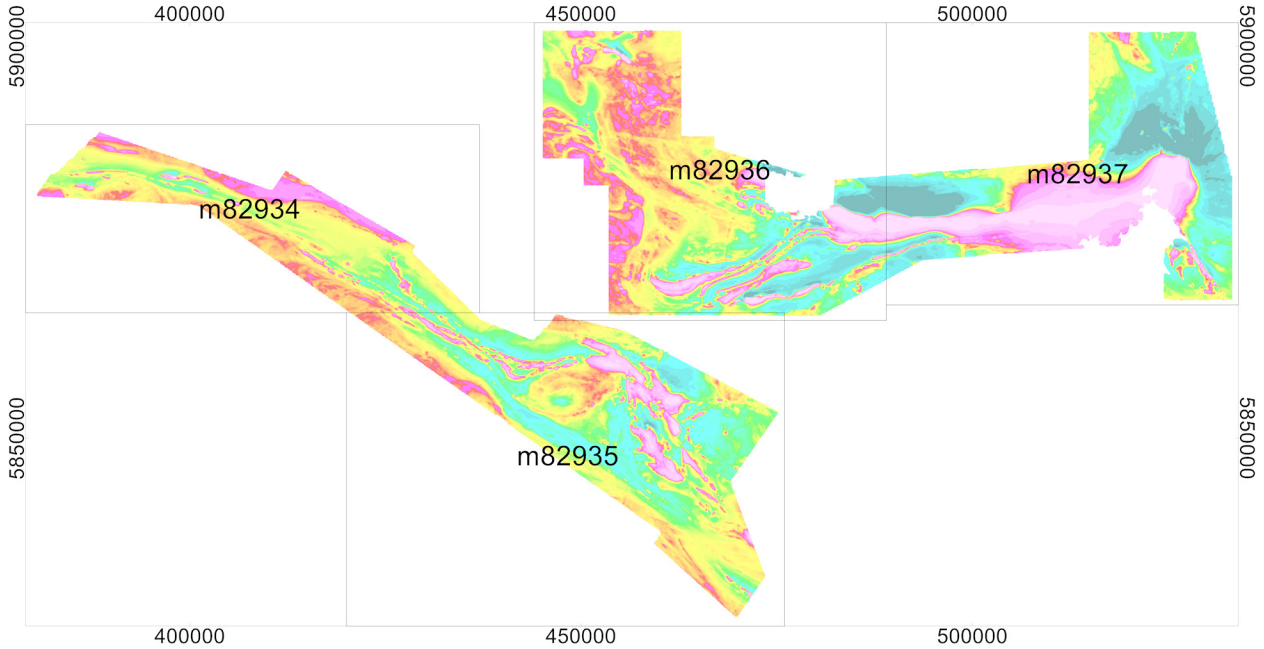

Figure 15. The tile layout for the digital 1:50 000 scale maps with a topographic layer is shown with associated map numbers where "M82XXX" indicates OGS Map 82XXX. The map exhibits colour-filled contours of the residual magnetic field, electromagnetic anomalies and flight lines.

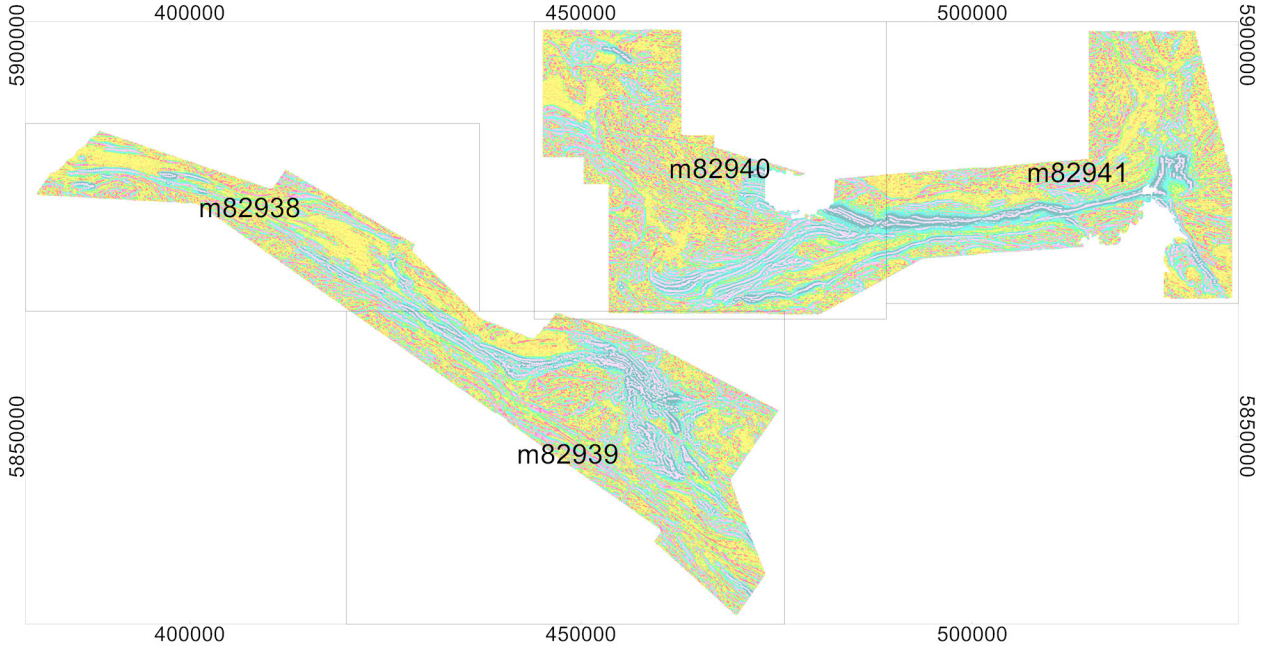

Figure 16. The tile layout for the digital 1:50 000 scale maps with a topographic layer is shown with associated map numbers where "M82XXX" indicates OGS Map 82XXX. The map exhibits colour shaded image of the second vertical derivative of the residual magnetic field, Keating coefficients and flight lines.

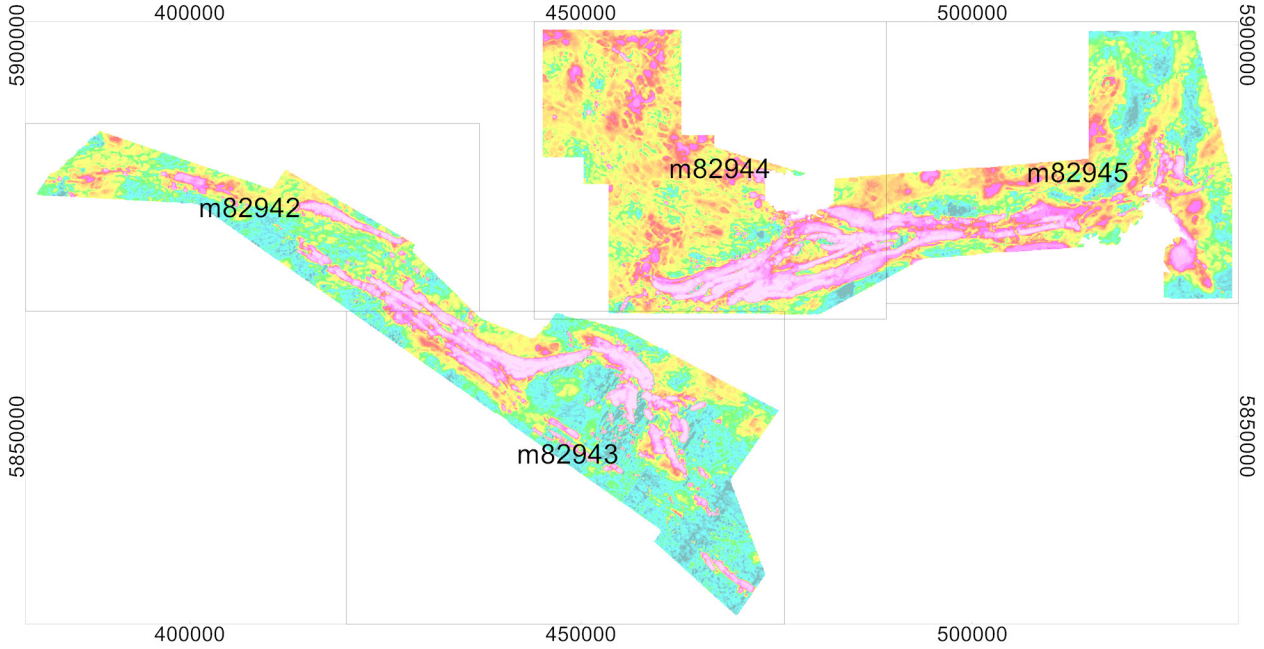

Figure 17. The tile layout for the digital 1:50 000 scale maps with a topographic layer is shown with associated map numbers where "M82XXX" indicates OGS Map 82XXX. The map exhibits the colour-filled contours of the EM decay constant, electromagnetic anomalies and flight lines.

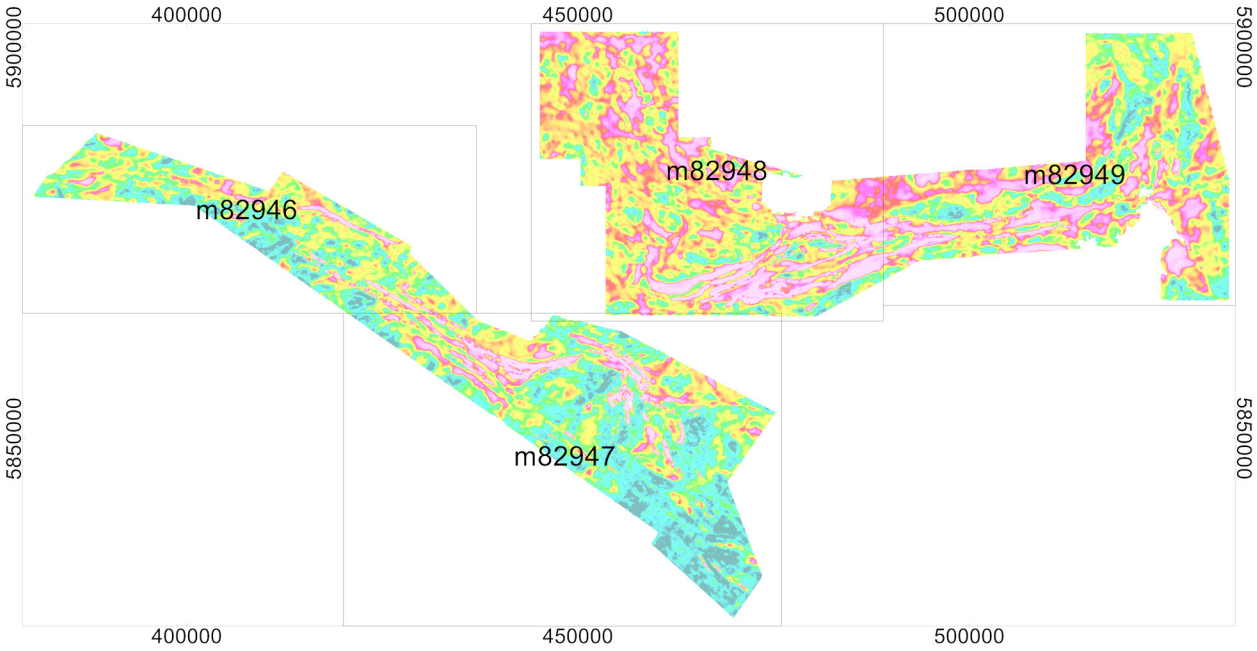

Figure 18. The tile layout for the digital 1:50 000 scale maps with a topographic layer is shown with associated map numbers where "M82XXX" indicates OGS Map 82XXX. The map exhibits the colour-filled contours of the apparent conductivity, electromagnetic anomalies and flight lines.

6.4. PROJECT REPORT

The survey report describes the data acquisition, processing, and final presentation of the survey results. The survey report is provided only digitally, in portable document format (*.pdf*).

6.5. FLIGHT VIDEOS

The digitally recorded video from each survey flight are provided in a compressed binary format on an external disc drive. Flight videos were delivered to the MENDM but are not part of the published Geophysical Data Set.

6.6. VECTOR FILES

Vector graphic files store the lines, shapes and colours that are plotted on a map as mathematical formulae; as a result they can be resized without losing detail or clarity.

They are created in Geosoft by exporting the selected layer as a *dxf* file. See Appendix A for the list of vector files provided.

6.7. GEO-REFERENCED IMAGE FILES

A GeoTIFF file has georeferenced information embedded in it such as projection and coordinates which allows the TIFF file to be spatially referenced.

They are created in Geosoft by exporting the selected layer as a geoTIFF file. See Appendix A for the list of GeoTIFFS provided.

6.8. VTEM STREAMED DATA

The VTEM streamed data are recorded at 192 kHz and is described in section 5.2 of this report.

Files containing stream data have extension ".c" and are provided in a separate hard-drive due to their large size. A flight usually contains several ".c" files recorded every ten (10) minutes and stored in binary format.

A typical ".c" file name is "vvv yy.mm.dd hh.mm.ss.c"

Where:

vvv: VTEM system serial number
yy: year
mm: month
dd: day
hh: hour
mm: minute
ss: second

VTEM streamed data were delivered to the MENDM but are not part of the published Geophysical Data Set.

7. Quality Assurance and Quality Control

Quality assurance and quality control (QA/QC) were undertaken by the survey contractor, Geotech Ltd., PGW (QA/QC Geophysicist), and MENDM. Stringent QA/QC was emphasized throughout the project so that the optimal geological signal was measured, archived and presented. The quality control procedures are summarized below.

7.1. PRE-PRODUCTION CALIBRATION AND TESTING

Test surveys were flown at the Sandy Lake sites to calibrate the magnetometer and TDEM systems respectively. These tests are presented in Appendix L.

In addition the following tests were carried out on the survey site:

1. Polarity Test – performed prior to the survey commencing. This test was designed to ensure that the polarity of the system is correct.
2. Aluminium Plate Test – performed prior to the survey commencing and at the end of every week. The test checked the sensitivity of the system during the survey period and ensured that the system was calibrated properly at all times.
3. Radar Altimeter Test – performed prior to survey commencing or if a new radar altimeter was installed. The test was performed to ensure the accuracy of the radar altimeter.
4. Full Waveform VTEM Calibration – performed prior to the survey commencing. This calibration is performed on the complete VTEM system installed in and connected to the

helicopter, using special calibration equipment. The procedure takes half-cycle files acquired and calculates a calibration file consisting of a single stacked half-cycle waveform. The purpose of the stacking is to attenuate natural and man-made magnetic signals, leaving only the response to the calibration signal.

7.2. DAILY CALIBRATIONS AND PRE-FLIGHT PRECAUTIONS

The TDEM system and magnetometer were sufficiently warmed up before each survey day to minimize temperature-related system drifting.

- Timing and synchronization of all recording instruments was checked for correct operation.
- Each flight included 2 background pre-flight and post-flight measurements for background and assessment of noise levels. The aircraft climbed to 500 m AGL (Above Ground Level) and maintained straight and level flight for one (1 minute or 5 km). A 'background check' was conducted at the beginning of each flight and repeated approximately every hour and after completing the last survey line of the flight.
- Each flight included 2 background measurements; pre-flight and post-flight for TDEM compensation and collection of the reference waveform.
- A test line of a minimum of 5 km long, with a variety of conductive responses, was flown daily at survey height.

7.3. DAILY FIELD QUALITY CONTROL

7.3.1. GENERAL

- Check that all the files are on the server as expected.
- Download and unzip the files. Make sure they were complete and not corrupted.
- Check the header of the airborne raw data files to ensure the system was configured properly.
- Pre-process and then import the data into the Geosoft® software.
- Plot the flight path in Google Earth and Geosoft® to verify that the data are complete and properly located and that the lines, as described in the flight logs, were flown.
- Check the flight path for crossing lines or lines that did not maintain proper separation.
- Plot the final flight path and look for problems, such as gaps and GPS busts.

7.3.2. ELECTROMAGNETIC DATA

- Visual check for shifts, excessive spiking, drift, etc.
- Correct/compensate the EM data.
- Identify the backgrounds and measure/log the EM noise levels including original and compensated channels. Ensure they are within specification
- Filter the EM data and check for drift or offsets
- After splitting the GDB into lines, check again

7.3.3. MAGNETIC DATA AND MAGNETIC BASE STATION

- Check the start and end time of base station record and ensure that it covers the full survey data.
- Check the base station for cultural noise and diurnal activity. Ensure the diurnal is within specifications.
- Check the airborne magnetic data for gaps, dropouts, or excessive noise

7.3.4. ALTITUDE

- Visually check the altitude particularly at the start and ends of lines.
- Calculate the average helicopter altitude and ensure that it meets specifications.

7.4. QUALITY CONTROL IN THE OFFICE

Data verification was performed by experienced geophysicists in the processing centre or on-site using a work station that is capable of reading, analysing and duplicating the data on a daily basis. This system was available to MENDM (QA/QC geophysicist) to monitor data acquisition and verification.

The work flow diagram provided below (Figure 19) shows the tests and checks on data applied during the course of the survey and subsequent processing. The red lines represent feedback loops that will send data back to be reprocessed or even re-flown so as to correct for any deficiencies detected either in the field during QA/QC or at the Data Processing centre where senior staff review incoming data sets.

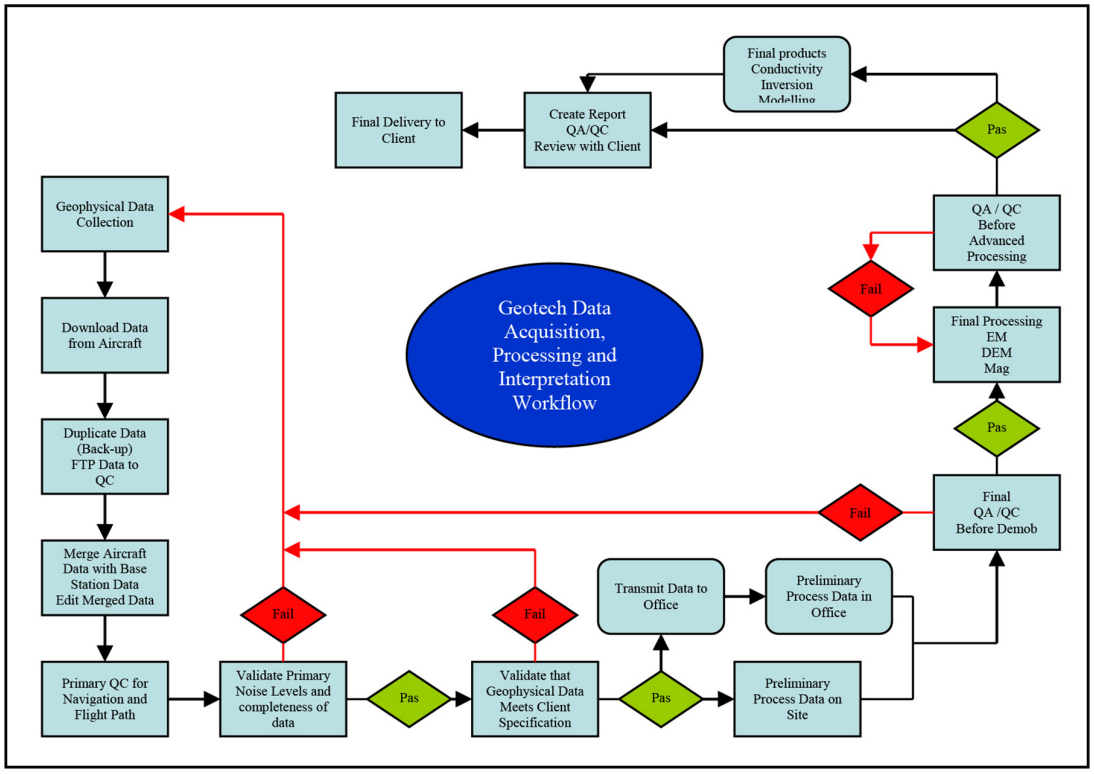

Figure 19. Data acquisition, data processing and interpretation workflow.

8. References

Gupta, V., Paterson, N., Reford, S., Kwan, K., Hatch, D. and MacLeod, I. 1989. Single master aeromagnetic grid and magnetic colour maps for the province of Ontario; *in* Summary of Field Work and Other Activities 1989, Ontario Geological Survey, Miscellaneous Paper 146, p.244-250.

Keating, P.B. 1995. A simple technique to identify magnetic anomalies due to kimberlite pipes; Exploration and Mining Geology, v.4, no.2, p.121-125.

McNeill, J.D. 1980. Applications of transient electromagnetic techniques; Technical Note 7, Geonics Ltd., Mississauga, Ontario.

Meju, M.A. 1998. Short Note: A simple method of transient electromagnetic data analysis; Geophysics, 63, p.405-410.

Naudy, H. and Dreyer, H. 1968. Essai de filtrage nonlinéaire appliqué aux profiles aeromagnétiques; Geophysical Prospecting, v.16, p.171-178.

Ontario Geological Survey 1999. Single master gravity and aeromagnetic data for Ontario; Ontario Geological Survey, Geophysical Data Set 1036.

———2003. Ontario airborne geophysical surveys, magnetic and electromagnetic data, Vickers area; Ontario Geological Survey, Geophysical Data Set 1106–revised.

———2011. 1:250 000 scale bedrock geology of Ontario; Ontario Geological Survey, Miscellaneous Release—Data 126–Revision 1.

Reford, S.W., Gupta, V.K., Paterson, N.R., Kwan, K.C.H. and Macleod, I.N. 1990. Ontario master aeromagnetic grid: A blueprint for detailed compilation of magnetic data on a regional scale; in Expanded Abstracts, Society of Exploration Geophysicists, 60th Annual International Meeting, San Francisco, v.1, p.617-619.

Satterly, J. 1938. Geology of the Sandy Lake area; Ontario Department of Mines, Annual Report, 1938, v.47, pt.7, p.1-43.

Stone, D. 1998. Precambrian geology of the Berens River area, northwest Ontario; Ontario Geological Survey, Open File Report 5963, 116p.

Appendix A. Geophysical Data File Layout

The files for the Sandy Lake and Favourable Lake Survey, Geophysical Data Set 1085, are archived on 2 three-volume sets of DVDs and are sold as separate products as follows:

ASCII format	Geophysical Data Set (GDS) 1085a volumes 1 to 3
Geosoft® binary format	Geophysical Data Set (GDS) 1085b volumes 1 to 3

The content of the ASCII and Geosoft® binary file types are identical. They are provided in both forms to suit the user's available software. The survey data are divided as follows:

Geophysical Data Set 1085a (DVD)

- Profile data
  a) Profile database of electromagnetic and magnetic data (10 Hz sampling) in ASCII (*.xyz*) format
- Gridded data in ASCII (*.gxf*) format:
  a) total (residual) field magnetics
  b) second vertical derivative of the total field magnetics
  c) decay constant
  d) apparent conductivity at -100m depth
  e) digital elevation model
- EM anomaly database in ASCII (*.csv*) format
- Keating correlation coefficient database in ASCII (*.csv*) format
- Vector files in *.dxf* format:
  a) flight path
  b) EM anomalies
  c) Keating correlation (kimberlite) anomalies
  d) total field magnetic contours
  e) decay constant contours
  f) apparent conductivity contours
- GEOTIFF images
  a) colour total field magnetics with base map
  b) colour shaded relief of second vertical derivative with base map
  c) colour decay constant with base map
  d) apparent conductivity at -100m, -150m, -200m and -250m depth with base map
- Waveform database in ASCII (*.xyz*) format
- Conductivity Depth Imaging (CDI) data:
  a) CDI database in Geosoft® Binary ASCII format
  b) Plotted CDI sections in portable document format (*.pdf*)
  c) Survey report in portable document format (*.pdf*)

Geophysical Data Set 1085b (DVD)

- Profile data
  a) Profile database of electromagnetic and magnetic data (10 Hz sampling) in Geosoft® Binary (*.gdb*) format
- Gridded data in Geosoft® Binary (*.grd*) format:
  a) total (residual) field magnetics
  b) second vertical derivative of the total field magnetics
  c) decay constant
  d) apparent conductivity at -100m, -150m, -200m and -250m depth
  e) digital elevation model
- EM anomaly database in Geosoft® Binary (*.gdb*) format
- Keating correlation coefficient database in Geosoft® Binary (*.gdb*) format
- Vector files in *.dxf* format:
  a) flight path
  b) EM anomalies
  c) Keating correlation (kimberlite) anomalies
  d) total field magnetic contours
  e) decay constant contours
  f) apparent conductivity contours
- GEOTIFF images
  a) colour total field magnetics with base map
  b) colour shaded relief of second vertical derivative with base map
  c) colour decay constant with base map
  d) apparent conductivity at -100m depth with base map
- Waveform database in Geosoft® (*.gdb*) format
- Conductivity Depth Imaging (CDI) data:
  a) CDI database in Geosoft® Binary (*.gdb*) format
  b) Plotted CDI sections in portable document format (*.pdf*)
  c) Survey report in portable document format (*.pdf*)

Appendix B. Profile Archive Definition

The profile data are provided in 2 formats, one binary and one ASCII.

ASCII XYZ and Geosoft® OASIS montaj™ binary database file (no compression) of electromagnetic, magnetic and ancillary data, sampled at 10 Hz

- SLMAGEM.XYZ (ASCII) for Sandy Lake Block
- SLMAGEM.GDB (Binary) for Sandy Lake Block
- FLMAGEM.XYZ (ASCII) for Favourable Lake Block
- FLMAGEM.GDB (Binary) for Favourable Lake Block

The contents of *.GDB/*.XYZ (both file types contain the same set of data channels) are summarized as follows:

- Magnetic/Electromagnetic/ Ancillary Line Data

In SLMAGEM.XYZ and FLMAGEM.XYZ the electromagnetic channel data are provided in individual channels with numerical indices (e.g., em_z_final_off[4] to em_z_final_off[46]) along with magnetic and ancillary channels. In SLMAGEM.GDB and FLMAGEM.GDB, the electromagnetic channel data are provided in array channels with 43 elements.

Table 6. Survey profile database channels.

Channel name	Units	Description
gps_x_raw	metres	raw GPS X
gps_y_raw	metres	raw GPS Y
gps_z_raw	metres	raw GPS Z
gps_x_final	decimal-degrees	differentially corrected GPS X (NAD83 datum)
gps_y_final	decimal-degrees	differentially corrected GPS Y (NAD83 datum)
gps_z_final	metres ASL	differentially corrected GPS Z (NAD83 datum)
x_nad83	metres	easting in UTM co-ordinates using NAD83 datum
y_nad83	metres	northing in UTM co-ordinates using NAD83 datum
lon_nad83	decimal-degrees	longitude using NAD83 datum
lat_nad83	decimal-degrees	latitude using NAD83 datum
radar_raw	metres above terrain	raw radar altimeter
radar_final	metres above terrain	corrected radar altimeter
dem	metres ASL	digital elevation model
fiducial		Fiducial
flight		flight number
line_number		full flight line number (flight line and part numbers)
line		flight line number
time_utc	seconds	utc time
date	YYYY/MM/DD	local date
height_mag	metres above terrain	magnetometer height
mag_base_final	nanoteslas	corrected magnetic base station data
mag_raw	nanoteslas	raw magnetic field
mag_diurn	nanoteslas	diurnally-corrected magnetic field
mag_lev	nanoteslas	levelled magnetic field
igrf	nanoteslas	local IGRF field
mag_igrf	nanoteslas	IGRF-corrected magnetic field
mag_final	nanoteslas	diurnally and IGRF-corrected magnetic field
cvg	nanoteslas per metre	calculated magnetic vertical derivative from mag_final
mag_gsclevel	nanoteslas	GSC levelled magnetic field

Channel name	Units	Description
cvg_gsclevel	nanoteslas per metre	calculated magnetic vertical derivative from mag_gsclevel
height_em	metres above terrain	electromagnetic receiver height
em_z_raw_off	(pV)/(A*m^4)	raw (stacked) dB/dt, Z-component, off-time channels 4 to 46
em_z_final_off	(pV)/(A*m^4)	filtered and leveled dB/dt, Z-component, off-time channels 4 to 46
em_bz_raw_off	(pV*ms)/(A*m^4)	raw (stacked) B-field, Z-component, off-time channels 4 to 46
em_bz_final_off	(pV*ms)/(A*m^4)	filtered and leveled B-field, Z-component, off-time channels 4 to 46
em_x_raw_off	(pV)/(A*m^4)	raw (stacked) dB/dT, X-component, off-time channels 20 to 46
em_x_final_off	(pV)/(A*m^4)	filtered and leveled dB/dT, X-component, off-time channels 20 to 46
em_fraserfilt_final_off	(pV)/(A*m^4)	Fraser filtered calculated from channel em_x_final_off, channels 20 to 46
em_bx_raw_off	(pV*ms)/(A*m^4)	raw (stacked) B-field, X-component, off-time channels 20 to 46
em_bx_final_off	(pV*ms)/(A*m^4)	filtered and leveled B-field, X-component, off-time channels 20 to 46
em_y_raw_off	(pV)/(A*m^4)	raw (stacked) dB/dT, Y-component, off-time channels 20 to 46
em_y_final_off	(pV)/(A*m^4)	filtered and leveled dB/dT, Y-component, off-time channels 20 to 46
em_by_raw_off	(pV*ms)/(A*m^4)	raw (stacked) B-field, Y-component, off-time channels 20 to 46
em_by_final_off	(pV*ms)/(A*m^4)	filtered and leveled B-field, Y-component, off-time channels 20 to 46
plm	microvolts	60 Hz power line monitor
taubf	microseconds	decay constant (tau) for B-field Z-component
tausf	microseconds	decay constant (tau) for dB/dt Z-component
nchan_bf		latest time channels of TAU calculation, B-field Z
nchan_sf		latest time channels of TAU calculation, dB/dt Z
appcond	siemens per metre	apparent conductivity

Appendix C. EM Anomaly Archive Definition

The electromagnetic anomaly data are provided in 2 formats, one ASCII and one binary:

- SLANOMALY.csv – ASCII comma-delimited Excel® format for Sandy Lake Block
- SLANOMALY.gdb – Geosoft® OASIS montaj™ binary database file for Sandy Lake Block
- FLANOMALY.csv – ASCII comma-delimited Excel® format for Favourable Lake Block
- FLANOMALY.gdb – Geosoft® OASIS montaj™ binary database file for Favourable Lake Block

Both file types contain the same set of data channels and are summarized as follows.

Table 7. EM anomaly database channels.

Channel name	Units	Description
x_nad83	metres	easting in UTM co-ordinates using NAD83 datum
y_nad83	metres	northing in UTM co-ordinates using NAD83 datum
lon_nad83	decimal-degrees	longitude using NAD83 datum
lat_nad83	decimal-degrees	latitude using NAD83 datum
dem	metres asl	digital elevation model
fiducial		Fiducial
flight		flight number
line		flight line number
time_utc	seconds	utc time
date	YYYY/MM/DD	local date
em_z_final_off	(pV)/(A*m^4)	filtered and leveled dB/dt, Z-component, off-time channels 4 to 46
em_bz_final_off	(pV*ms)/(A*m^4)	filtered and leveled B-field, Z-component, off-time channels 4 to 46
tausf	microseconds	decay constant (tau) for dB/dt Z-component
appcond	Siemens per metre	apparent conductivity
height_em	metres above terrain	electromagnetic receiver height
anomaly_no		nth anomaly along the survey line
anomaly_ID		Alpha identifier
anomaly_type_letter		anomaly classification, “thick” (K) or “thin” (N) anomaly
anomaly_type_no		anomaly classification (i.e. anomaly grade), 1 to 6 from the weakest to the strongest
conductance_dBdt	Siemens	apparent conductance, calculated from dB/dt data
conductance_bfield	Siemens	apparent conductance, calculated from B-field data
depth_to_conductor	metres	Depth to conductor
heading	degrees	direction of flight
survey_number		Government survey number
nchan_z		Number of off-time channels deflected
cultural		Flagged channel for anomalies identified as cultural

Appendix D. Keating Correlation Archive Definition

The Keating kimberlite pipe correlation coefficient data are provided in 2 formats, one ASCII and one binary:

- SLKC.csv – ASCII comma-delimited format for Sandy Lake Block
- SLKC.gdb – Geosoft® OASIS montaj™ binary database file for Sandy Lake Block
- FLKC.csv – ASCII comma-delimited format for Favourable Lake Block
- FLKC.gdb – Geosoft® OASIS montaj™ binary database file for Favourable Lake Block

Both file types contain the same set of data channels and are summarized as follows.

Table 8. Keating correlation database channels.

Channel name	Units	Description
x_nad83	metres	easting in UTM co-ordinates using NAD83 datum
y_nad83	metres	northing in UTM co-ordinates using NAD83 datum
lon_nad83	decimal-degrees	longitude using NAD83 datum
lat_nad83	decimal-degrees	latitude using NAD83 datum
corr_coeff	percent	correction coefficient
pos_coeff	percent	positive correction coefficient
neg_coeff	percent	negative correction coefficient
norm_error	percent	standard error normalized to amplitude
amplitude	nanoteslas	peak-to-peak anomaly amplitude within window

Appendix E. Grid Archive Definition

The gridded data are provided in 2 formats, one ASCII and one binary:

- *.gxf - Geosoft® ASCII Grid eXchange Format (no compression)
- *.grd - Geosoft® OASIS montaj™ binary grid file (no compression)

Grids are NAD83 UTM Zone 15 North for Sandy Lake Block and Favourable Lake Block, with a grid cell size of 40 m x 40 m.

Grids in Geosoft® GRD and GXF format are summarized as follows.

- SL1VD83: Calculated First Vertical Derivative of TMI (nT/m) for Sandy Lake Block
- SL1VDGSC83: Calculated First Vertical Derivative of the "GSC levelled" Residual Magnetic Field (nT/m) for Sandy Lake Block
- SL2VD83: Calculated Second Vertical Derivative of TMI (nT/m^2) for Sandy Lake Block
- SL2VDGSC83: Calculated Second Vertical Derivative of the "GSC levelled" Residual Magnetic Field (nT/m^2) for Sandy Lake Block
- SLDCBZ83: TDEM Decay Constant B field Z Component (µsec) for Sandy Lake Block
- SLDCZ83: TDEM Decay Constant dBz/dt Z Component (µsec) for Sandy Lake Block
- SLCON83: TDEM Apparent Conductivity depth slice 100 m below surface (mS/m) for Sandy Lake Block
- SLDEM83: Digital Elevation Model (metres) for Sandy Lake Block
- SLEMBZ3683: TDEM of B field Z component at index 36
- SLEMZ1083: TDEM of dB/dt of Z component at index 10
- SLEMZ2583: TDEM of dB/dt of Z component at index 25
- SLEMZ4083: TDEM of dB/dt of Z component at index 40
- SLMAG83: Total Magnetic Intensity (nT) for Sandy Lake Block
- SLMAGGSC83: GSC Levelled Total Magnetic Intensity (nT) for Sandy Lake Block
- SLPLM83: 60Hz power line monitor
- FL1VD83: Calculated First Vertical Derivative of TMI (nT/m) for Favourable Lake Block
- FL1VDGSC83: Calculated First Vertical Derivative of the "GSC levelled" Residual Magnetic Field (nT/m) for Favourable Lake Block
- FL2VD83: Calculated Second Vertical Derivative of TMI (nT/m^2) for Favourable Lake Block
- FL2VDGSC83: Calculated Second Vertical Derivative of the "GSC levelled" Residual Magnetic Field (nT/m^2) for Favourable Lake Block
- FLDCBZ83: TDEM Decay Constant B field Z Component (µsec) for Favourable Lake Block
- FLDCZ83: TDEM Decay Constant Z Component (µsec) for Favourable Lake Block
- FLCON83: TDEM Apparent Conductivity depth slice 100 m below surface (mS/m) for

Favourable Lake Block

- FLDEM83: Digital Elevation Model (metres) for Favourable Lake Block
- FLEMBZ3683: TDEM of B field Z component at index 36
- FLEMZ1083: TDEM of dB/dt of Z component at index 10
- FLEMZ2583: TDEM of dB/dt of Z component at index 25
- FLEMZ4083: TDEM of dB/dt of Z component at index 40
- FLMAG83: Total Magnetic Intensity (nT) for Favourable Lake Block
- FLMAGGSC83: GSC Levelled Total Magnetic Intensity (nT) for Favourable Lake Block
- FLPLM83: 60Hz powerline monitor

A Geosoft® .GRD file has a .GI metadata file associated with it, containing grid projection information.

Appendix F. Geotiff and Vector Archive Definition

GeoTIFF Images

Geographically referenced colour images, incorporating a planimetric base, are provided in GeoTIFF format for use in GIS applications:

- SLMAG83.TIF – Colour residual, GSC levelled, magnetic field grid plotted on a planimetric base for Sandy Lake Block
- SL2VD83.TIF – Shaded colour image of the second vertical derivative of the residual magnetic field on a planimetric base for Sandy Lake Block
- SLDCZ83.TIF – Colour decay constant on a planimetric base for Sandy Lake Block
- SLCON83_DepthSlice_-100.TIF – Colour apparent conductivity on a planimetric base 100 m below surface for Sandy Lake Block
- SLCON83_DepthSlice_-150.TIF – Colour apparent conductivity on a planimetric base 150 m below surface for Sandy Lake Block
- SLCON83_DepthSlice_-200.TIF – Colour apparent conductivity on a planimetric base 200 m below surface for Sandy Lake Block
- SLCON83_DepthSlice_-250.TIF – Colour apparent conductivity on a planimetric base 250 m below surface for Sandy Lake Block

- FLMAG83.TIF – Colour residual, GSC levelled, magnetic field grid plotted on a planimetric base for Favourable Lake Block
- FL2VD83.TIF – Shaded colour image of the second vertical derivative of the residual magnetic field on a planimetric base for Favourable Lake Block
- FLDCZ83.TIF – Colour decay constant on a planimetric base for Favourable Lake Block
- FLCON83_DepthSlice_-100.TIF – Colour apparent conductivity on a planimetric base 100 m below surface for Favourable Lake Block
- FLCON83_DepthSlice_-150.TIF – Colour apparent conductivity on a planimetric base 150 m below surface for Favourable Lake Block
- FLCON83_DepthSlice_-200.TIF – Colour apparent conductivity on a planimetric base 200 m below surface for Favourable Lake Block
- FLCON83_DepthSlice_-250.TIF – Colour apparent conductivity on a planimetric base 250 m below surface for Favourable Lake Block

Vector Archives

Vector line work from the map is provided in DXF (v12) ASCII format using the following naming convention:

- SLPATH83_20K.DXF – flight path of the survey area from 1:20 000 scale maps for Sandy Lake Block
- SLKC83_20K.DXF – Keating correlation targets from 1:20 000 scale maps for Sandy Lake Block
- SLMAG83_20K.DXF – contours of the GSC levelled, residual magnetic field in nT from 1:20 000 scale maps for Sandy Lake Block
- SLDCZ83_20K.DXF – contours of the Z coil decay constant in µsec from 1:20 000 scale maps for Sandy Lake Block

- SLCON83_20K.DXF – contours of the apparent conductivity100 m below surface in (mS/m) from 1:20 000 scale maps for Sandy Lake Block
- SLEM83_20K.DXF – electromagnetic anomaly symbols from 1:20 000 scale maps for Sandy Lake Block
- FLPATH83_20K.DXF – flight path of the survey area from 1:20 000 scale maps for Favourable Lake Block
- FLKC83_20K.DXF – Keating correlation targets from 1:20 000 scale maps for Favourable Lake Block
- FLMAG83_20K.DXF – contours of the GSC levelled, residual magnetic field in nT from 1:20 000 scale maps for Favourable Lake Block
- FLDCZ83_20K.DXF – contours of the Z coil decay constant in μsec from 1:20 000 scale maps for Favourable Lake Block
- FLCON83_20K.DXF – contours of the apparent conductivity 100 m below surface in (mS/m) from 1:20 000 scale maps for Favourable Lake Block
- FLEM83_20K.DXF – electromagnetic anomaly symbols from 1:20 000 scale maps for Favourable Lake Block

The layers within the DXF files correspond to the various object types found therein and have intuitive names.

Appendix G. Waveform and Conductivity Depth Image Archive Definition

The databases of the transmitter reference waveform are provided in binary and ASCII formats. The Conductivity Depth Image (CDI) databases are provided in binary format:

Transmitter Current Waveform

SL_VTEM07_Waveform.gdb – Geosoft® OASIS montaj™ binary database file for Sandy Lake Block, VTEM #07 system

SL_VTEM07_Waveform.XYZ – ASCII file for Sandy Lake Block, VTEM #07 system

SL_VTEM15_Waveform.gdb – Geosoft® OASIS montaj™ binary database file for Sandy Lake Block, VTEM #15 system

SL_VTEM15_Waveform.XYZ – ASCII file for Sandy Lake Block, VTEM #15 system

FL_VTEM07_Waveform.gdb – Geosoft® OASIS montaj™ binary database file for Favourable Lake Block, VTEM #07 system

FL_VTEM07_Waveform.XYZ – ASCII file for Favourable Lake Block, VTEM #07 system

FL_VTEM15_Waveform.gdb – Geosoft® OASIS montaj™ binary database file for Favourable Lake Block, VTEM #15 system

FL_VTEM15_Waveform.XYZ – ASCII file for Favourable Lake Block, VTEM #15 system

Descriptions of the data channels are provided below.

Geosoft database for the VTEM waveform

Table 9. VTEM Waveform database channels.

Channel name	Description
Time:	Sampling rate interval, 5.2083 microseconds
Tx_Current:	Output current of the transmitter (amps)

Conductivity Depth Image

GL170151_SL_CDI.gdb – Geosoft® OASIS montaj™ binary database file for Sandy Lake Block
GL170151_FL_CDI.gdb – Geosoft® OASIS montaj™ binary database file for Favourable Lake Block
Geosoft database for conductivity depth image (CDI) data format

Table 10. CDI database channels.

Channel name	Units	Description
x_nad83	metres	easting in UTM co-ordinates using NAD83 datum
y_nad83	metres	northing in UTM co-ordinates using NAD83 datum
dist	metres	distance from the beginning of the line
depth	metres	array channel, depth from the surface
z	metres	array channel, depth from sea level
appres	ohm.m	array channel, apparent resistivity
appcond	Siemens per metre	array channel, apparent conductivity

Channel name	Units	Description
tr	metres	electromagnetic receiver height from sea level
topo	metres	digital elevation model
height_em	metres	electromagnetic receiver height
em_z_final_off	pV/(A*m^4)	array channel, filtered and leveled dB/dt, Z-component, off-time
mag_gsclevel	nanoteslas	GSC levelled magnetic field
cvg_gscl	nanoteslas per metre	calculated magnetic vertical derivative from mag_gsclevel
doi	metres	Depth of Investigation: a measure of VTEM depth effectiveness
power		60Hz power line monitor

Grids of horizontal depth slices of apparent conductivity are provided in Geosoft® binary grid format. The grids are summarized in Table 11 below:

Table 11. Apparent conductivity depth slice grids.

Grid name	Survey block	Description
SL_cdiatdepth025m.grd	Sandy Lake	apparent conductivity 25m below surface
SL_cdiatdepth050m.grd	Sandy Lake	apparent conductivity 50m below surface
SL_cdiatdepth075m.grd	Sandy Lake	apparent conductivity 75m below surface
SL_cdiatdepth100m.grd	Sandy Lake	apparent conductivity 100m below surface
SL_cdiatdepth125m.grd	Sandy Lake	apparent conductivity 125m below surface
SL_cdiatdepth150m.grd	Sandy Lake	apparent conductivity 150m below surface
SL_cdiatdepth175m.grd	Sandy Lake	apparent conductivity 175m below surface
SL_cdiatdepth200m.grd	Sandy Lake	apparent conductivity 200m below surface
SL_cdiatdepth225m.grd	Sandy Lake	apparent conductivity 225m below surface
SL_cdiatdepth250m.grd	Sandy Lake	apparent conductivity 250m below surface
SL_cdiatdepth275m.grd	Sandy Lake	apparent conductivity 275m below surface
SL_cdiatdepth300m.grd	Sandy Lake	apparent conductivity 300m below surface
SL_cdiatdepth325m.grd	Sandy Lake	apparent conductivity 325m below surface
SL_cdiatdepth350m.grd	Sandy Lake	apparent conductivity 350m below surface
SL_cdiatdepth375m.grd	Sandy Lake	apparent conductivity 375m below surface
SL_cdiatdepth400m.grd	Sandy Lake	apparent conductivity 400m below surface
SL_cdiatdepth425m.grd	Sandy Lake	apparent conductivity 425m below surface
SL_cdiatdepth450m.grd	Sandy Lake	apparent conductivity 450m below surface
SL_cdiatdepth475m.grd	Sandy Lake	apparent conductivity 475m below surface
SL_cdiatdepth500m.grd	Sandy Lake	apparent conductivity 500m below surface
SL_cdiatdepth525m.grd	Sandy Lake	apparent conductivity 525m below surface
SL_cdiatdepth550m.grd	Sandy Lake	apparent conductivity 550m below surface
SL_cdiatdepth575m.grd	Sandy Lake	apparent conductivity 575m below surface
SL_cdiatdepth600m.grd	Sandy Lake	apparent conductivity 600m below surface
SL_cdiatdepth625m.grd	Sandy Lake	apparent conductivity 625m below surface
SL_cdiatdepth650m.grd	Sandy Lake	apparent conductivity 650m below surface
SL_cdiatdepth675m.grd	Sandy Lake	apparent conductivity 675m below surface
SL_cdiatdepth700m.grd	Sandy Lake	apparent conductivity 700m below surface
FL_cdiatdepth025m.grd	Favourable Lake	apparent conductivity 25m below surface
FL_cdiatdepth050m.grd	Favourable Lake	apparent conductivity 50m below surface

Grid name	Survey block	Description
FL_cdiatdepth075m.grd	Favourable Lake	apparent conductivity 75m below surface
FL_cdiatdepth100m.grd	Favourable Lake	apparent conductivity 100m below surface
FL_cdiatdepth125m.grd	Favourable Lake	apparent conductivity 125m below surface
FL_cdiatdepth150m.grd	Favourable Lake	apparent conductivity 150m below surface
FL_cdiatdepth175m.grd	Favourable Lake	apparent conductivity 175m below surface
FL_cdiatdepth200m.grd	Favourable Lake	apparent conductivity 200m below surface
FL_cdiatdepth225m.grd	Favourable Lake	apparent conductivity 225m below surface
FL_cdiatdepth250m.grd	Favourable Lake	apparent conductivity 250m below surface
FL_cdiatdepth275m.grd	Favourable Lake	apparent conductivity 275m below surface
FL_cdiatdepth300m.grd	Favourable Lake	apparent conductivity 300m below surface
FL_cdiatdepth325m.grd	Favourable Lake	apparent conductivity 325m below surface
FL_cdiatdepth350m.grd	Favourable Lake	apparent conductivity 350m below surface
FL_cdiatdepth375m.grd	Favourable Lake	apparent conductivity 375m below surface
FL_cdiatdepth400m.grd	Favourable Lake	apparent conductivity 400m below surface
FL_cdiatdepth425m.grd	Favourable Lake	apparent conductivity 425m below surface
FL_cdiatdepth450m.grd	Favourable Lake	apparent conductivity 450m below surface
FL_cdiatdepth475m.grd	Favourable Lake	apparent conductivity 475m below surface
FL_cdiatdepth500m.grd	Favourable Lake	apparent conductivity 500m below surface
FL_cdiatdepth525m.grd	Favourable Lake	apparent conductivity 525m below surface
FL_cdiatdepth550m.grd	Favourable Lake	apparent conductivity 550m below surface
FL_cdiatdepth575m.grd	Favourable Lake	apparent conductivity 575m below surface
FL_cdiatdepth600m.grd	Favourable Lake	apparent conductivity 600m below surface
FL_cdiatdepth625m.grd	Favourable Lake	apparent conductivity 625m below surface
FL_cdiatdepth650m.grd	Favourable Lake	apparent conductivity 650m below surface
FL_cdiatdepth675m.grd	Favourable Lake	apparent conductivity 675m below surface
FL_cdiatdepth700m.grd	Favourable Lake	apparent conductivity 700m below surface

The following Geosoft® voxels of apparent conductivity are provided:

SL_CDI_AppCond_clip_win.geosoft_voxel – CDI voxel for Sandy Lake Block

FL_CDI_AppCond_clip_win.geosoft_voxel – CDI voxel for Favourable Lake Block

In addition, PDF files of plotted CDI sections (one per flight line) are presented in the following files:

- SLMAGEM_CDI_Sections_All_Lines(singleZON) – CDI sections with common colour scheme for Sandy Lake Block
- FLMAGEM_CDI_Sections_All_Lines(singleZON) – CDI sections with common colour scheme for Favourable Lake Block

Appendix H. Survey Block Co-Ordinates

Table 12. Sandy Lake Block co-ordinates.

Sandy Lake Block	
WGS84 UTM Zone 15N	
X	Y
453500	5865850
453500	5882300
450300	5882300
450300	5885800
445150	5885800
445150	5901850
462750	5901850
462750	5888350
467000	5888350
467000	5886850
481200	5882600
514900	5885300
514900	5901600
528450	5901600
533200	5883000
533200	5867850
524500	5867850
524500	5875100
493650	5872950
480500	5865850
453500	5865850

Table 13. Favourable Lake Block Co-ordinates.

Favourable Lake Block	
WGS84 UTM Zone 15N	
X	Y
388300	5888850
382719	5883513
382171	5883541
380458	5881082
401000	5879950
460450	5838150
459450	5836750
469950	5827250
473400	5832200
468900	5844250
475150	5853150
455550	5863450
446800	5865600
443900	5862200
437100	5864850
428200	5873600
428700	5874350
412150	5883900
410350	5881400

Appendix I. General Modelling Results of the VTEM System

Introduction

The VTEM system is based on a concentric or central loop design, whereby, the receiver is positioned at the centre of a transmitter loop that produces a primary field. The wave form is a bipolar, modified square wave with a turn-on and turn-off at each end.

During turn-on and turn-off, a time varying field is produced (dB/dt) and an electromotive force (emf) is created as a finite impulse response. A current ring around the transmitter loop moves outward and downward as time progresses. When conductive rocks and mineralization are encountered, a secondary field is created by mutual induction and measured by the receiver at the centre of the transmitter loop.

Efficient modelling of the results can be carried out on regularly shaped geometries, thus yielding close approximations to the parameters of the measured targets. The following is a description of a series of common models made for the purpose of promoting a general understanding of the measured results.

A set of models has been produced for the Geotech VTEM®Plus system dB/dt Z- and X-components (*see* models in Figures I-1 to I-6). The Maxwell ™ modelling program (EMIT Technology Pty. Ltd. Midland, WA, AU) used to generate the following responses assumes a resistive half-space. The reader is encouraged to review these models, so as to get a general understanding of the responses as they apply to survey results. While these models do not begin to cover all possibilities, they give a general perspective on the simple and most commonly encountered anomalies.

As the plate dips and departs from the vertical position, the peaks become asymmetrical.

As the dip increases, the aspect ratio (Min/Max) decreases and this aspect ratio can be used as an empirical guide to dip angles from near 90º to about 30º. The method is not sensitive enough where dips are less than about 30º.

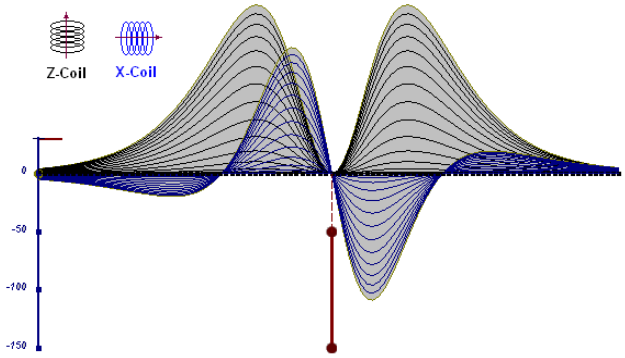

Figure I-1. vertical thin plate

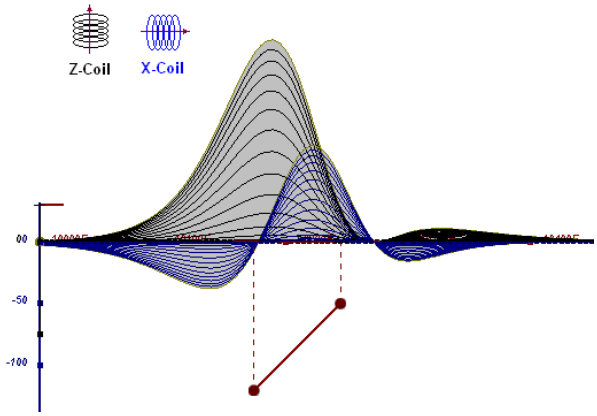

Figure I-2. inclined thin plate

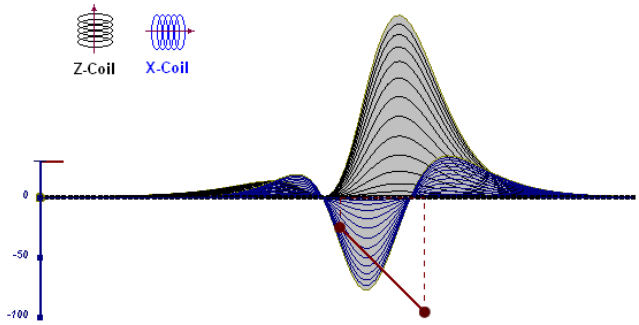

Figure I-3. inclined thin plate

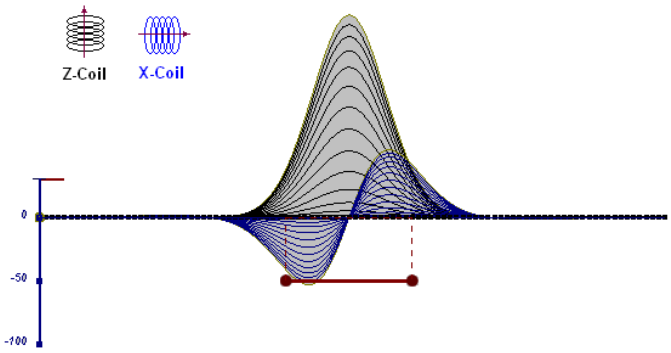

Figure I-4. horizontal thin plate

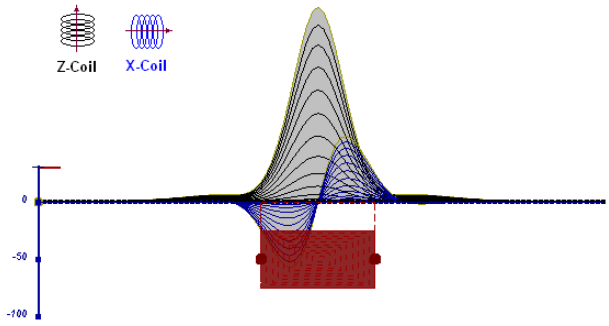

Figure I-5. horizontal thick plate (linear scale of the response)

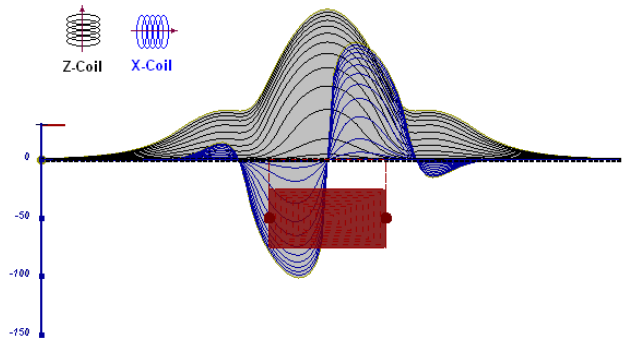

Figure I-6. horizontal thick plate (log scale of the response)

Appendix J. EM Time Constant (Tau) Analysis

Estimation of time constant parameter in transient electromagnetic method is one of the steps towards the extraction of the information about conductances beneath the surface from TEM measurements.

The most reliable method to discriminate or rank conductors from overburden, background or one and other is by calculating the EM field decay time constant (TAU parameter), which directly depends on conductance despite their depth and accordingly amplitude of the response.

Theory

As established in electromagnetic theory, the magnitude of the electromotive force (emf) induced is proportional to the time rate of change of primary magnetic field at the conductor. This emf causes eddy currents to flow in the conductor with a characteristic transient decay, whose time constant (Tau) is a function of the conductance of the survey target or conductivity and geometry (including dimensions) of the target. The decaying currents generate a proportional secondary magnetic field, the time rate of change of which is measured by the receiver coil as induced voltage during the off time.

The receiver coil output voltage ($\mathbf{e_0}$) is proportional (α) to the time rate of change of the secondary magnetic field and has the form,

$$e_0 \ \alpha \ (1 / \tau)\, e^{-(t/\tau)}$$

Where,
τ = L/R is the characteristic time constant of the target (TAU)
R = resistance
L = inductance

From the expression, conductive targets that have small value of resistance and hence large value of τ (tau) yield signals with small initial amplitude that decays relatively slowly with progress of time. Conversely, signals from poorly conducting targets that have large resistance value and small τ, have high initial amplitude but decay rapidly with time (Figure J-1).

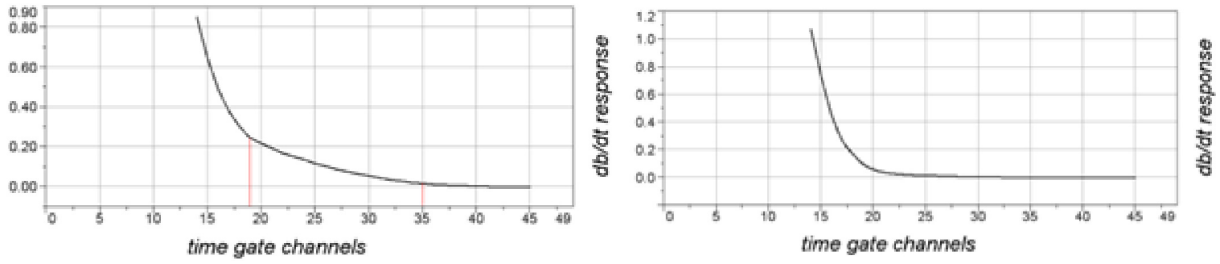

Figure J-1. Left – example of off-time decay curve of good conductor, right – poor conductor.

EM Time Constant (Tau) Calculation

The EM time constant (TAU) is a general measure of the speed of decay of the electromagnetic response and indicates the presence of eddy currents in conductive sources as well as reflecting the "conductance quality" of a source. Although TAU can be calculated using either the measured dB/dt decay or the calculated B-field decay, dB/dt is commonly preferred due to better stability (S/N) relating to signal noise. Generally, TAU calculated on base of early time response reflects both near surface overburden and poor conductors whereas, in the late ranges of time, deep and more conductive sources, respectively. For example early time TAU distribution in an area that indicates conductive overburden is shown in Figure J-2. In Figure J-3, the full time range is displayed, showing the expression of a deep, highly conductive target in the left side of the image.

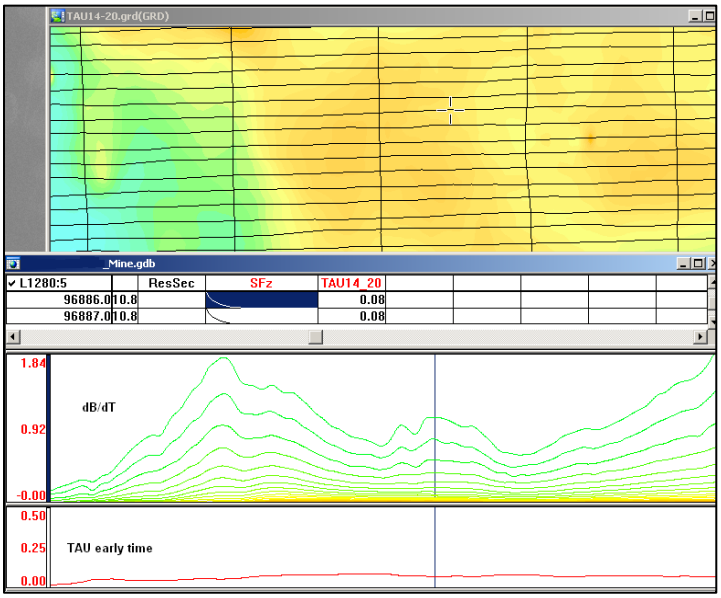

Figure J-2. Map of early time TAU. Area with overburden conductive layer and local sources.

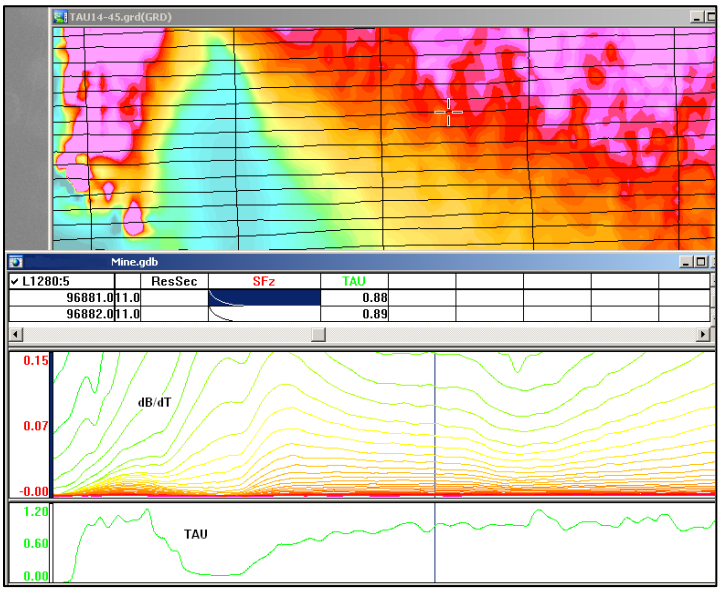

Figure J-3. Map of full time range TAU with EM anomaly due to deep highly conductive target.

There are many advantages of TAU maps:

- TAU depends only on one parameter (conductance) in contrast to response magnitude;
- TAU is integral parameter, which covers time range and all conductive zones and targets are displayed independently of their depth and conductivity on a single map.
- Very good differential resolution in complex conductive places with many sources with different conductivity.
- Signs of the presence of good conductive targets are amplified and emphasized independently of their depth and level of response accordingly.

In the examples shown in Figures J-4 and J-5, 3 local targets are defined, each of them with a different depth of burial, as indicated on the resistivity depth image (RDI). All are very good conductors but the deeper target (number 2) has a relatively weak dB/dt signal yet also features the strongest total TAU (Figure J-6). This example highlights the benefit of TAU analysis in terms of an additional target discrimination tool.

The EM time constants for dB/dt and B-field were calculated using the "sliding Tau" in-house program developed at Geotech. The principle of the calculation is based on using of time window (4 time channels) which is sliding along the curve decay and looking for latest time channels which have a response above the level of noise and decay. The EM decays are obtained from all available decay channels, starting at the latest channel. Time constants are taken from a least square fit of a straight-line (log/linear space) over the last 4 gates above a preset signal threshold level (Figure J-4). Threshold settings are pointed in the "label" property of TAU database channels. The sliding Tau method determines that, as the amplitudes increase, the time-constant is taken at progressively later times in the EM decay. Conversely, as the amplitudes decrease, Tau is taken at progressively earlier times in the decay. If the maximum signal amplitude falls below the threshold, or becomes negative for any of the 4 time gates, then Tau is not calculated and is assigned a value of "dummy" by default.

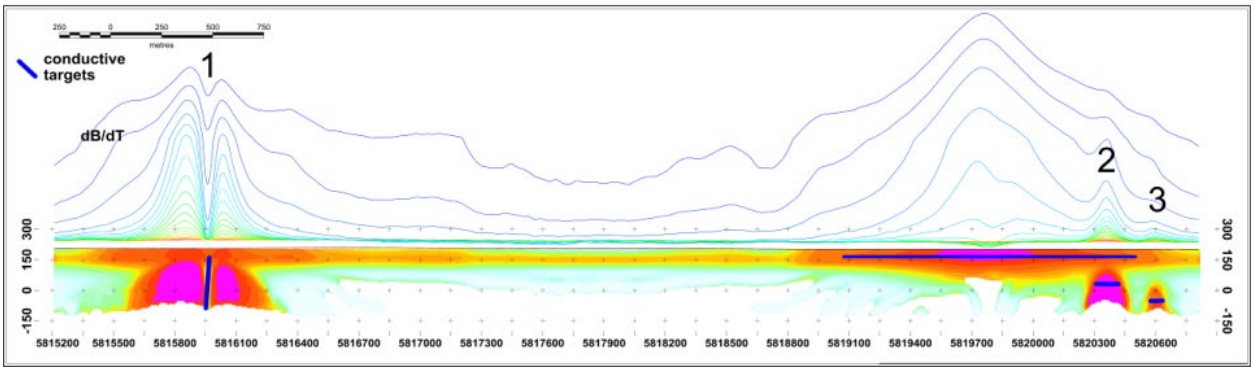

Figure J-4. dB/dt profile and RDI with different depths of targets.

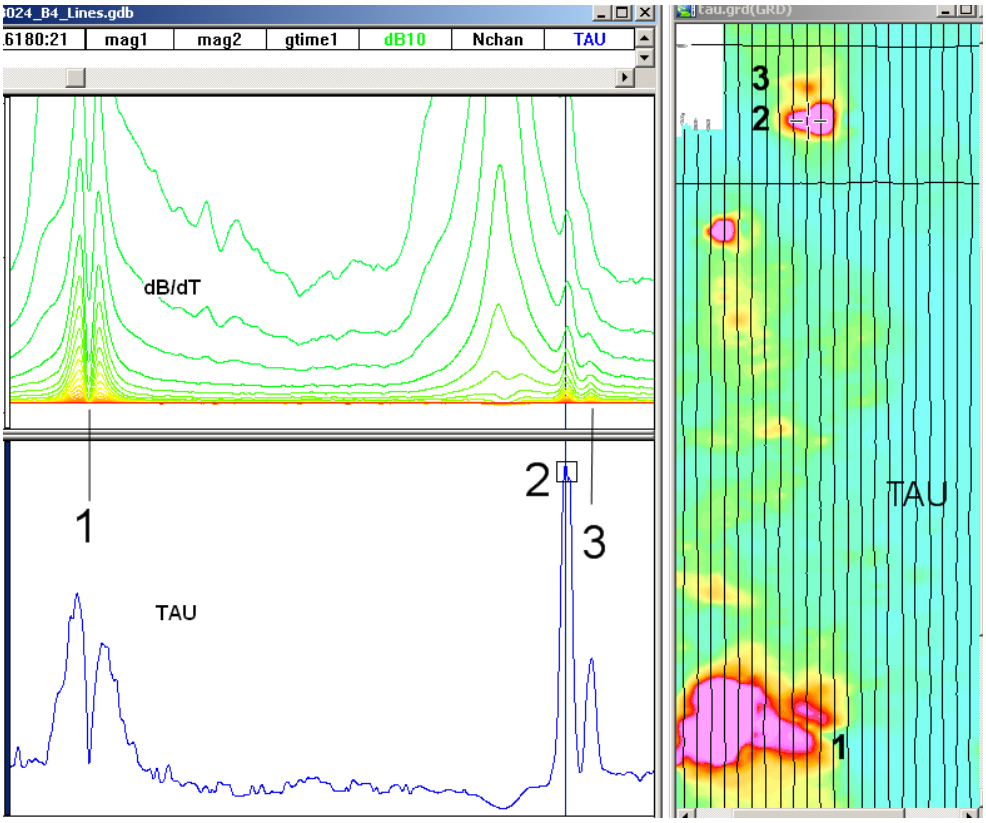

Figure J-5. Map of total TAU and dB/dt profile.

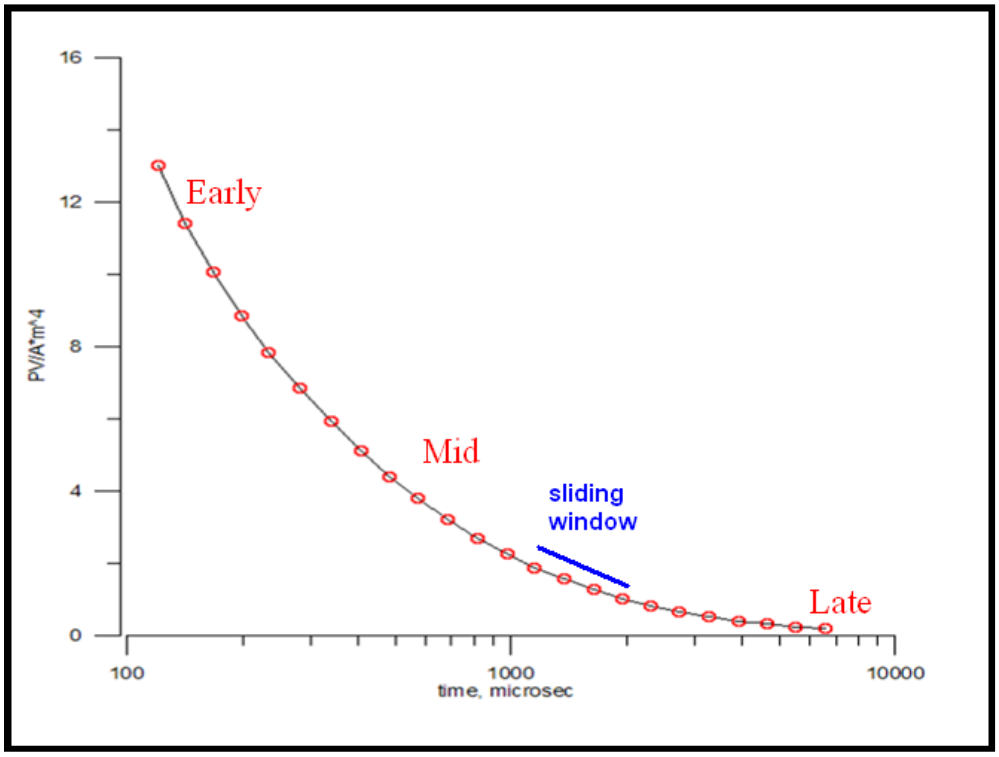

Figure J-6. Typical dB/dt decays of VTEM data.

Appendix K. TEM Resistivity Depth Imaging (RDI)

Resistivity depth imaging (RDI) is technique used to rapidly convert EM profile decay data into an equivalent resistivity versus depth cross-section, by deconvolution of the measured TEM data. The used RDI algorithm of resistivity-depth transformation is based on scheme of the apparent resistivity transform of Meju (1998) and TEM response from conductive half-space. The program was developed by Alexander Prikhodko for Geotech Ltd. (2011) and depth calibrated based on forward plate modelling for VTEM system configuration (Figures K-1 to 11).

RDIs provide reasonable indications of conductor relative depth and vertical extent, as well as accurate 1D layered-earth apparent conductivity/resistivity structure across VTEM flight lines.

Approximate depth of investigation of a TEM system, image of secondary field distribution in half space, effective resistivity, initial geometry and position of conductive targets is the information obtained on base of the RDIs.

Maxwell forward modeling with RDI sections from the synthetic responses (VTEM system)

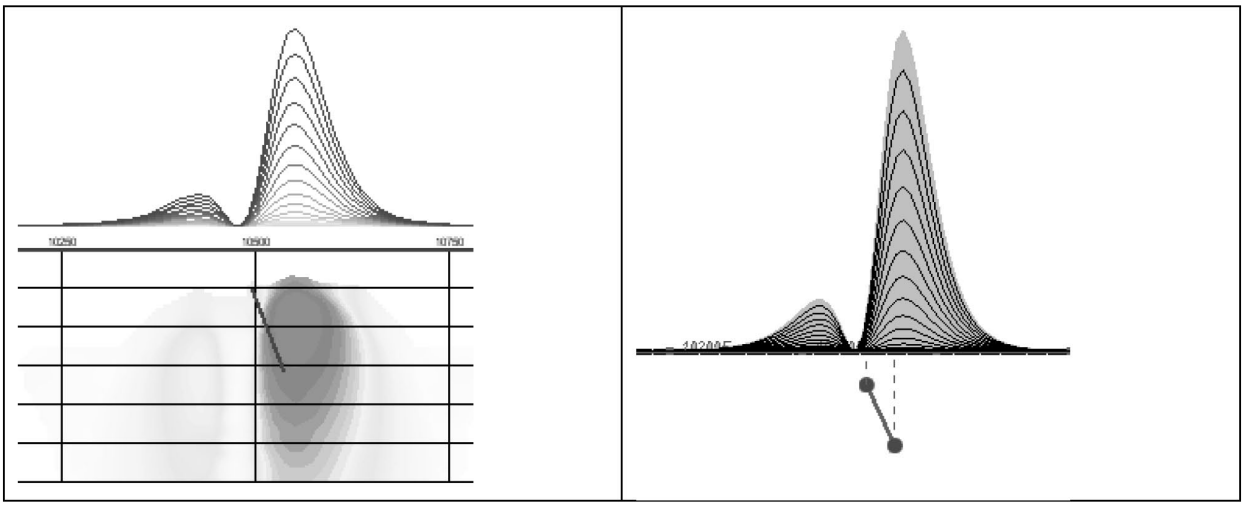

Figure K-1: Maxwell plate model and RDI from the calculated response for conductive "thin" plate (depth 50 m, dip 65 degree, depth extend 100 m).

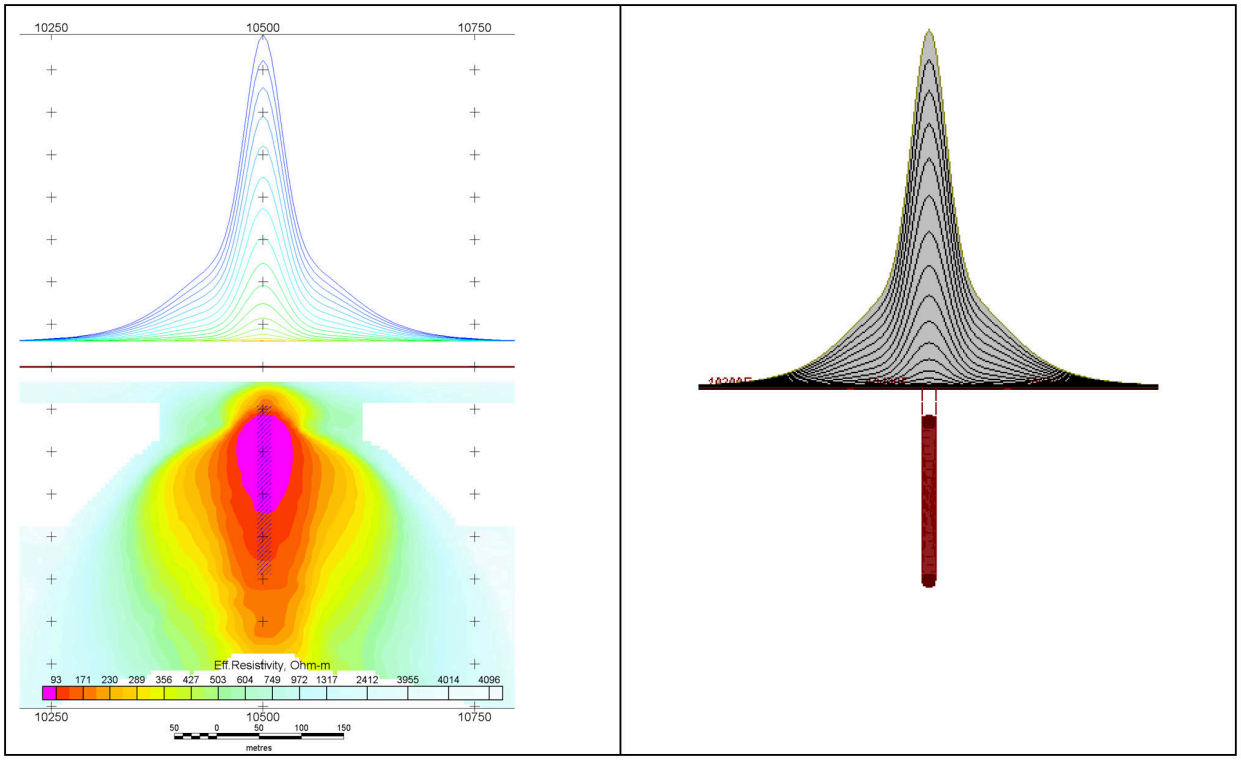

Figure K-2: Maxwell plate model and RDI from the calculated response for "thick" plate 18 m thickness, depth 50 m, depth extend 200 m).

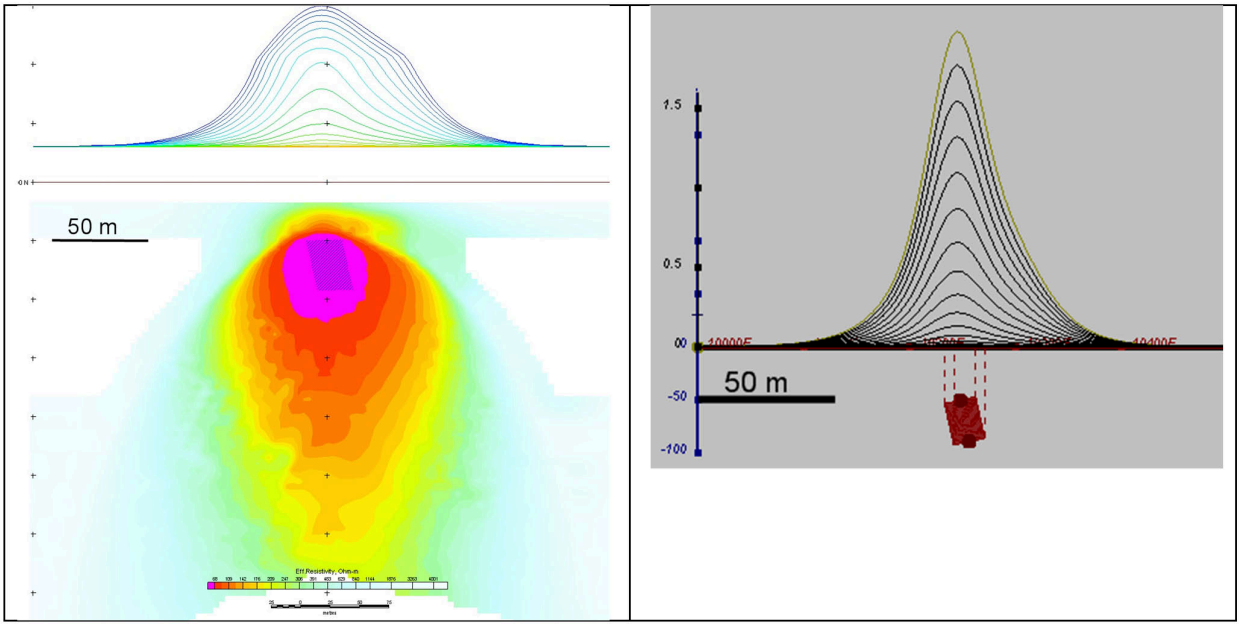

Figure K-3: Maxwell plate model and RDI from the calculated response for bulk ("thick") 100 m length, 40 m depth extend, 30 m thickness

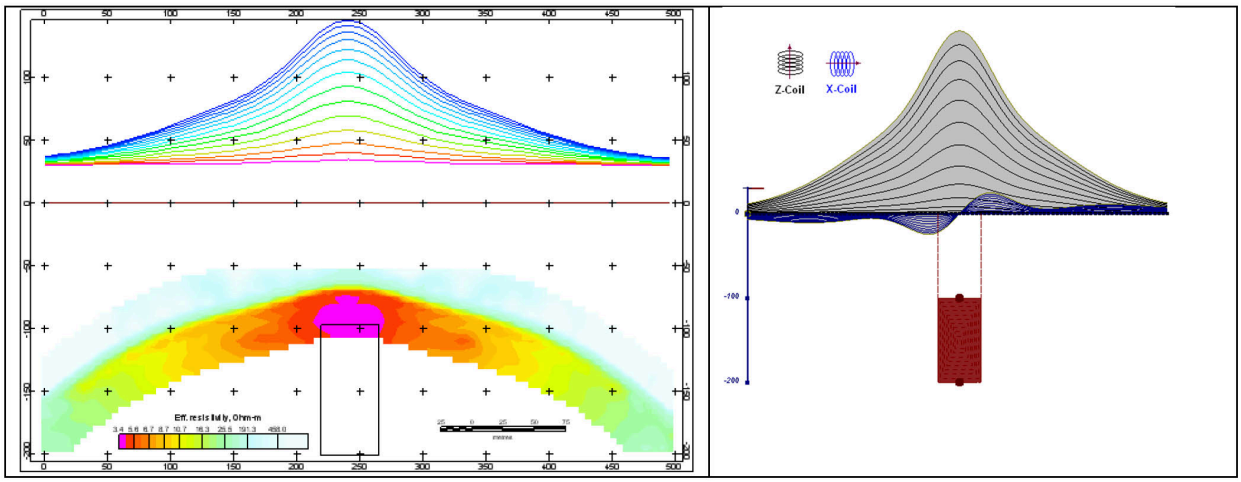

Figure K-4: Maxwell plate model and RDI from the calculated response for "thick" vertical target (depth 100 m, depth extend 100 m). 19-44 chan.

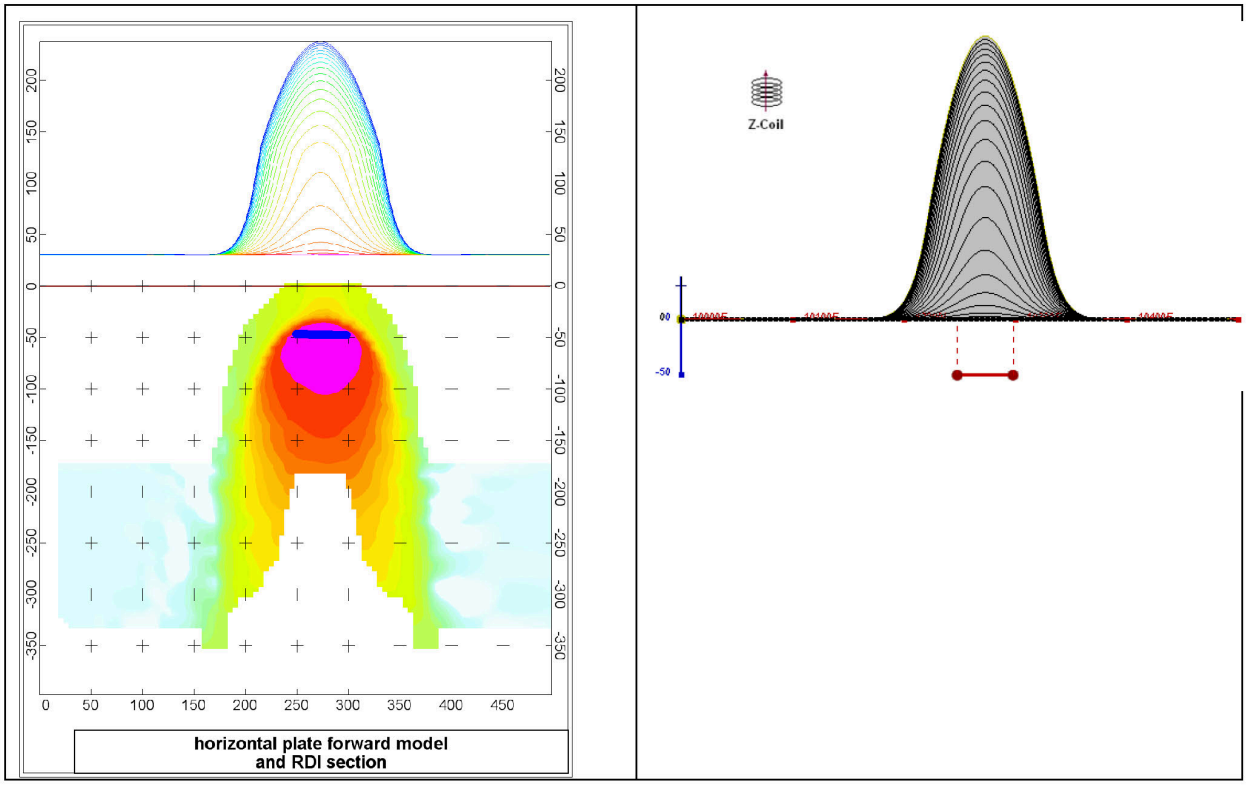

Figure K-5: Maxwell plate model and RDI from the calculated response for horizontal thin plate (depth 50 m, dim 50x100 m). 15-44 chan.

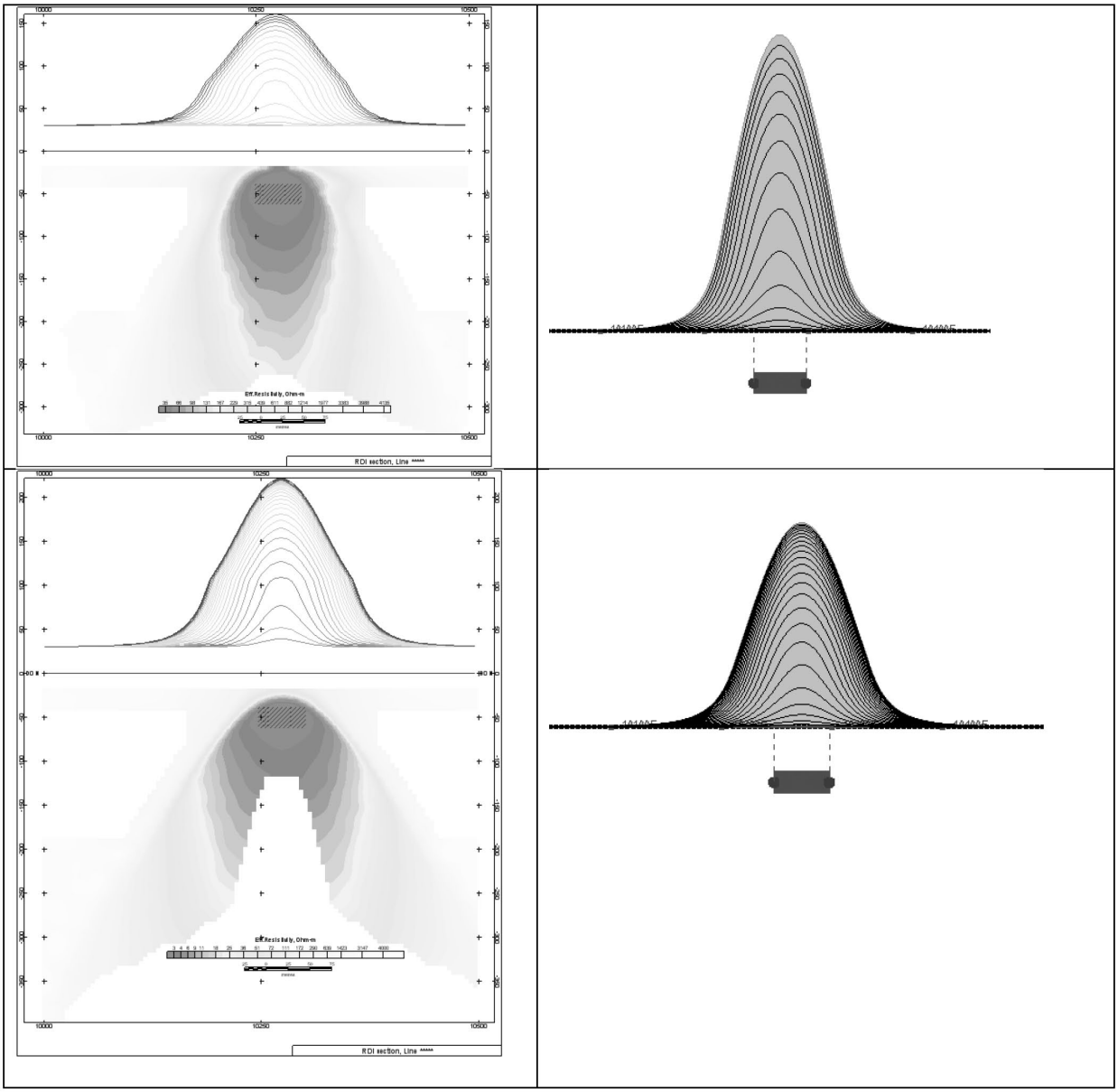

Figure K-6: Maxwell plate model and RDI from the calculated response for horizontal thick (20m) plate – less conductive (on the top), more conductive (below)

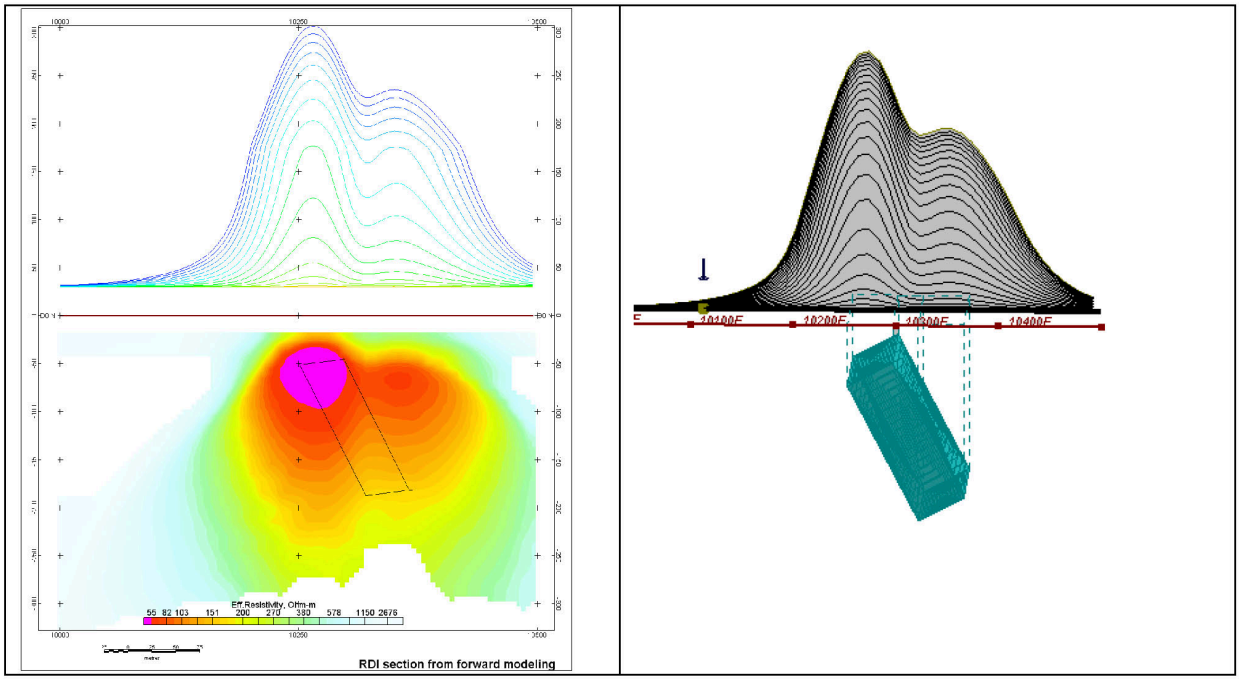

Figure K-7: Maxwell plate model and RDI from the calculated response for inclined thick (50m) plate. Depth extends 150 m, depth to the target 50 m.

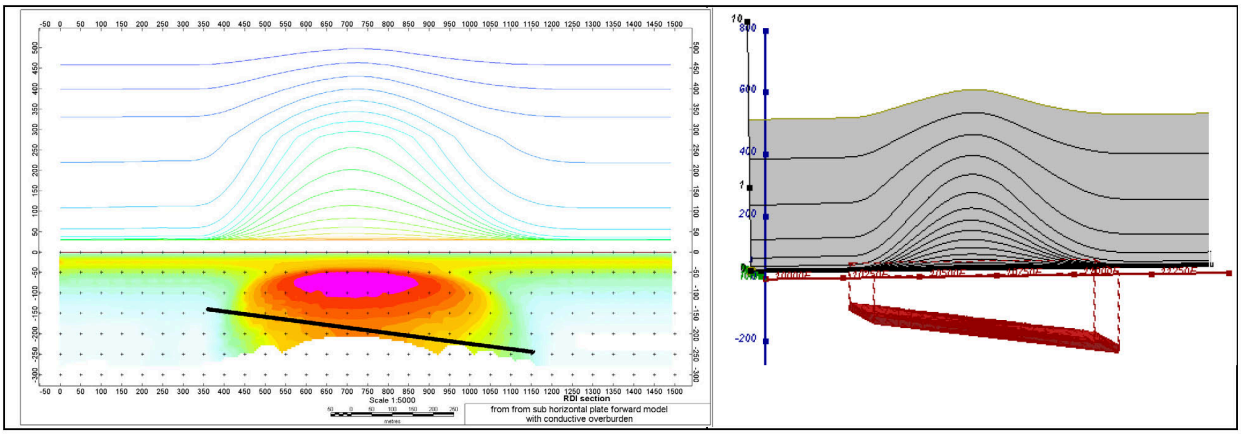

Figure K-8: Maxwell plate model and RDI from the calculated response for the long, wide and deep subhorizontal plate (depth 140 m, dim 25x500x800 m) with conductive overburden.

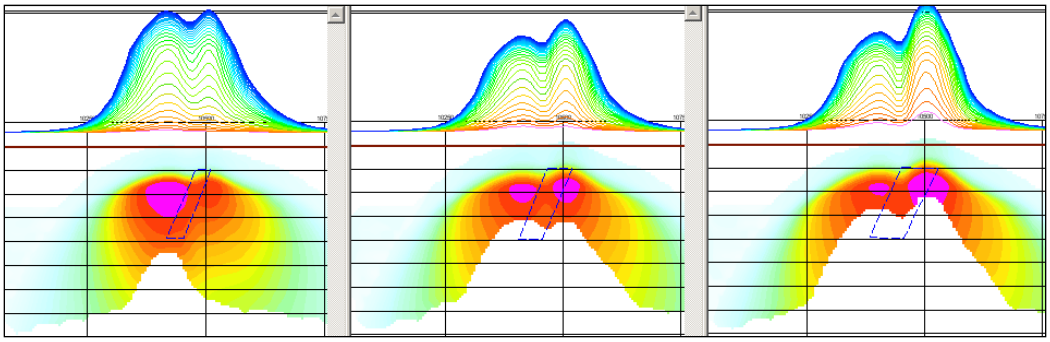

Figure K-9: Maxwell plate models and RDIs from the calculated response for "thick" dipping plates (35, 50, 75 m thickness), depth 50 m, conductivity 2.5 S/m.

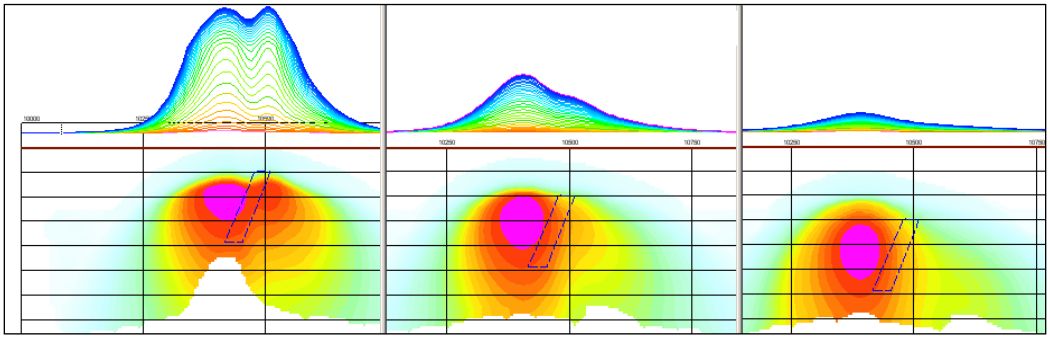

Figure K-10: Maxwell plate models and RDIs from the calculated response for "thick" (35 m thickness) dipping plate on different depth (50, 100, 150 m), conductivity 2.5 S/m.

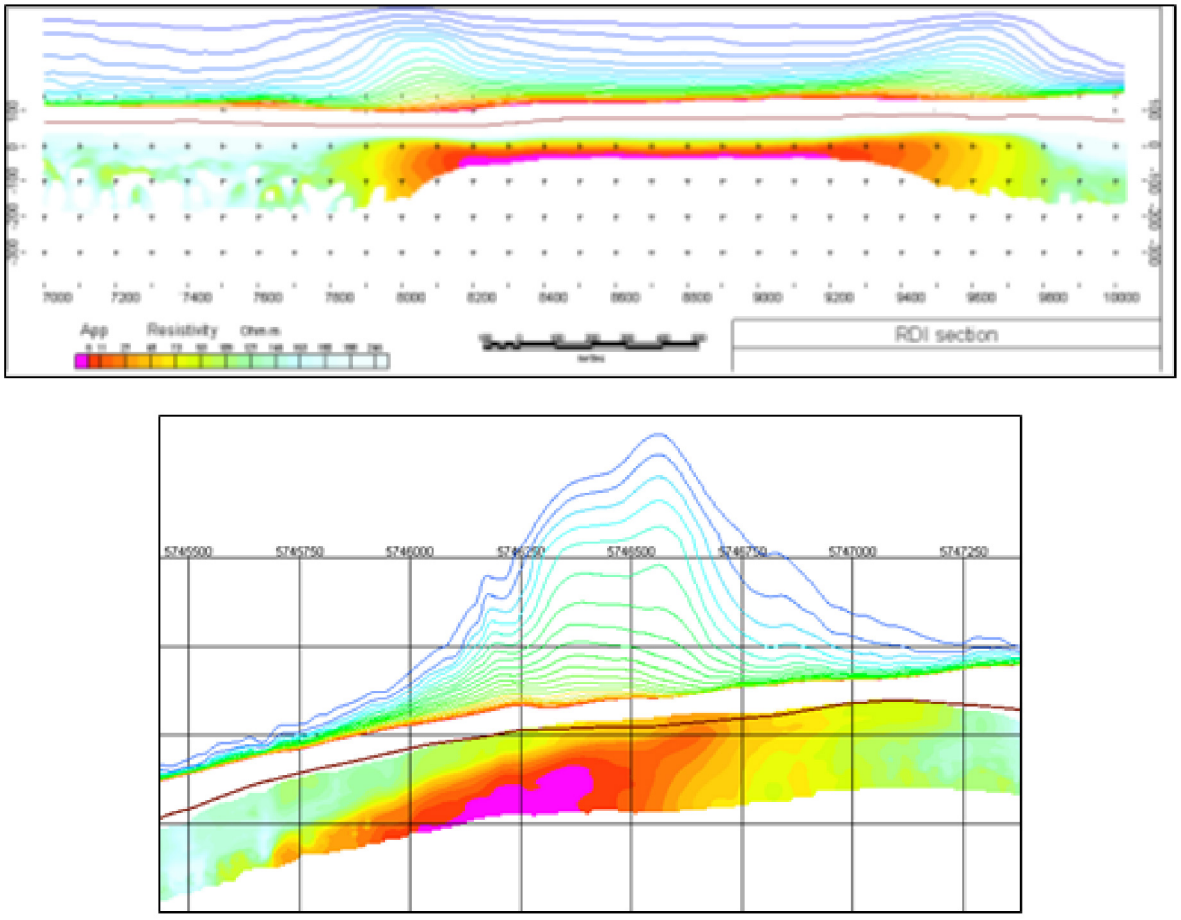

Figure K-11: RDI section for the real horizontal and slightly dipping conductive layers

FORMS OF RDI PRESENTATION

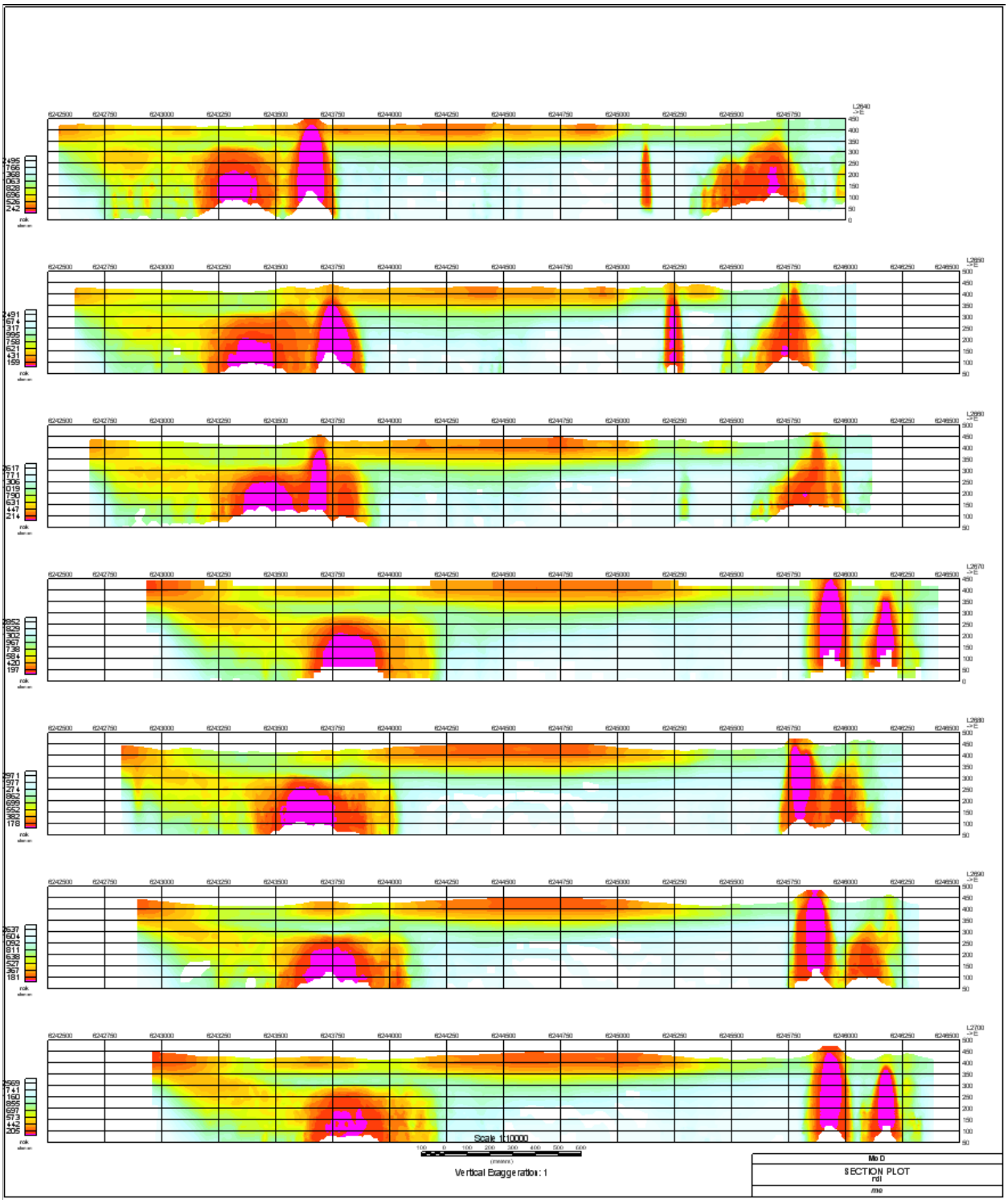

Figure K-12: Presentation of series of lines.

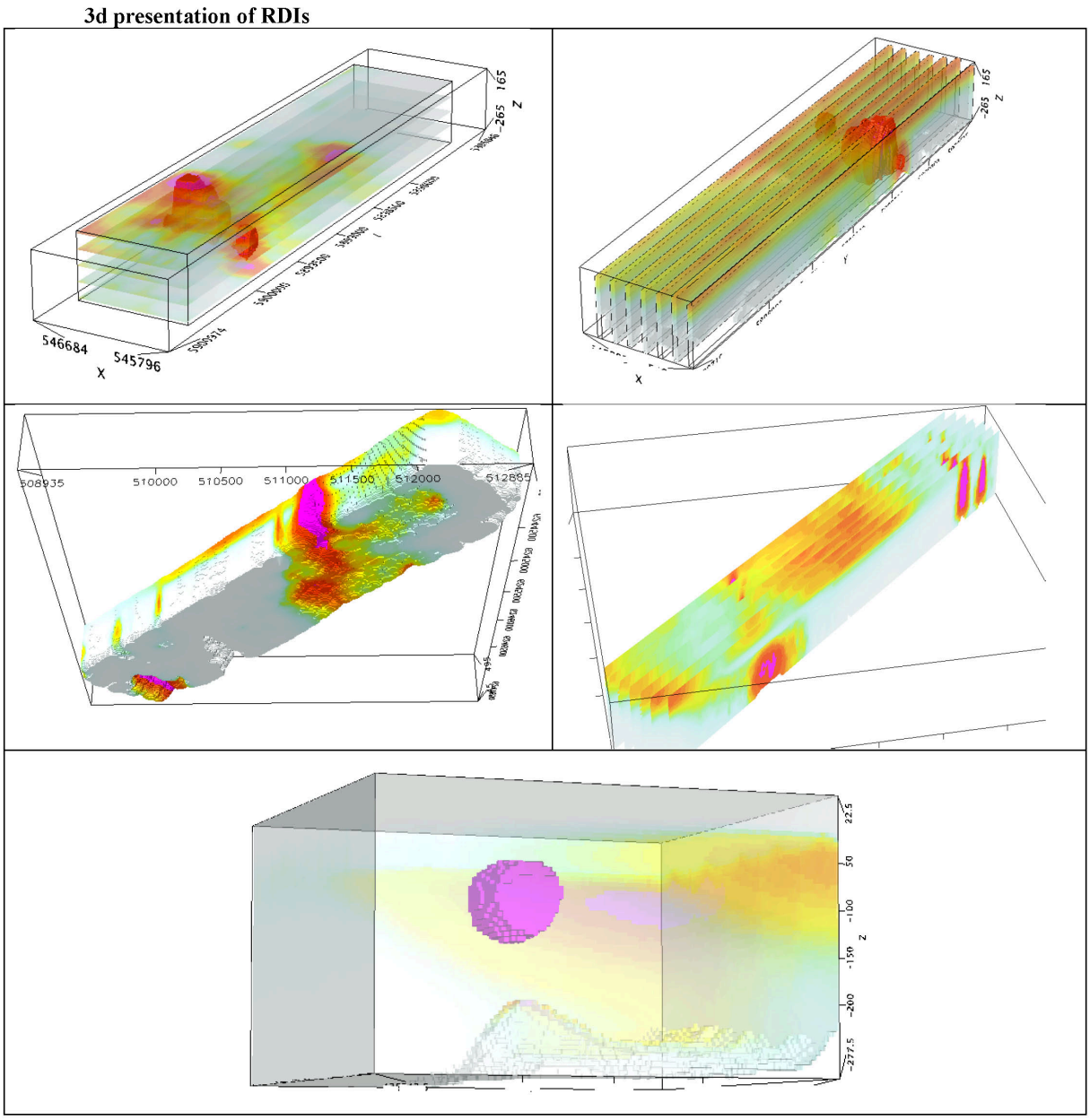

Figure K-13: 3-D presentation of RDIs.

Apparent Resistivity Depth Slices plans:

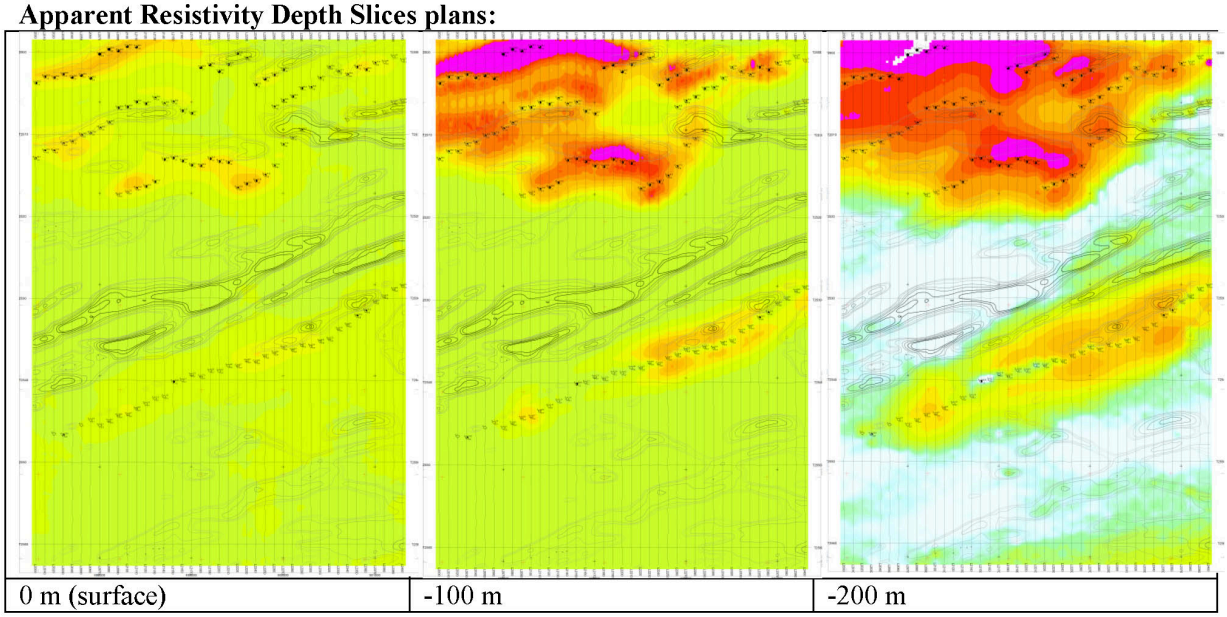

Figure K-14: Apparent resistivity depth slices plans.

3d views of apparent resistivity depth slices:

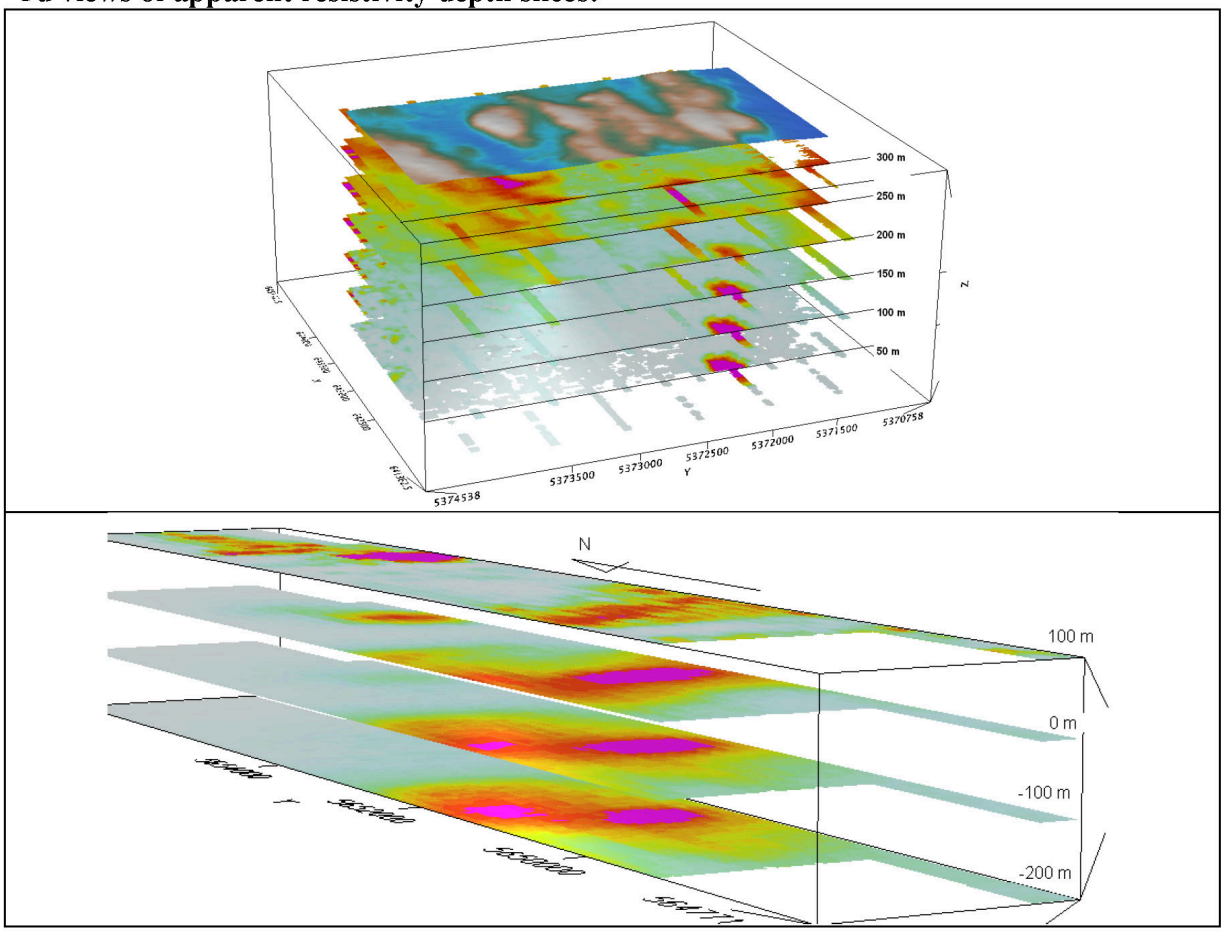

Figure K-15: 3-D views of resistivity depth slices.

Real base metal targets in comparison with RDIs:

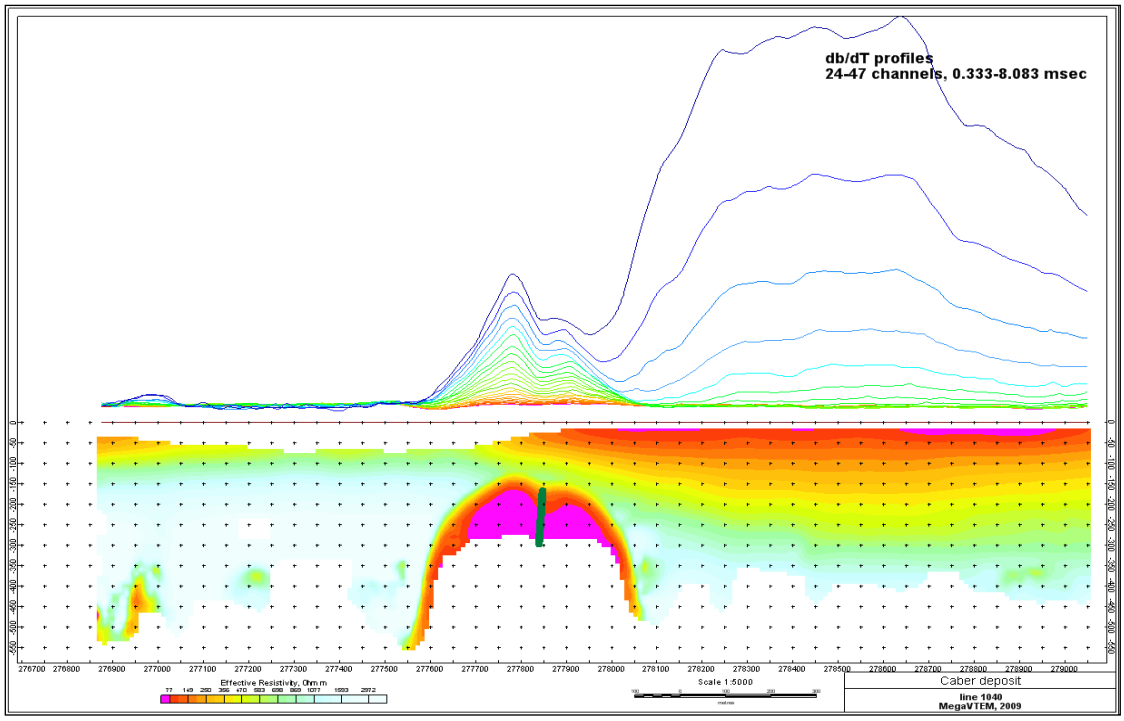

Figure K-16: RDI section of the line over Caber deposit ("thin" subvertical plate target and conductive overburden).

3d RDI voxels with base metals ore bodies (Middle East):

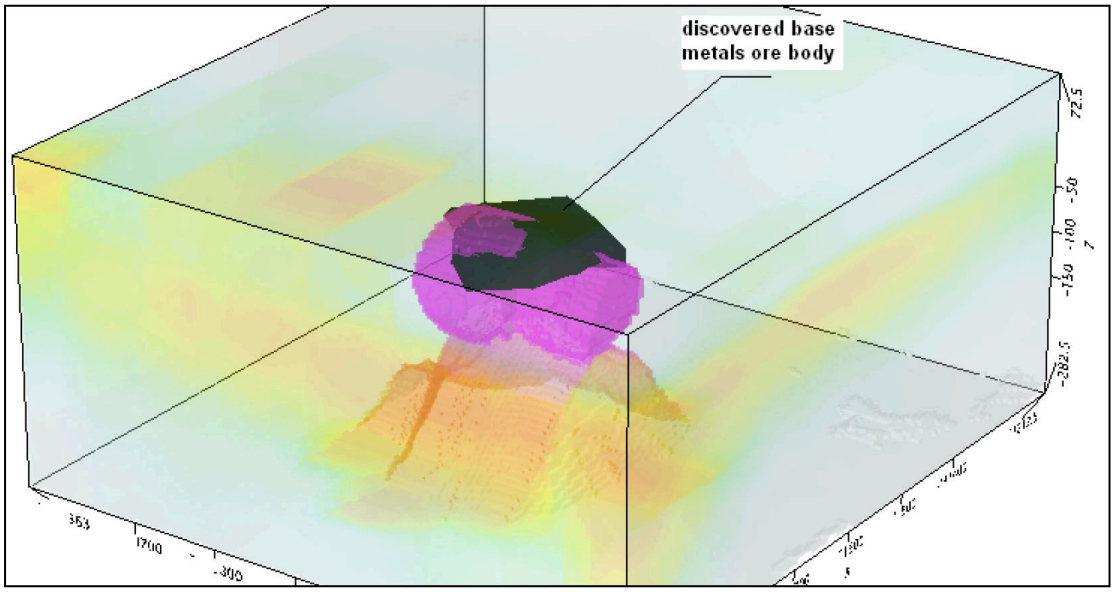

Figure K-17: 3-D RDI voxels with base metals ore bodies (Middle East).

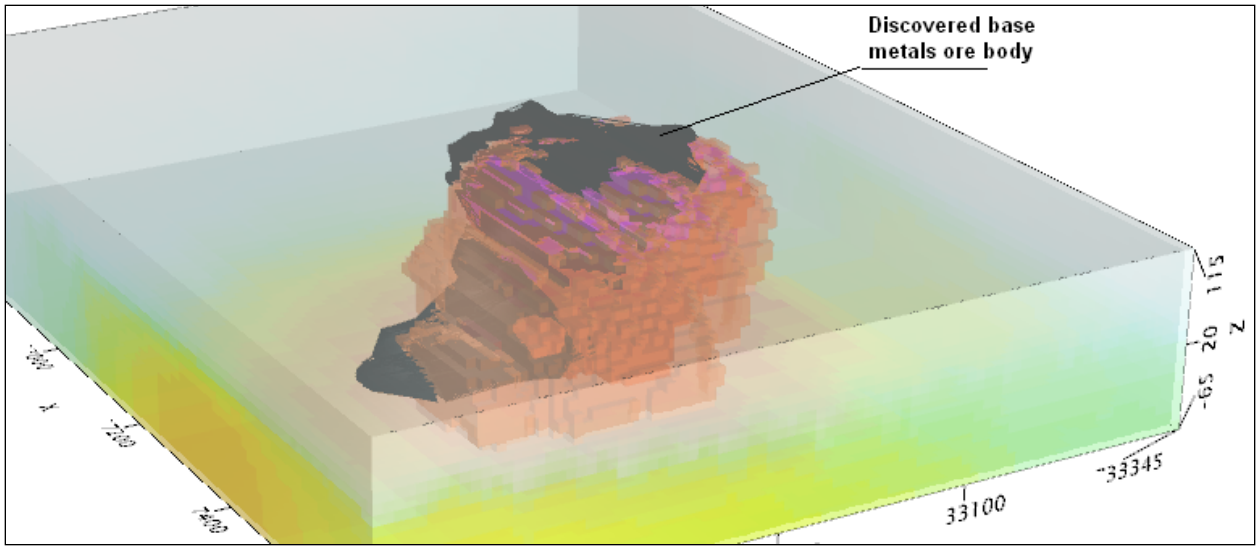

Figure K-18: 3-D RDI voxels with discovered base metals ore body.

Appendix L. Test Sites and Calibrations

MOREWOOD TEST SITE

The Morewood test was flown to ensure that the aeromagnetic system measures the total field values with an absolute accuracy of 10 nT or less after the aircraft has been compensated. This test requires that data is recorded coincidentally with the data from the nearby Ottawa magnetic observatory.

With the magnetic sensor at 1500 feet, the 4 cardinal headings are flown, repeating the entire test twice for a total of 8 passes. The test was performed on July 5, 2017 as presented in Figure L-1, and results in Figure L-2.

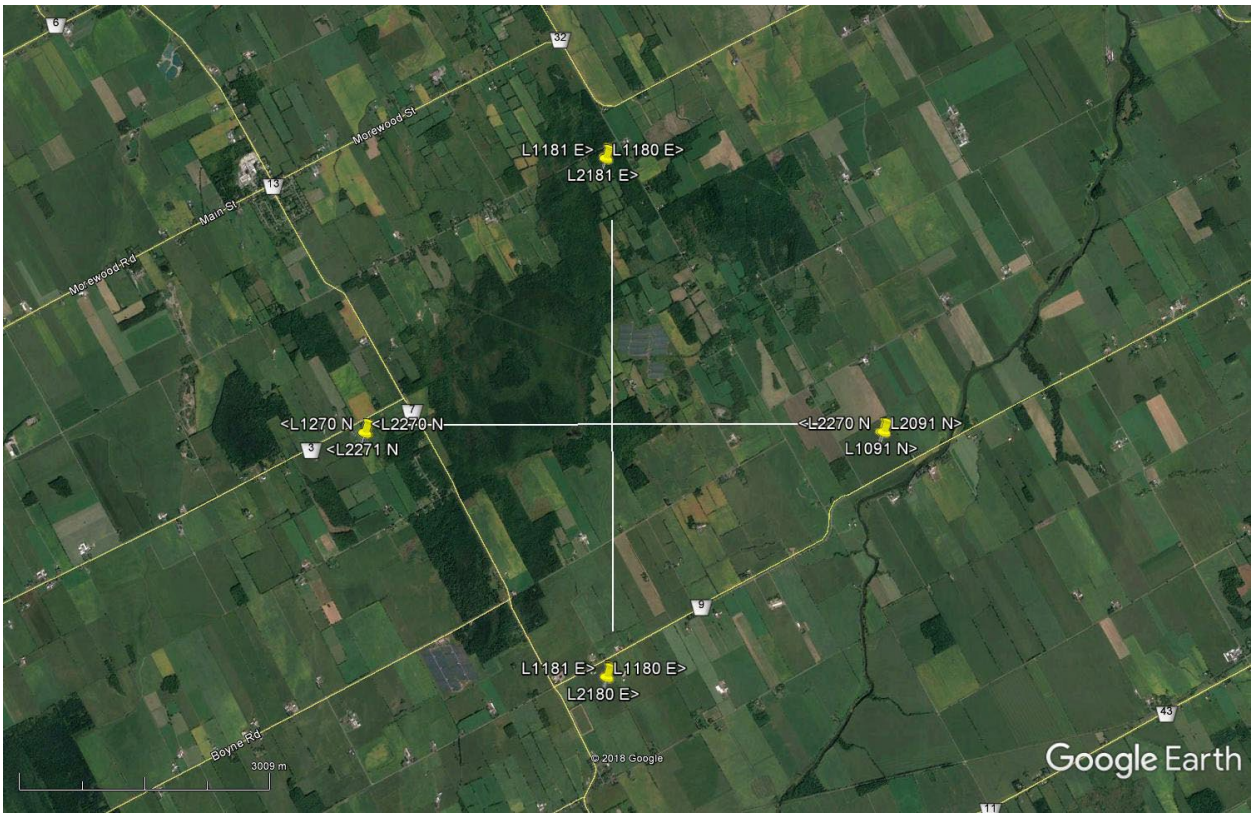

Figure L-1. Morewood test lines shown on Google Earth™ (July 5, 2017).

AEROMAGNETIC SURVEY SYSTEM CALIBRATION TEST RANGES AT MOREWOOD, ONTARIO

AIRCRAFT TYPE AND REGISTRATION: Astar B3 C-FKOI
ORGANIZATION (COMPANY): Geotech Limited
MAGNETOMETER TYPE: G-822A
MAGNETOMETER SERIAL NUMBER:
COMPILED BY: N.Fiset

DATE: 05/07/2017 DD/MM/YYYY
HEIGHT FLOWN: 1500 FEET
SAMPLING RATE: 10 / SECOND
DATA ACQUISITION SYSTEM: Geotech DAQ
GSC 12/99

Direction of flight across the Crossroads	Time that Survey Aircraft was over the Crossroads (HH/MM/SS) Greenwich Mean Time	Total Field Value (nT) Recorded in Survey Aircraft over Crossroads (T1)	Observatory Diurnal Reading at Previous Minute i.e. Hours + Minutes (T2) from Printout	Observatory Diurnal Reading at Subsequent Minute i.e. H hours + (M + 1) mins. (T3) from Printout	Interpolated Observatory Diurnal Reading at Time H hours + M mins + S sec T4 = T2 + S (T3 - T2) ----- 60	Calculated Observatory Value T5 = T4 - C*	Error Value T6 = T1 - T5
EXAMPLE	20:34:40 Z	56840.4 nT	57397.5 nT	57398.3 nT	57398.0 nT	56842.0 nT	-1.6 nT
2360 N	13:44:15.5	53617.5			54259.0	53620.3	-2.8
2180 S	13:49:23.6	53618.4			54259.5	53620.8	-2.4
2090 E	14:07:17.2	53616.2			54257.1	53618.4	-2.2
2270 W	14:11:51.4	53616.1			54256.7	53618.0	-1.9
2361 N	13:54:39.3	53617.2			54258.6	53619.9	-2.7
2181 S	13:59:37.4	53616.7			54257.7	53619.0	-2.3
2091 E	14:16:15.3	53615.0			54255.9	53617.2	-2.2
2271 W	14:20:56.7	53614.9			54255.6	53616.9	-2.0

*C is the difference in the total field between the Blackburn or Meanook Observatory value (O) and the value (B) at the point above the crossroads at a given height. Blackburn Observatory: 1500 Feet, C = (O-B) = 638.7 nT
Meanook Observatory: 1000 Feet, C = (O-B) = 0 nT; 500 Feet, C = 0 nT Total = -18.5 nT

Average North-South Heading Error (T6 North - T6 South) = -0.4 nT
Average East-West Heading Error (T6 East - T6 West) = -0.25 nT Number of Passes for Average = 8 2.31 nT

The completed document must be forwarded to the GSC Project Leader prior to the start of field operations and a copy must be attached to the next weekly report.

Figure L-2. Aeromagnetic survey system calibration test ranges at Morewood, Ontario.

REID–MAHAFFEY TEST SITE

The Reid–Mahaffey test, located near Timmins, is flown as a prerequisite to all surveys for the Government of Ontario Ministry of Energy, Northern Development and Mines (MENDM) to ensure that the airborne electromagnetic system is operational and responds to a broad range of electromagnetic responses at different depths below surface.

Sixteen (16) traverse lines are flown at 200 m line spacing and north–south oriented, similar to the survey specifications of the Sandy Lake Block. Four (4) tie-lines are flown perpendicular to traverse lines, as indicated in the tables below and in Figure L-3. The test was performed with EM bird terrain clearance of 30 m. These lines were flown on July 12, 2017.

Line orientation for the Reid–Mahaffey Test is listed in the tables below.

Table 14. Traverse lines.

Traverse lines	Direction
10	N to S
20	S to N
30	N to S
40	S to N
50	N to S
60	S to N
70	N to S
80	S to N
90	N to S
100	S to N
110	N to S
120	S to N
130	N to S
140	S to N
150	N to S
160	S to N
Traverse lines	**Direction**
10	N to S
20	S to N
30	N to S
40	S to N
50	N to S
60	S to N
70	N to S
80	S to N
90	N to S
100	S to N
110	N to S
120	S to N
130	N to S
140	S to N
150	N to S
160	S to N

Table 15. Tie lines.

Tie lines	Direction
9010	W to E
9020	E to W
9030	W to E
9040	E to W

On the location of line 40, 6 additional lines are flown in the north to south direction at different level of EM bird terrain clearance: 50 m, 75 m, 100 m, 125 m, and 150 m, as indicated in table below. These lines were flown on July 12, 2017.

Table 16. EM bird terrain clearance on line 40, Reid–Mahaffey Test.

Location of L40	EM bird altitude (m)
4050	50
4075	75
4100	100
4125	125
4150	150
4200	200

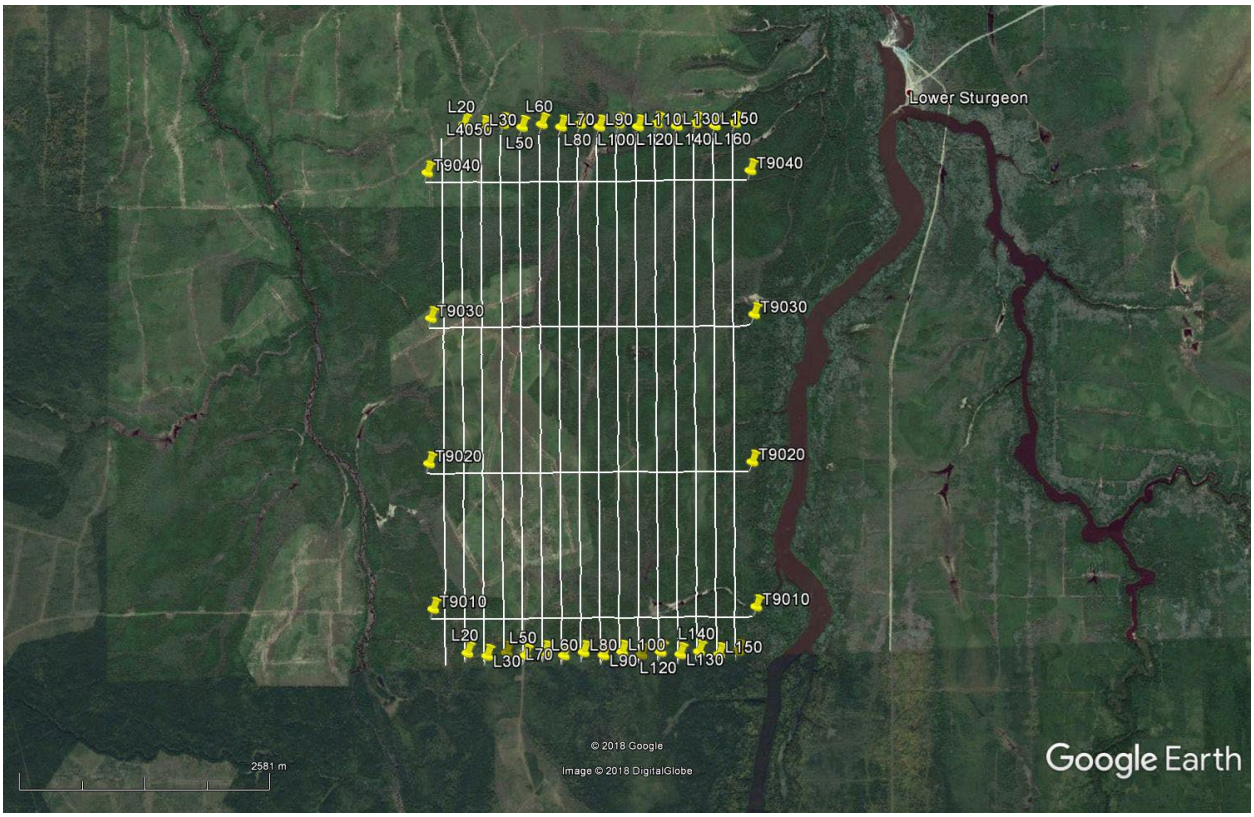

Figure L-3. Reid–Mahaffey Test lines on Google Earth™ (July 12, 2017).

Data acquired in Reid–Mahaffey was processed and presented in a Geosoft database and grids. Additional products include the selection of anomalies, resistivity-depth images (RDI) and apparent conductivity depth slices.

FULL WAVEFORM VTEM CALIBRATION

The calibration is performed with the completely assembled VTEM system connected to the helicopter at the survey site on the ground. Measurements of the half-cycles are collected and used to calculate a sensor calibration consisting of a single stacked half-cycle waveform. The purpose of the stacking is to attenuate natural and man-made magnetic signals, leaving only the response to the calibration signal. The stacked half-cycle allows the transfer functions between the receiver and data acquisition system, $H_D(\omega)$, and current sensor and data acquisition system, $H_R(\omega)$, to be determined. These transfer functions are used as a part of the system response correction during processing to correct the half-cycle waveforms and data acquired on a survey flight to a common transfer function:

$$D(\omega) = [H_C(\omega)/H_D(\omega)]\, D_R(\omega)$$

$$A(\omega) = [H_C(\omega)/H_R(\omega)]\, A_R(\omega)$$

where $H_C(\omega)$ is the common transfer function, and $D_R(\omega)$ and $A_R(\omega)$ are the FFT's of the raw receiver and current sensor responses recorded by the data acquisition system.

This process allows for the receiver response, $R(\omega)$, to become independent of the sensor characteristics determined by the transfer functions $H_D(\omega)$ and $H_R(\omega)$ and acts similar to a deconvolution of the data.

$$R(\omega) = \frac{D(\omega)I(\omega)}{A(\omega)}$$

where, $D(\omega)$ is the FFT of the actual receiver data sample $D(t)$, $I(\omega)$ is the FFT of a reference or "Ideal waveform" and $A(\omega)$ is the FFT of the actual waveform.

HIGH ALTITUDE CALIBRATION

The high altitude calibration is conducted on each survey flight. At the beginning and at the end of each flight the helicopter climbs at 2500 to 3000 feet above ground to check the EM "zero level". When at the required altitude, at least 60 seconds of data were acquired in normal operation mode.

Reference transmitter current and receiver voltage waveforms, each sampled at 192 kHz, were also recorded at high altitude for all survey flights. The recorded waveforms were transformed into an ideal form, having zero current at the beginning of the off-time, by the full waveform calibration (*see* "Full Waveform VTEM Calibration").

The final delivered data set contains these processed windowed high altitude data for the one hundred and fifty four (154) survey flights in Geosoft® database format (Appendix G). A graphical representation of a VTEM waveform is shown in Figure 5.

ALUMINIUM PLATE TEST

This test is performed on ground to verify the sensitivity of the system. An aluminium plate of known conductive response is positioned in alternated positions (vertical and horizontal) for about 10 seconds for 3 time measurements. Response of corresponding dB/dt and B-field data is then verified.

Results of the test performed on January 27, 2018 is presented in a Geosoft® database view below. When the aluminum plate is horizontal with respect to the loop, measured signal will show positive response, indicating a proper polarity (Figure L-4).

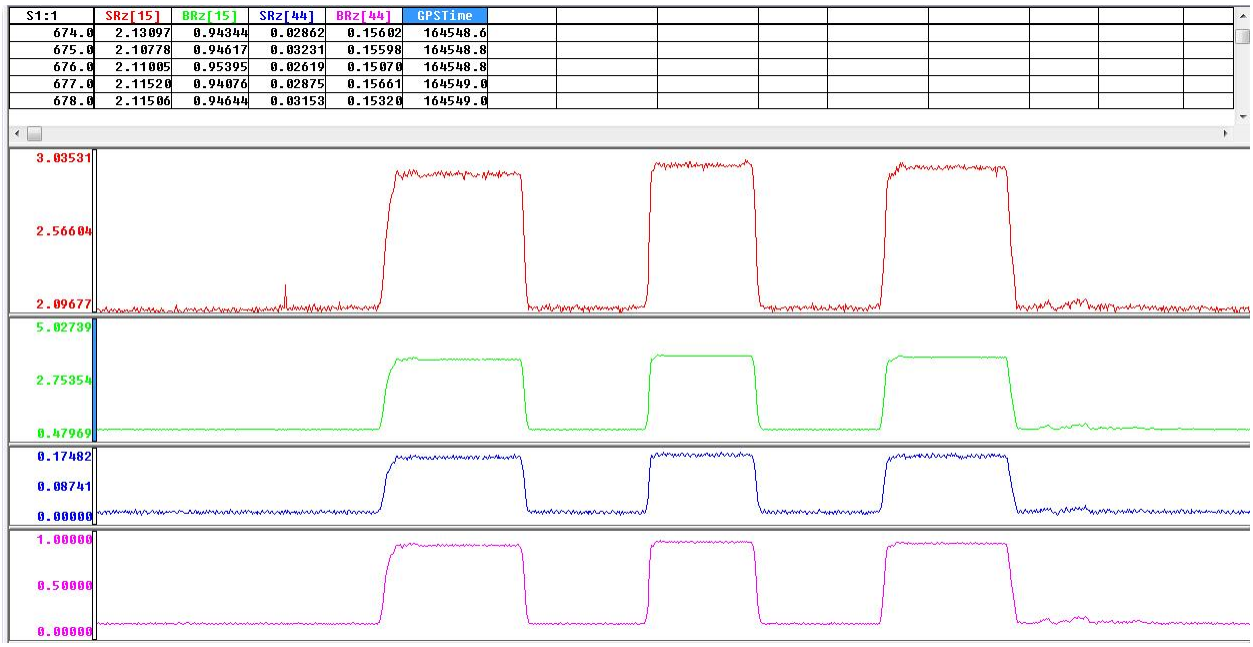

Figure L-4. Plate test results performed on January 27, 2018.

TEST LINES

Daily test lines were acquired to ensure that the airborne system is operating repeatability and as expected. Three test line locations were selected, 2 of them were flown in an east to west direction and one was flown in a north to south direction, as presented in figure below (Figure L-5).

Figure L-5. Location of test lines flown in a daily basis.

RADAR ALTIMETER CALIBRATION TEST

The purpose of the radar altimeter calibration is to verify the performance of radar altimeter readings using the GPS elevation data as the reference.

The calibration is performed flying over the same spot at various altitudes, ranging from 30 m (100 feet) to 183 m (600 feet). The selected spot has known elevation and flat terrain, repeated on land and water. This test was performed on each aircraft at the beginning of the survey July 20 (Figure L-6) and July 24, 2018 (Figure L-7), upon arrival of a replacement aircrafts, and at the end of the survey on March 19 and March 22, 2018.

As observed in the graphical results presented below, where the GPS elevations versus radar readings are plotted, the relationship between radar and GPS readings are linear, and the radar readings are very accurate (R^2~1.0), for the range of flying heights to be expected for the survey.

Radar checks were preformed once per day. These checks consisted of the ground crew communicating with the operator/pilot via radio when the tail of the system would leave the ground.

Table 17. Radar altimeter calibration data from tests performed on July 20, 2017.

Nominal Altitude above ground (m)	Radar Altitude Raw Data (m)	DGPS Altitude Ellipsoidal Height (m)	DTM = DGPS - Radar Alt Ellipsoidal Height WGS84 (m)	DGPS Altitude (ALT) ALT=DGPS - AVERAGE(DTM) (m)
85.34	86.85	383.4	296.55	88.28
89.92	88.83	384.4	295.57	89.28
100.58	104.28	399.4	295.12	104.28
120.40	118.95	414.7	295.75	119.58
150.88	156.41	449.0	292.59	153.88

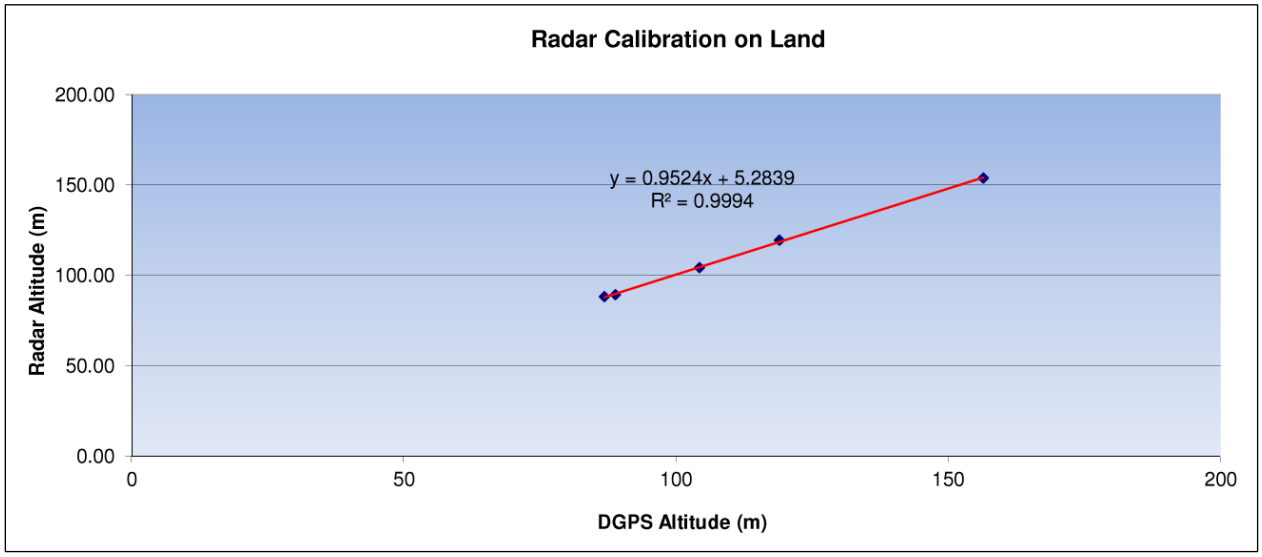

Figure L-6. Radar altimeter test results performed on July 20, 2017.

Table 18. Radar altimeter calibration data from tests performed on July 24, 2017.

Nominal Altitude above ground (m)	Radar Altitude Raw Data (m)	DGPS Altitude Ellipsoidal Height (m)	DTM = DGPS - Radar Alt Ellipsoidal Height WGS84 (m)	DGPS Altitude (ALT) ALT=DGPS - AVERAGE(DTM) (m)
85.34	86.85	379	292.15	89.78
89.92	88.83	383.2	294.37	93.98
100.58	104.28	390.5	286.22	101.28
121.92	118.95	414.3	295.35	125.08
152.40	156.41	434.3	277.99	145.18

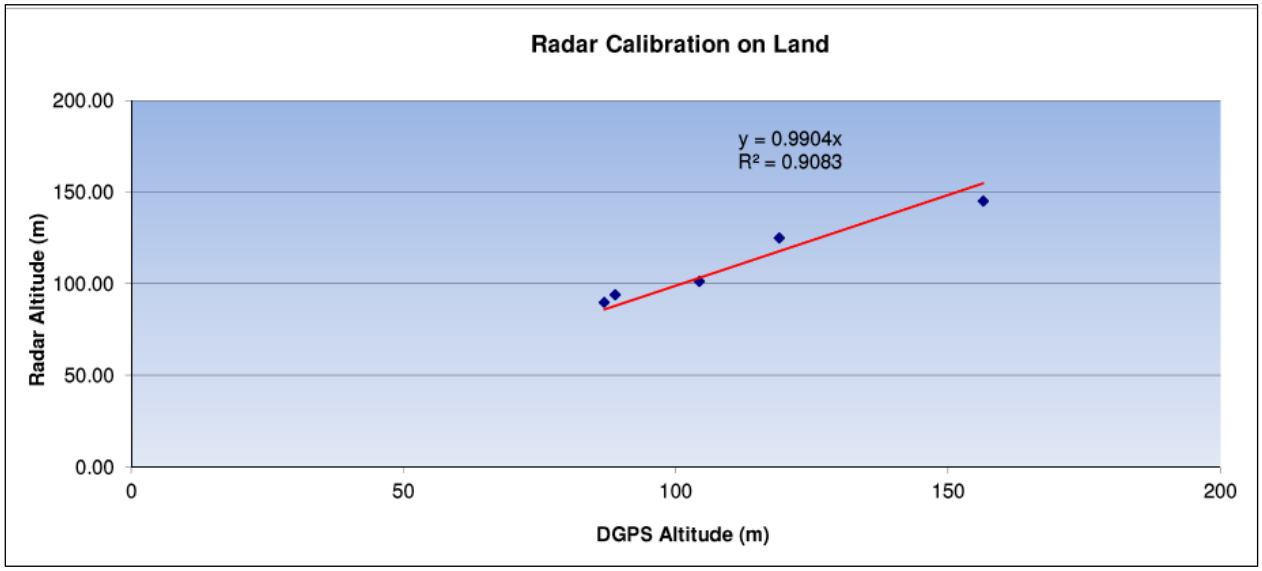

Figure L-7. Radar altimeter test results performed on July 24, 2017.

MAGNETOMETER CLOVERLEAF TESTS

Calibration flights are performed to verify the heading errors of the magnetometer in the 4 cardinal directions. The TDEM data is analyzed during this process as well to confirm data quality in terms of response to turns and varying wind conditions.

This test is performed at the beginning of the project, once per month during the course of the project, and at the end of the project on March 19, 2018 (Figure L-8) and March 22, 2018 (Figure L-9).

Test Date: March 19, 2018 (VTEM07)

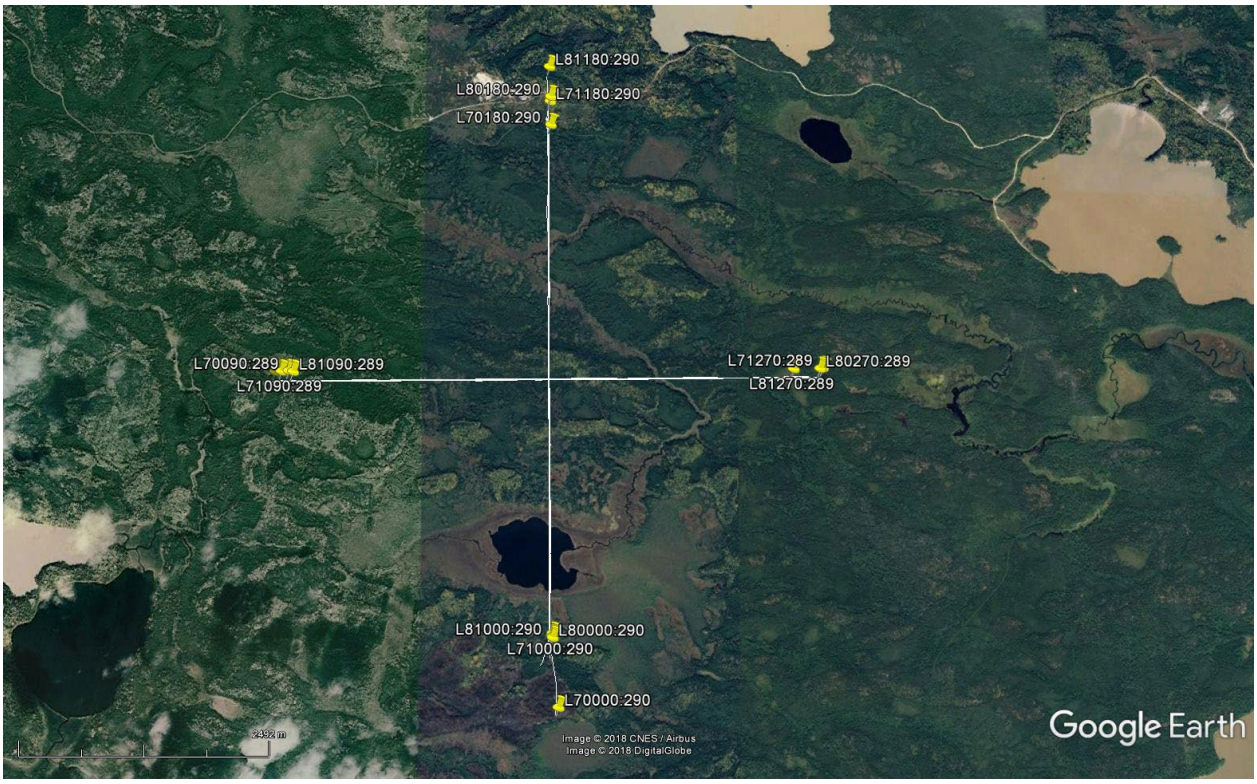

Figure L-8. Flight path of Heading test performed on March 19, 2018.

Table 19. Raw Heading data (Mag channel is diurnally corrected and lagged), March 19, 2018 (VTEM07).

	Direction	Line #	Fiducial	Mag
pass 1	0	L70000	75657.0	57628.6
	90	L70090	64685.7	57629.9
	180	L70180	75929.8	57629.5
	270	L70270	64369.5	57630.3
pass 2	0	L71000	76215.2	57630.3
	90	L71090	65292.5	57629.1
	180	L71180	76483.9	57628.9
	270	L71270	64989.0	57631.1

Table 20. Heading Effect coefficients, March 19, 2018 (VTEM07).

Direction	Heading Correction
0	0.26
90	0.21
180	0.51
270	-0.99

Table 21. Heading corrected data, March 19, 2018 (VTEM07).

Direction	Line #	Fiducial	Mag Corr
0	L70000	75657.0	57628.9
90	L70090	64685.7	57630.1
180	L70180	75929.8	57630.0
270	L70270	64369.5	57629.3
0	L71000	76215.2	57630.6
90	L71090	65292.5	57629.3
180	L71180	76483.9	57629.4
270	L71270	64989.0	57630.1

Test Date: March 22, 2018 (VTEM15)

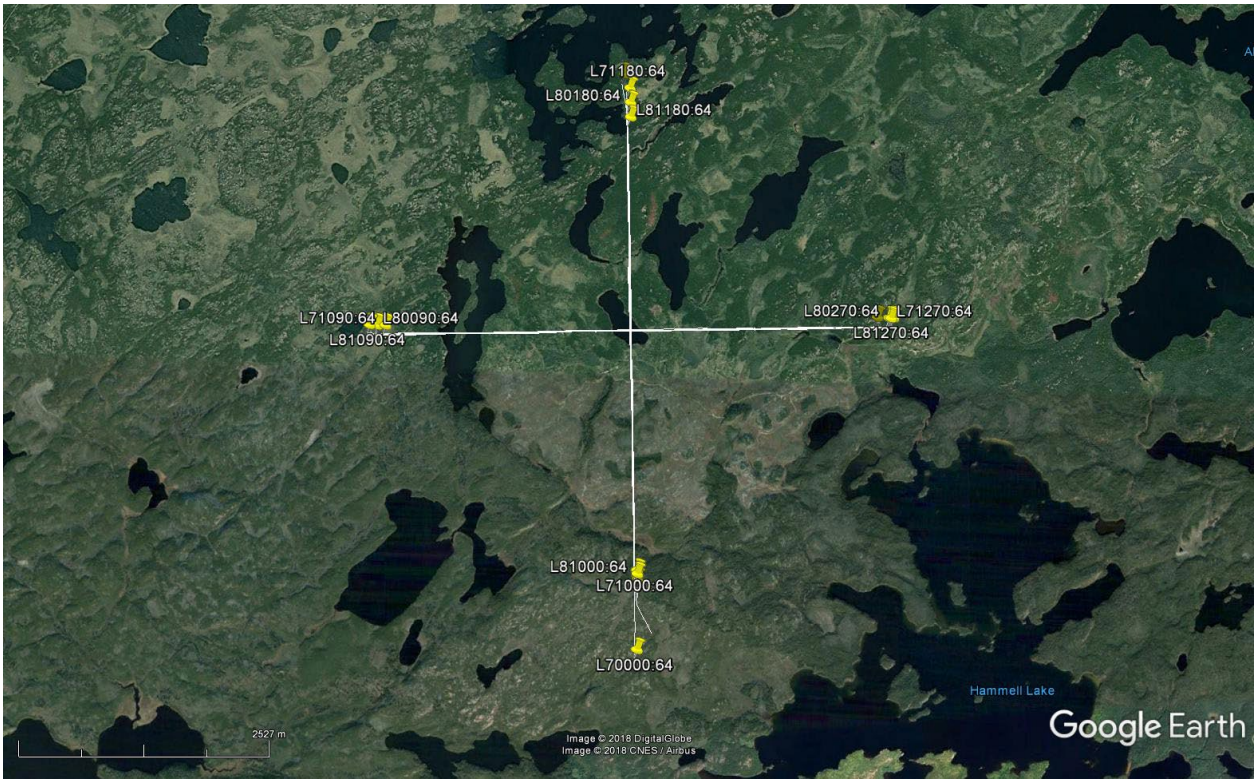

Figure L-9. Flight path of Heading test performed on March 22, 2018.

Table 22. Raw Heading data (Mag channel is diurnally corrected and lagged), March 22, 2018 (VTEM15).

	Direction	Line #	Fiducial	Mag1
pass 1	0	L70000	55883.5	57164.4
	90	L70090	60544.6	57164.2
	180	L70180	56152.0	57164.8
	270	L70270	60831.5	57167.7
pass 2	0	L71000	56416.7	57163.5
	90	L71090	61111.7	57167.9
	180	L71180	56700.3	57166.1
	270	L71270	61396.7	57164.2

Table 23. Heading Effect coefficients, March 22, 2018 (VTEM15).

Direction	Heading Correction
0	1.40
90	-0.70
180	-0.10
270	-0.60

Table 24. Heading corrected data, March 22, 2018 (VTEM15).

Direction	Line #	Fiducial	Mag Corr
0	L70000	55883.5	57165.8
90	L70090	60544.6	57163.5
180	L70180	56152.0	57164.7
270	L70270	60831.5	57167.1
0	L71000	56416.7	57164.9
90	L71090	61111.7	57167.2
180	L71180	56700.3	57166.0
270	L71270	61396.7	57163.6